Computational Investigations of Surface-Normal Pneumatic Active Aerodynamic Load Control for Lift Enhancement and Separation Mitigation in High-Lift Systems

Sheida Hosseini

C. P. van Dam

Shishir Pandya

NASA Advanced Modeling and Simulation Seminar

July 9, 2020

Motivation

Active Flow Control for high-lift systems

For large twin-engine transport jet *

- $C_{L_{max}}$ — $+1\% C_{L_{max}} \propto$ 4400 lb (~22 passengers)
- L/D — +1%L/D $\propto$ 2800 lb (~14 passengers)
- C_L modulation in the linear lift regime — +0.10 $\Delta C_L \propto$ 14 in reduction in $h_{landing\ gear}$ $\propto$ 1400 lb (~7 passenger)


B787 flap system
Source: C.P. van Dam

* P. Meredith, "Viscous phenomena affecting high-lift systems and suggestions for future CFD development. High-lift System Aerodynamics," AGARD CP 515, pp. 19(1)–19(8), 1993.

Active Flow Control (AFC)

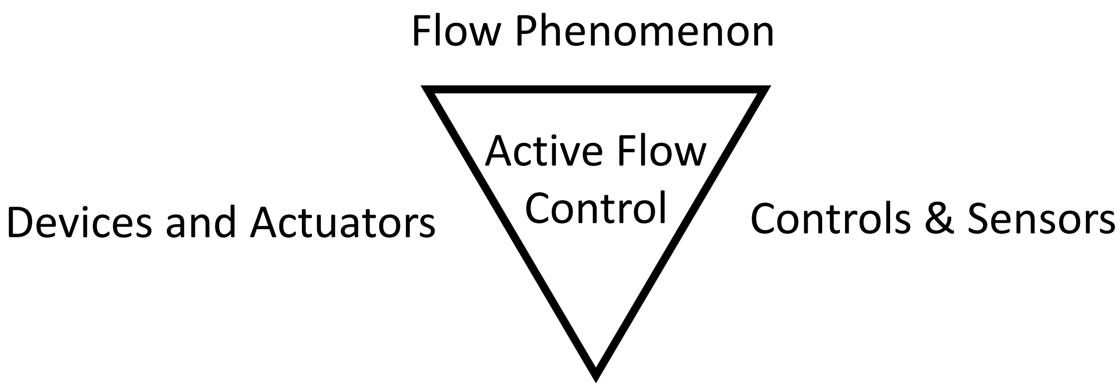

Separation Mitigation

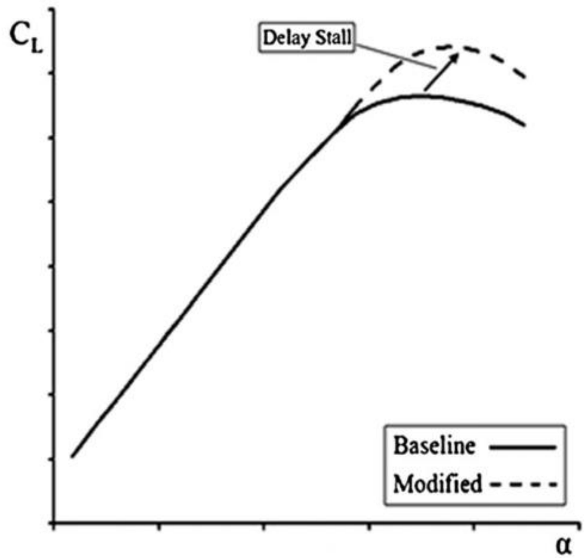

Load Control *

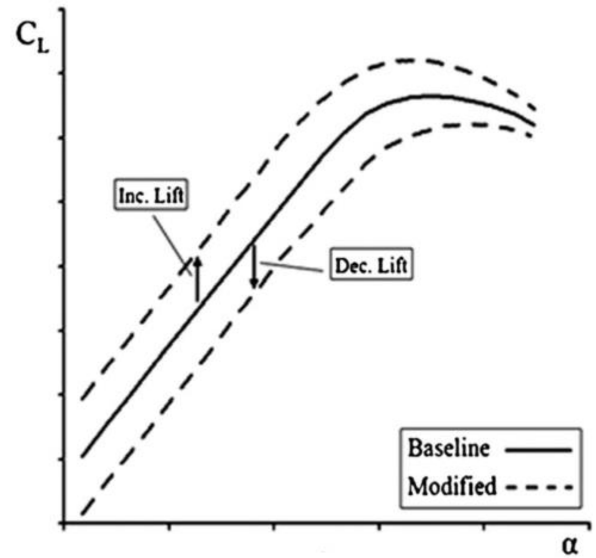

*Lift curve is taken from : Johnson, S. J., Baker, J. P., van Dam, C. P., and Berg, D., “An overview of active load control techniques for wind turbines with an emphasis on microtabs," Wind Energy: An International Journal for Progress and Applications in Wind Power Conversion Technology 13(2-3), 2010, pp. 239-253.

Microtab and Microjet

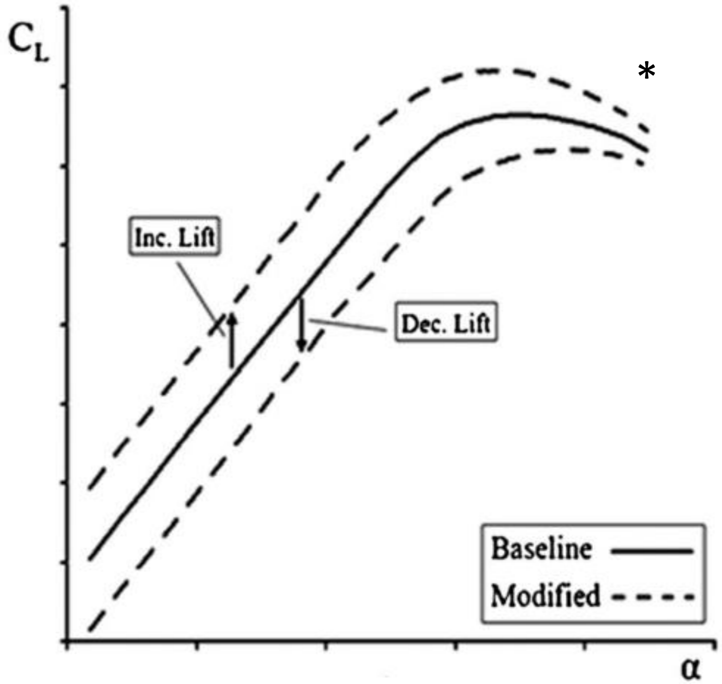

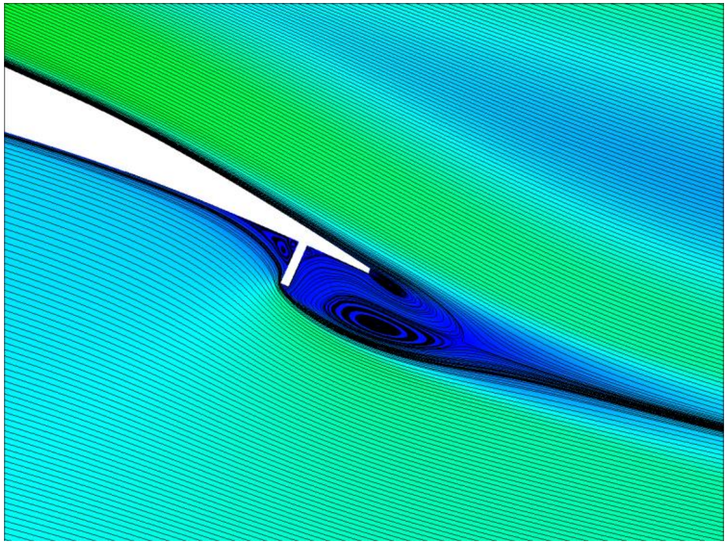

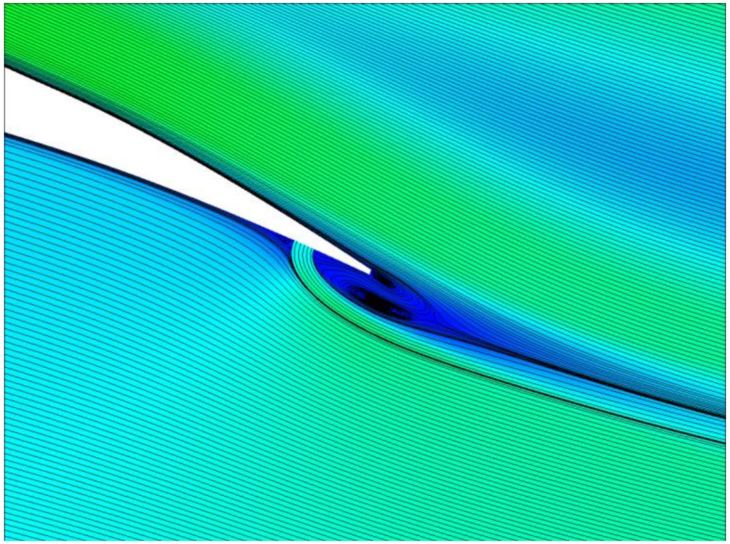

* Lift curve is taken from : Johnson, S. J., Baker, J. P., van Dam, C. P., and Berg, D., “An overview of active load control techniques for wind turbines with an emphasis on microtabs," Wind Energy: An International Journal for Progress and Applications in Wind Power Conversion Technology 13(2-3), 2010, pp. 239-253.

Theoretical Developments

Assume: thin jet, inviscid, irrotational, and doesn't mix with the flow external to the jet

$$p_1 + \frac{1}{2}\rho_\infty u_1^2 = p_2 + \frac{1}{2}\rho_\infty u_2^2$$

$$p_1 + \frac{1}{2}\rho_j v_1^2 = p_2 + \frac{1}{2}\rho_j v_2^2$$

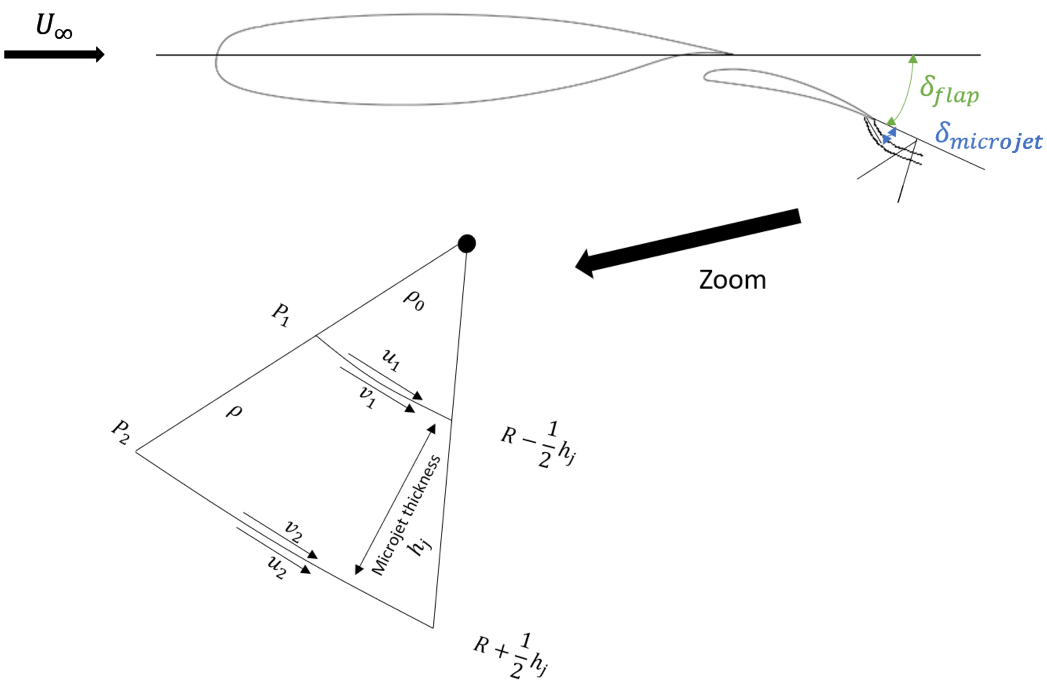

Theoretical Developments

$$p_1 - p_2 = \frac{1}{2}\rho_\infty u_2^2 - \frac{1}{2}\rho_\infty u_1^2 \quad (1)$$

$$p_1 - p_2 = \frac{1}{2}\rho_j v_2^2 - \frac{1}{2}\rho_j v_1^2 \quad (2)$$

$$u_1^2 - u_2^2 = \frac{\rho_j}{\rho_\infty}(v_1^2 - v_2^2) \quad (3)$$

$$(u_1 - u_2)(u_1 + u_2) = \frac{\rho_j}{\rho_\infty}(v_1 - v_2)(v_1 + v_2) \quad (4)$$

Irrotational flow assumption

$$\Gamma = \oint \vec{v}\, d\vec{l} = 0.$$

$$v_1(R - \frac{1}{2}h_j) = v_2(R + \frac{1}{2}h_j) \quad (5)$$

$$v_1 - v_2 = \frac{h_j}{2R}(v_1 + v_2) \quad (6)$$

Substitute (6) in (4)

$$(u_1 - u_2)(u_1 + u_2) = \frac{\rho_j}{\rho_\infty}(v_1 + v_2)\frac{h_j}{2R}(v_1 + v_2) \quad (7)$$

Assume small perturbations, and that u velocity is outside of boundary layer, entrainment region and recirculation region

$$U_\infty = \tfrac{1}{2}(u_1 + u_2) \text{ and } U_j = \tfrac{1}{2}(v_1 + v_2).$$

$$2U_\infty(u_1 - u_2) = \frac{\rho_j}{\rho_\infty}\frac{h_j}{2R}4U_j$$

$$u_1 - u_2 = \frac{\rho_j U_j^2 h_j}{\rho_\infty U_\infty R}$$

$$\gamma_j = u_1 - u_2 = \frac{\rho_j U_j^2 h_j}{\rho_\infty U_\infty R}$$

$$p_1 - p_2 = -\rho_j U_j h_j / R$$

Violates the Kutta Condition!!

Theoretical Developments

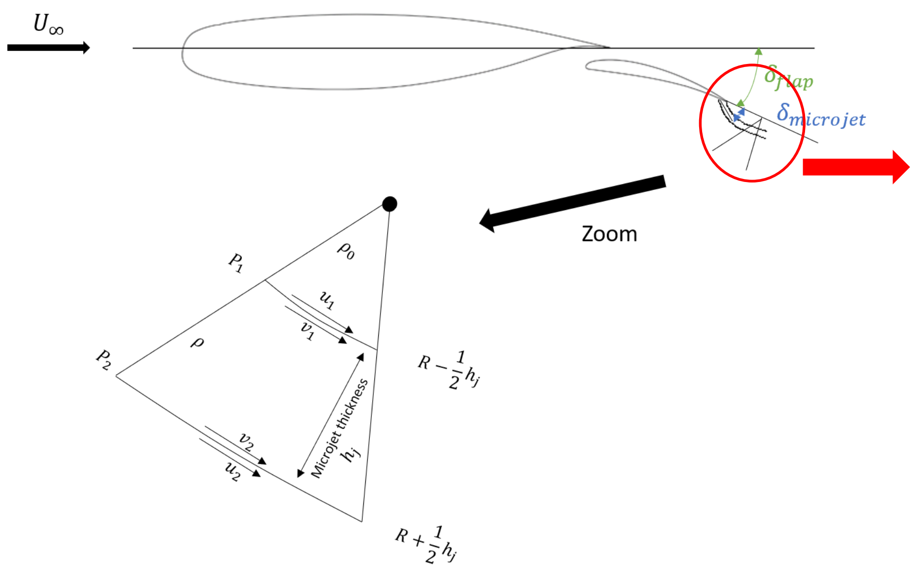

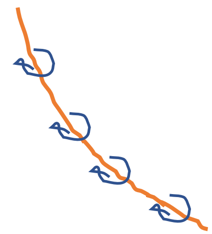

$$L = \rho_j U_j \Gamma_j + \rho_\infty U_\infty \Gamma_{\text{airfoils}}$$

$$\Gamma_j = \int_o^\infty \gamma_j ds = \int_o^\infty \frac{\rho_j U_j^2 h_j}{\rho_\infty U_\infty R} ds$$

$$\Gamma_{\text{airfoil}} = \int_o^{TE_{\text{main element}}} \gamma_{\text{main element}} dl + \int_o^{TE_{\text{flap element}}} \gamma_{\text{flap element}} dl$$

Lift is augmented due to

i) Reaction due to the vertical component of the microjet momentum force

ii) Due to the vertical component of the pressure on the airfoil surface which is modified by the asymmetry microjet creates in the flow-field

Theoretical Developments

Optimal Location for Circulation Control

$$C_l = \frac{L'}{\frac{1}{2}\rho U_\infty^2 c} = 2\pi(A_0 + \frac{A_1}{2}) \qquad A_0 = \alpha - \frac{1}{\pi}\int_0^\pi \frac{d\eta_c}{dx}d\theta \qquad A_1 = \frac{2}{\pi}\int_0^\pi \frac{d\eta_c}{dx}cos\theta d\theta$$

$$C_l = 2\pi(\alpha + \frac{1}{\pi}\int_0^\pi (cos\theta - 1)\frac{d\eta_c}{dx}d\theta) \qquad C_l = 2\pi\left(\alpha + \frac{2}{\pi}\int_{\frac{x}{c}=0}^{1} \frac{d(\frac{\eta_c}{c})}{d(\frac{x}{c})}\frac{\sqrt{\frac{x}{c}(1-\frac{x}{c})}}{\frac{x}{c}-1}d(\frac{x}{c})\right)$$

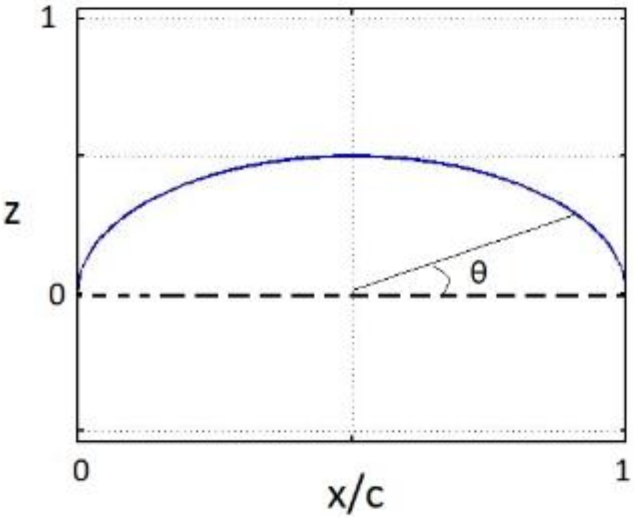

The effect of airfoil camber is maximum at the TE and vanishes at the LE

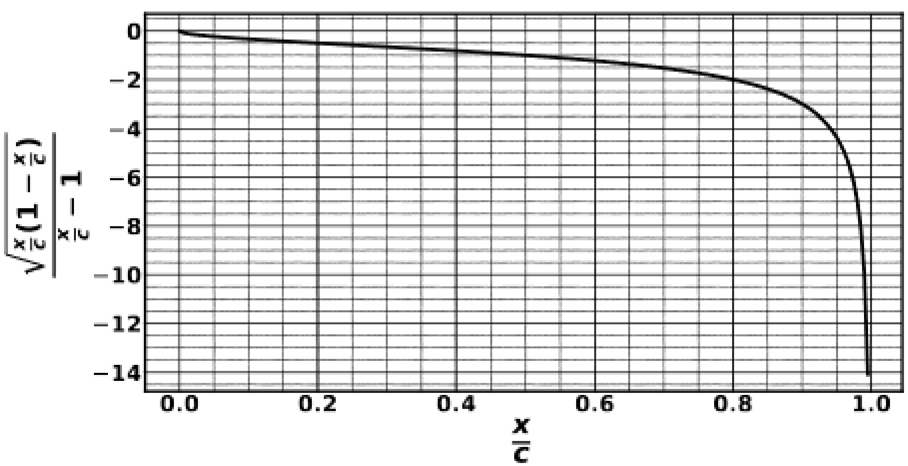

$\frac{d(\frac{\eta_c}{c})}{d(\frac{x}{c})} > 0$ Largest lift reduction due to camber at the TE

$\frac{d(\frac{\eta_c}{c})}{d(\frac{x}{c})} < 0$ Largest lift increase due to camber at the TE

Project Scope

- **Selection of airfoil configuration**
- **CFD validation / computational sensitivities**
  - Surface and volume grid sensitivities
  - Grid connectivity
  - Solver sensitivities
  - Turbulence model
  - Transition modeling
  - Far field extent
- **2D microjet configuration studies**
  - Microjet and microtab comparison
  - Microjets effects over angle of attack range
  - Control volume analysis
  - Momentum coefficient sweeps
  - Microjet chordwise location and width
  - Initial power requirement analysis
  - Microjet inlet velocity profile and effects of modeling as boundary condition vs. plenum
  - Varying flap deflection and separation effects
  - Pulsed vs. steady microjet
  - Mach number and Reynolds number effects
- **Extensive CFD studies of microjets**
  - 2.5-D: Microjet effects on infinite sheared wing
  - 3D: Application of microjets on CRM

Publications:

- Journal of Aircraft in progress
- Journal of Aircraft paper in review
- Journal of Aircraft paper DOI: 10.2514/1.C035248
- AIAA paper 2019-3498 (Aviation 2019)
- AIAA paper 2019-0590 (SciTech 2019)
- AIAA paper 2018-0559 (SciTech 2018)

Computational Studies

- Summary of the computational setup on baseline multi-element airfoil NLR7301
- 2D investigations on the NLR7301 flaps 20° and 30°
- 2.5D (infinite sheared wing) the NLR7301 flap 30°
- CRM-HL in landing configuration

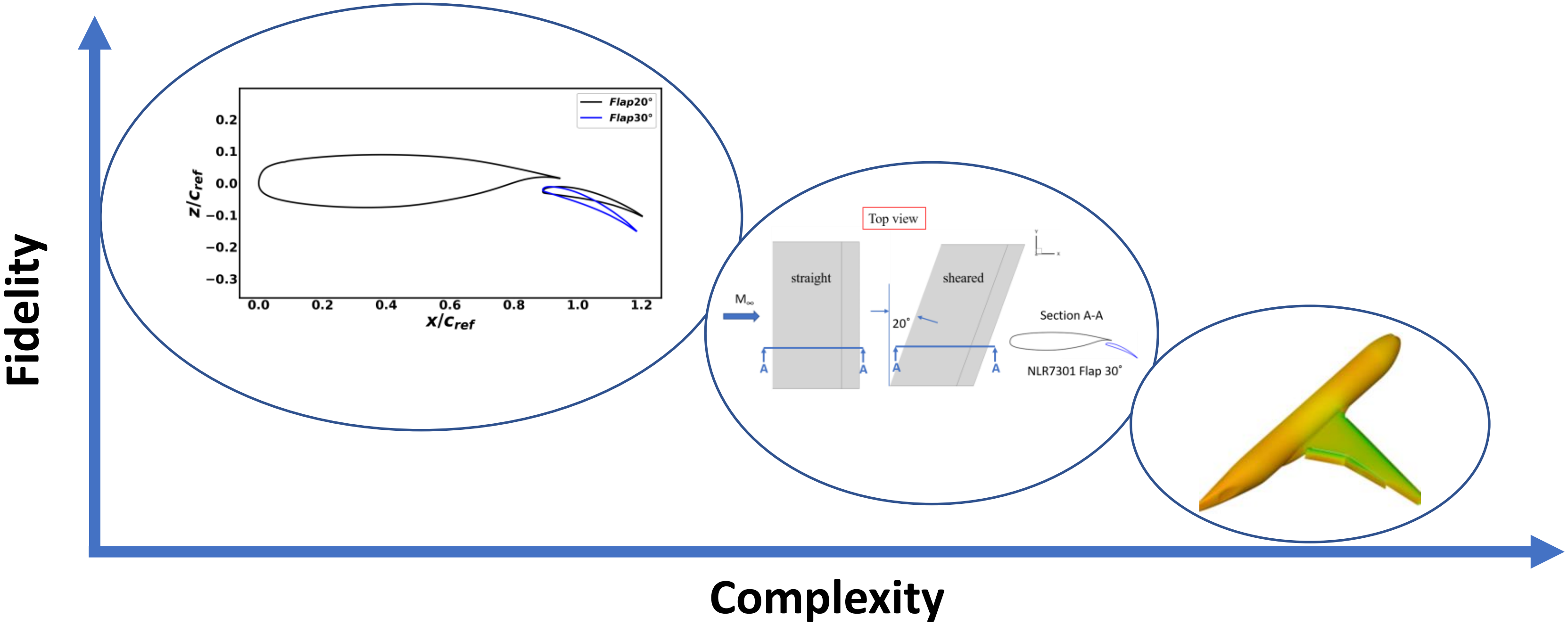

Computational Studies

- Summary of the computational setup on baseline multi-element airfoil NLR7301
- 2D investigations on the NLR7301 flaps 20° and 30°
- 2.5D (infinite sheared wing) the NLR7301 flap 30°
- CRM-HL in landing configuration

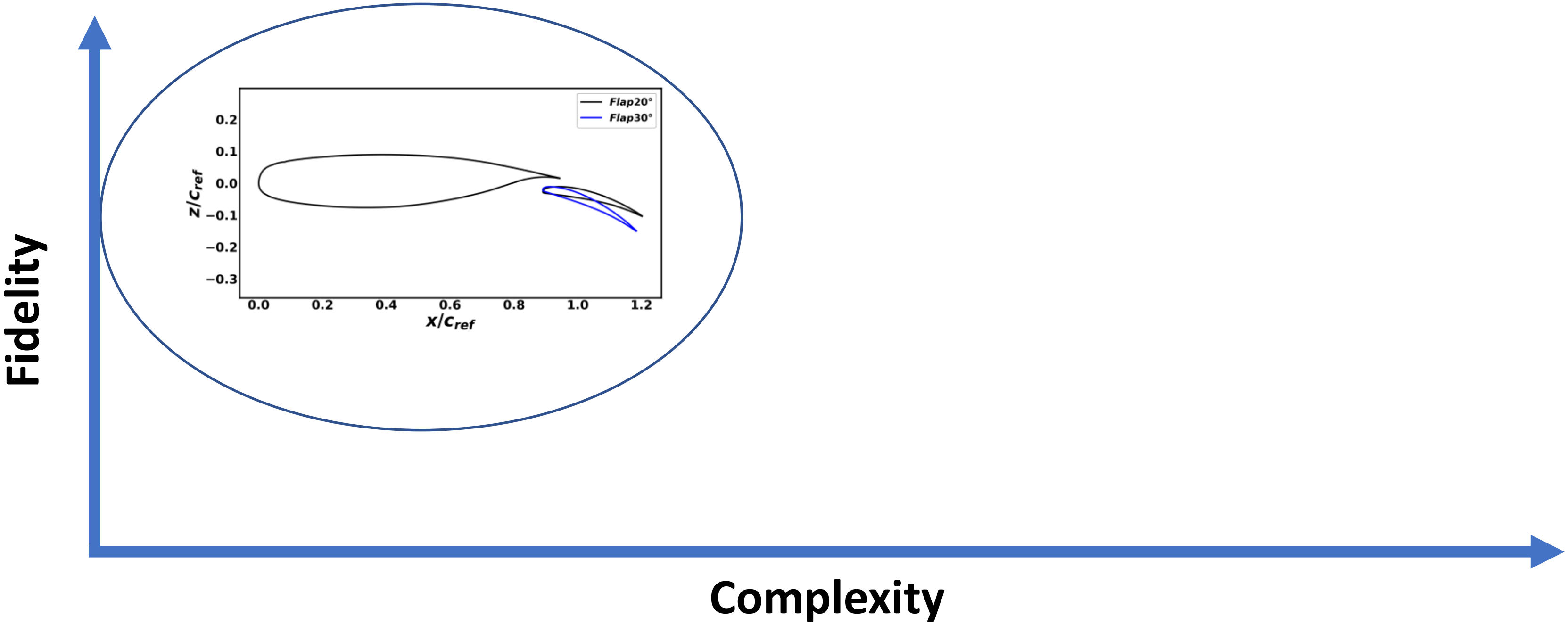

Airfoil Definition*

- NLR7301: flap chord is 32%c_{ref}
  - Flap deflection 20°, overlap 0.053 c_{ref}, gap 0.026 c_{ref}
  - 2-dimensional $\alpha = 6°$, $Re = 2.51E6$, and $M = 0.185$

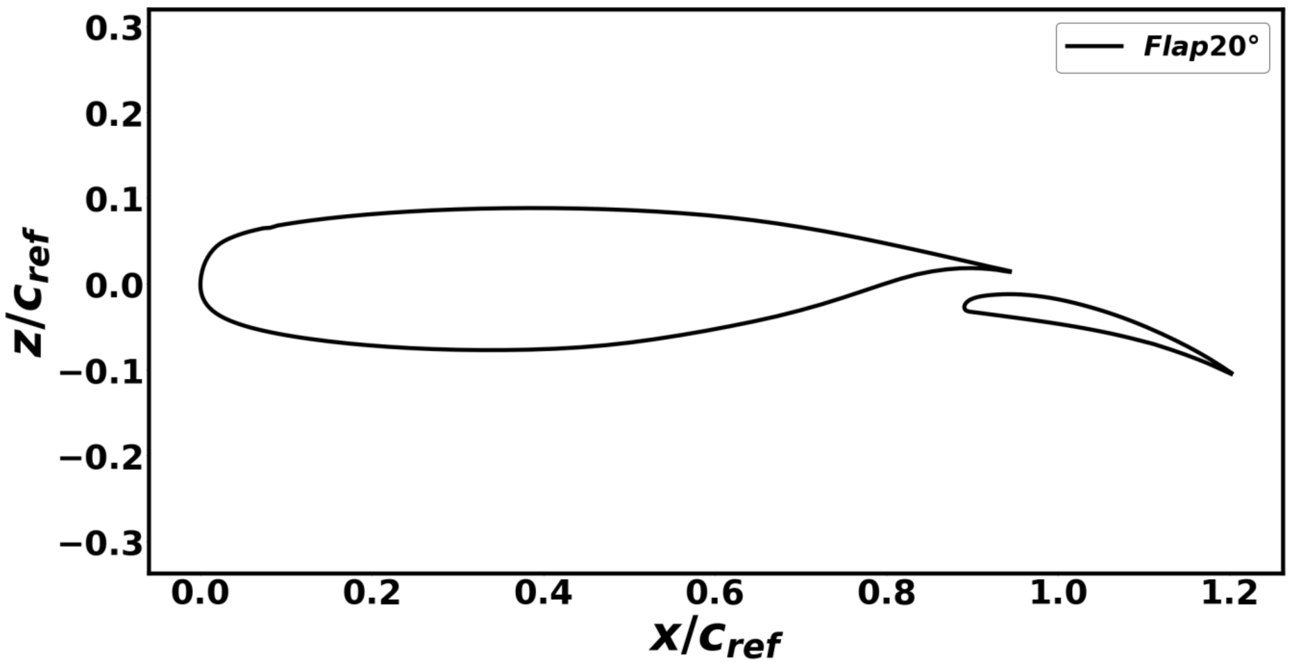

*Vandenberg, B. and Oskam, B., "Boundary layer measurements on a two-dimensional wing with flap and a comparison with calculations," In AGARD Turbulent Boundary Layers 14 p (SEE N80-27647 18-34), 1980.

Airfoil Definition

- NLR7301: flap chord is 32%c_{ref}
  - Flap deflection 20°, overlap 0.053 c_{ref}, gap 0.026 c_{ref}
  - 2-dimensional $\alpha = 6°$, $Re = 2.51E6$, and $M = 0.185$

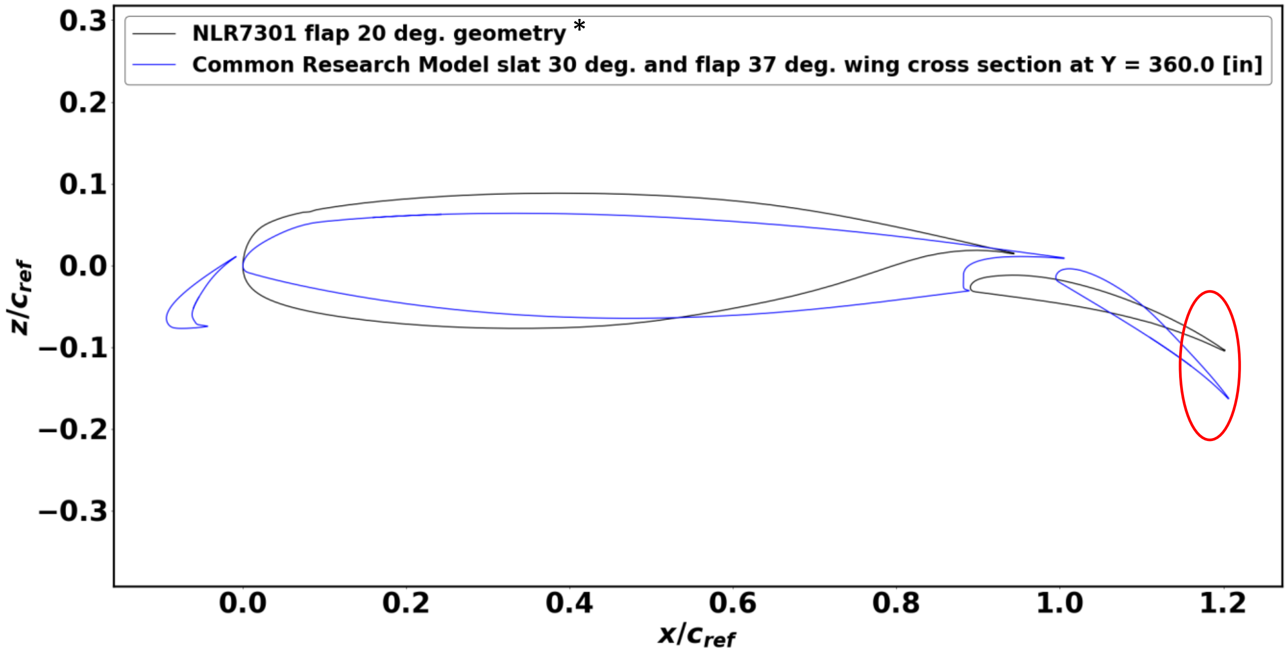

*Vandenberg, B. and Oskam, B., “Boundary layer measurements on a two-dimensional wing with flap and a comparison with calculations," In AGARD Turbulent Boundary Layers 14 p (SEE N80-27647 18-34), 1980.

2-D CFD Setup Summary

- Extensive CFD sensitivity study (solver, grid, connectivity, turbulence model, transition) conducted in 2018
- Overset grid technology
  - O-grid topology growing 10,000c away
  - DCF mesh connectivity
- RANS OVERFLOW 2
  - 3rd order accurate and ARC3D diagonalized approximate factorization with matrix artificial dissipation
  - SST turbulence model

ΔCd discrepancy transition related
CFD – fully turbulent
Exp – free transition

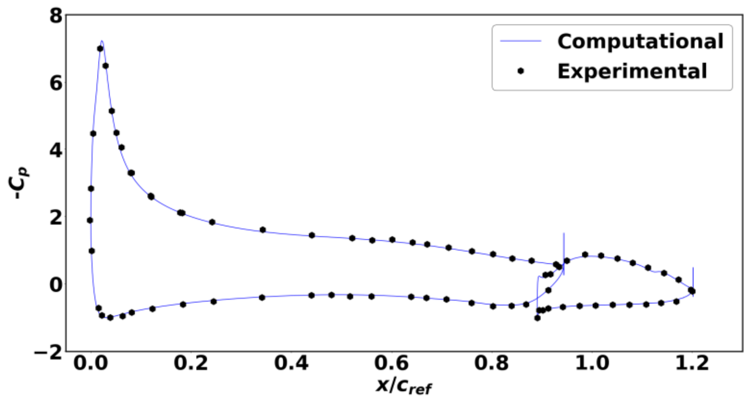

Clock Time[min] on 48 Haswell Processors	C_l	$\Delta C_l\%$ w.r.t resp. exp.	C_d	$\Delta C_d\%$ w.r.t resp. exp.
30.35	2.41	0.4%	0.0250	7.0%

Computational Studies

- Summary of the computational setup on baseline multi-element airfoil NLR7301
- 2D investigations on the NLR7301 flaps 20˚ and 30˚
- 2.5D (infinite sheared wing) the NLR7301 flap 30˚
- CRM-HL in landing configuration

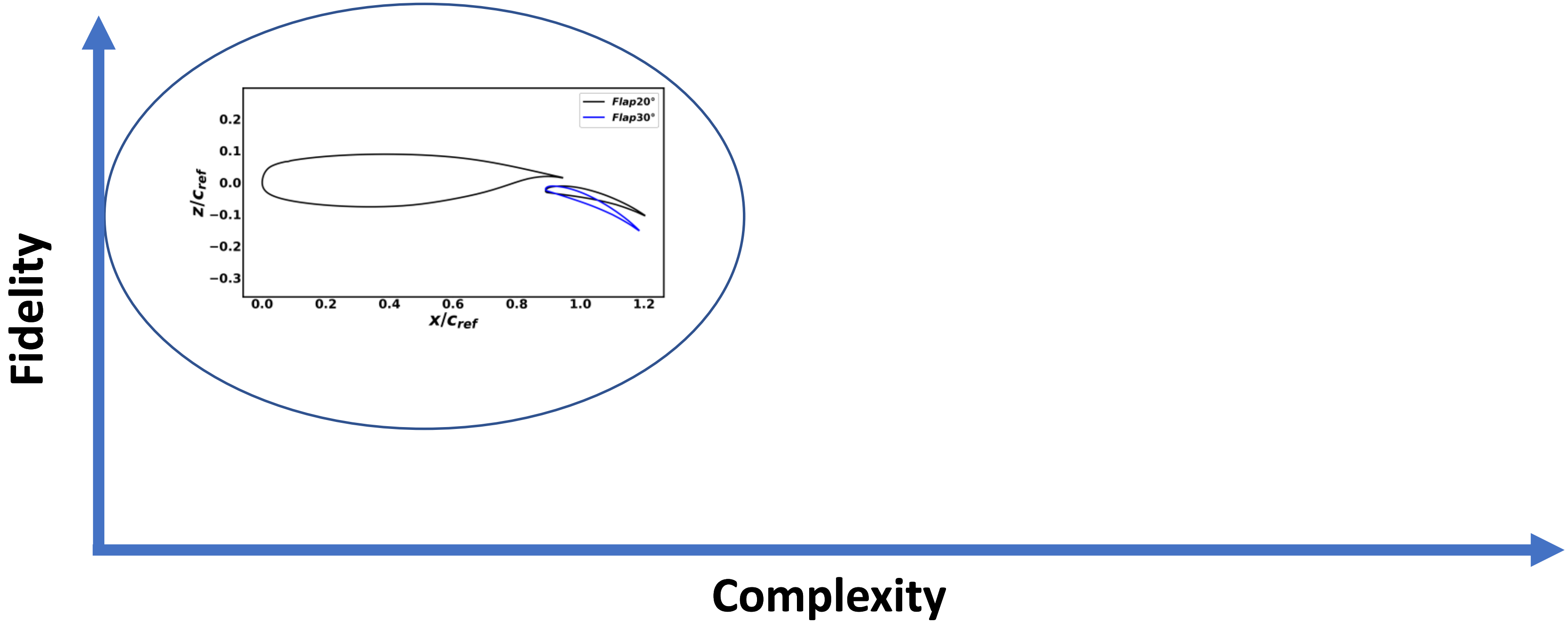

Microtab and Microjet Modeling

2D

α=6°, Re = 2.51E6, and Ma = 0.185

Tab 1%c in height and 0.2%c thickness

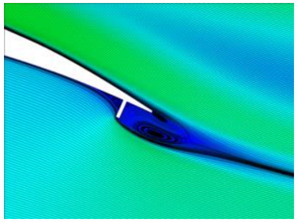

$$C\mu = \frac{\dot{m}_j U_j}{\frac{1}{2}\rho_\infty U_\infty^2 S_{ref}} \xrightarrow{\dot{m}_j = (\rho U A)_j} C\mu = \frac{\rho_j U_j^2 h_j b}{\frac{1}{2}\rho_\infty U_\infty^2 b\, c} \xrightarrow{Incompressible} C\mu = 2\frac{U_j^2}{U_\infty^2}\frac{h_j}{c}$$

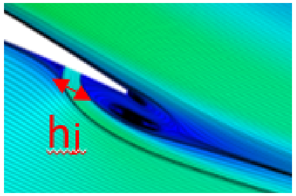

Configuration	$\frac{U_j}{U_\infty}$	C_μ	h_j	location
Initial microjet	1.0	0.010	$0.005c_{ref}$	$95\%C_{flap}$

- All the simulations for microjet in the presentation are time-accurate. The results shared are time-averaged.
- The simulations for microtab are steady.

Microtab and Microjet Modeling

2D

α=6°, Re = 2.51E6, and Ma = 0.185

	C_l	C_d
Baseline (no AFC)	2.409	0.02499
Microtab	2.640	0.02965
Microjet		

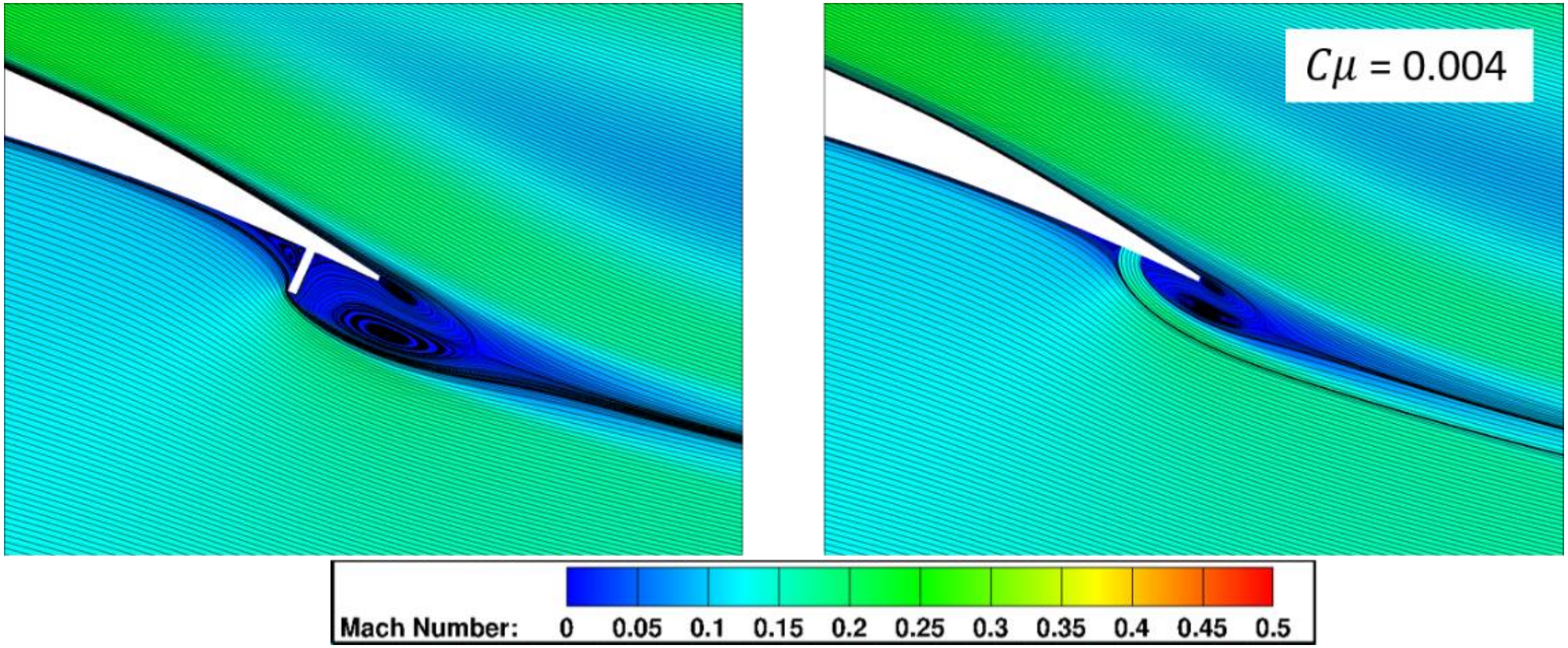

Microtab and Microjet Modeling

2D

α=6°, Re = 2.51E6, and Ma = 0.185

	C_l	C_d
Baseline (no AFC)	2.409	0.02499
Microtab	2.640	0.02965
Microjet	2.640	0.02232

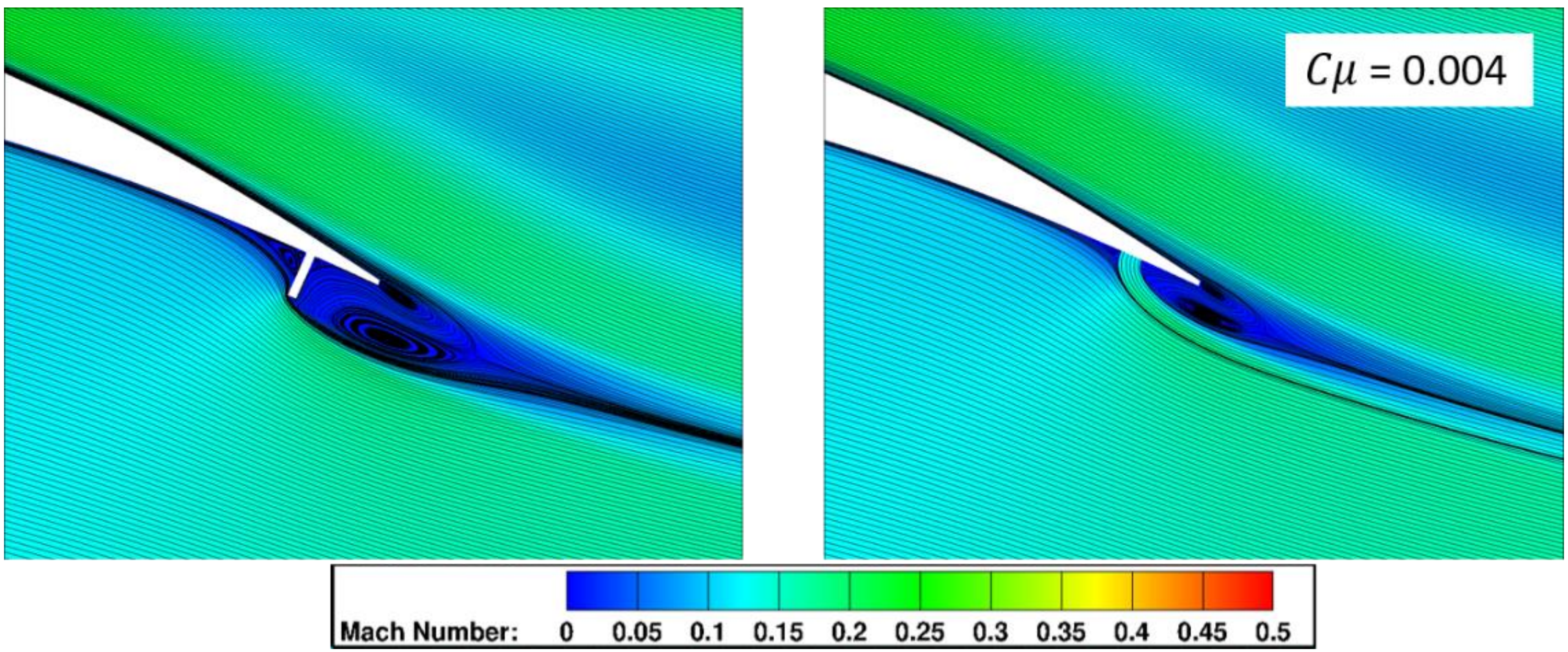

Flap 20 Lift and Drag Investigation

2D

α=6°, Re = 2.51E6, and Ma = 0.185

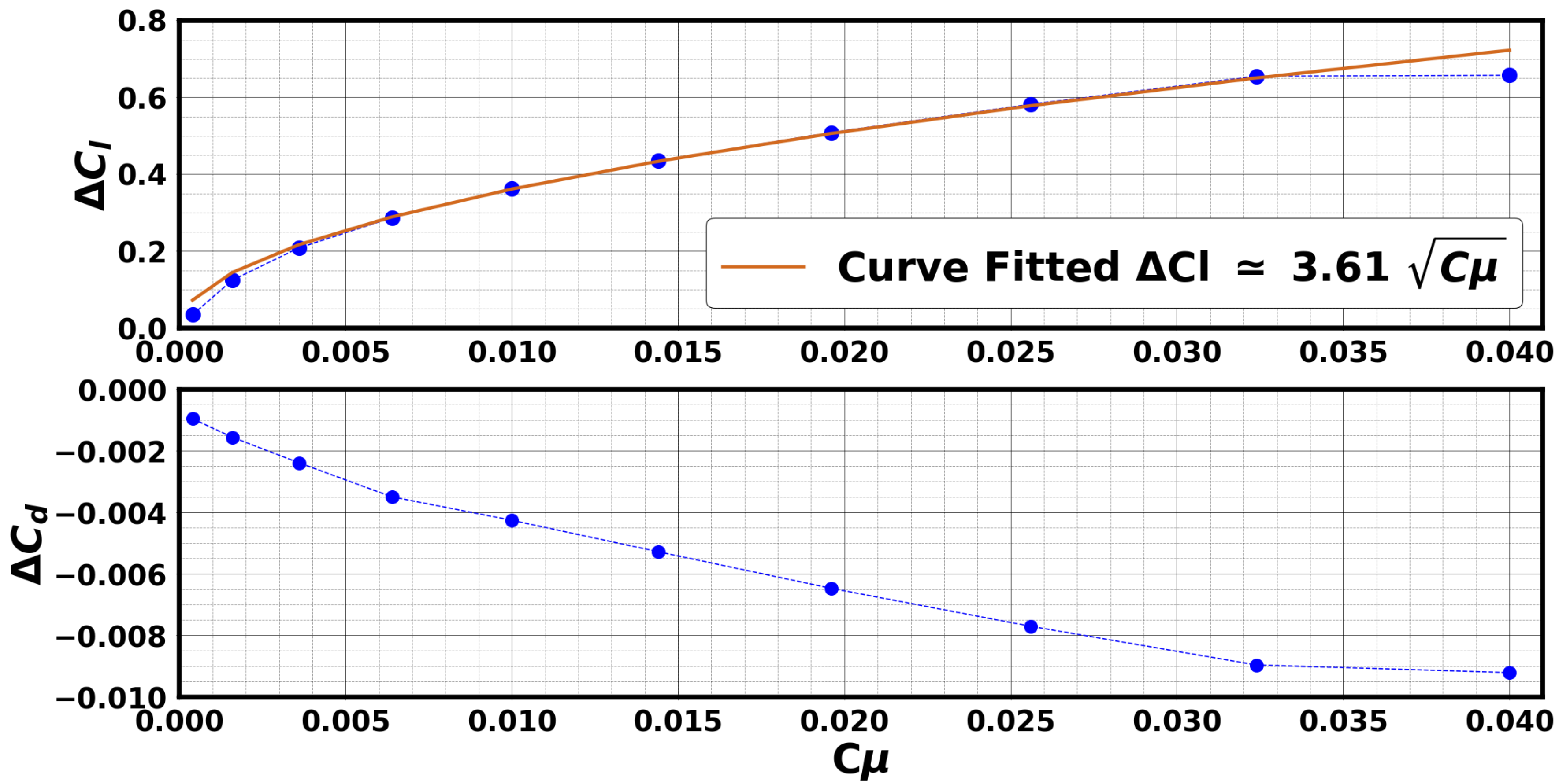

Drag Validation

α=0°, Re = 2.51E6, and Ma = 0.185, C_μ = 0.01

Case	Integrated at	C_l	C_d
Pressure-side microjet	Surface	2.011	0.01550
Pressure-side microjet	0.3c far-field	2.011	0.01551
Pressure-side microjet	0.5c far-field	2.011	0.01551
Pressure-side microjet	0.7c far-field	2.011	0.01551

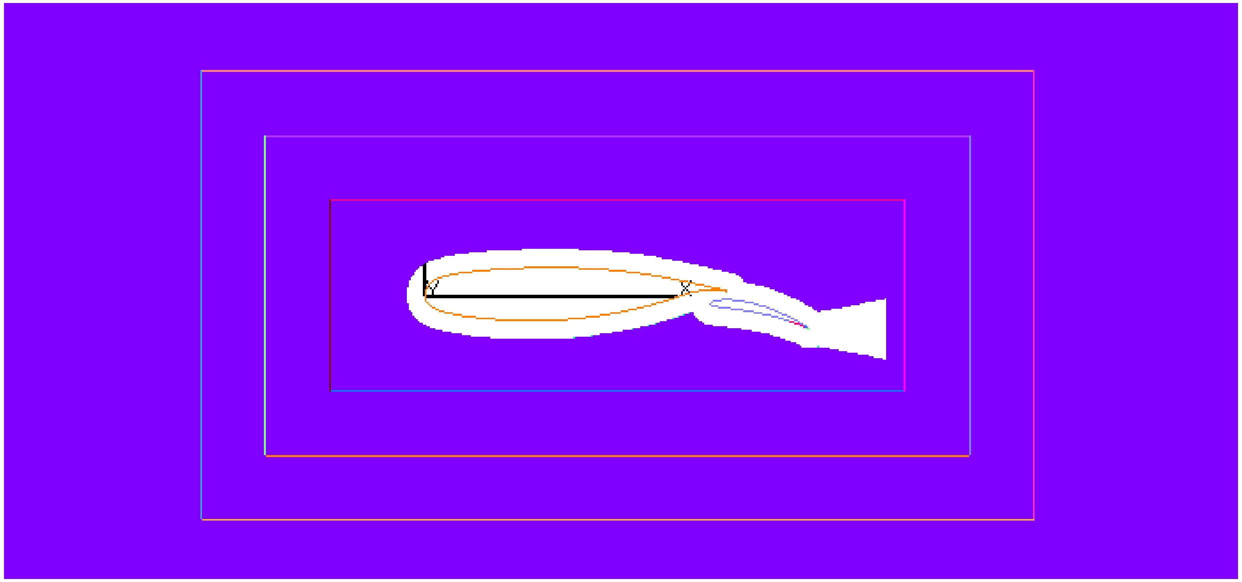

Spot Checks: Literature*

Symmetric airfoil

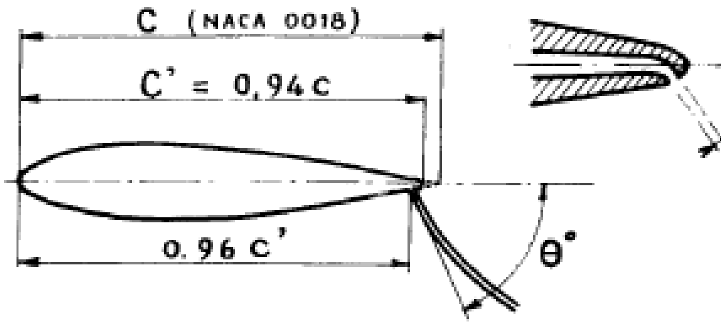

$$\Delta C_L = 3.9\sqrt{C_\mu} \cdot \sin\theta$$

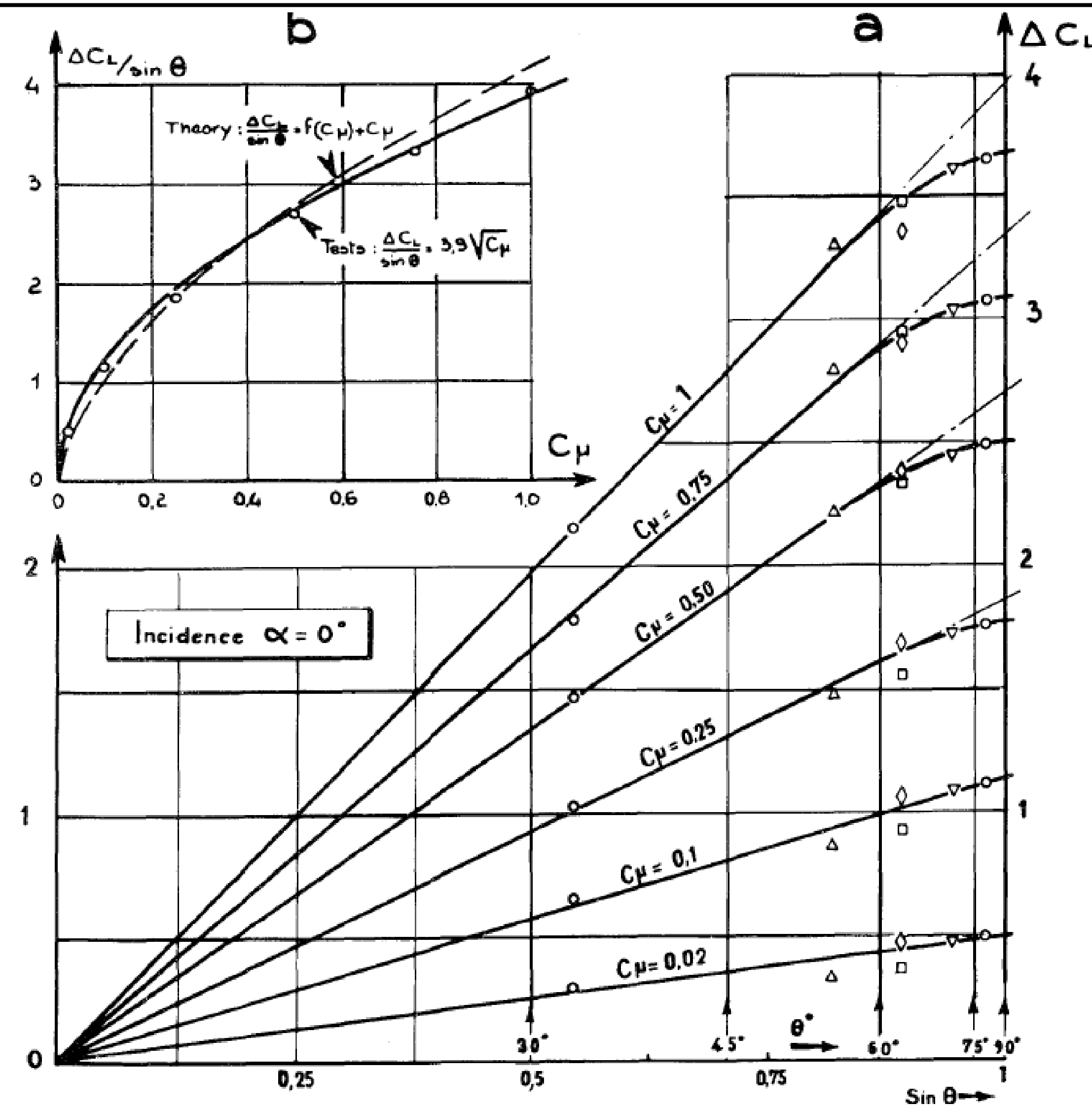

*L. Malavard, P. Poisson-Quinton, and P. Jousserandot, “Theoretical and experimental investigations of circulation control,” T.M. Berthoff and DC. Hazen (translators), Princeton University Department of Aeronautical Engineering, Report 356, 1956.

Spot Checks: Literature*

Symmetric airfoil

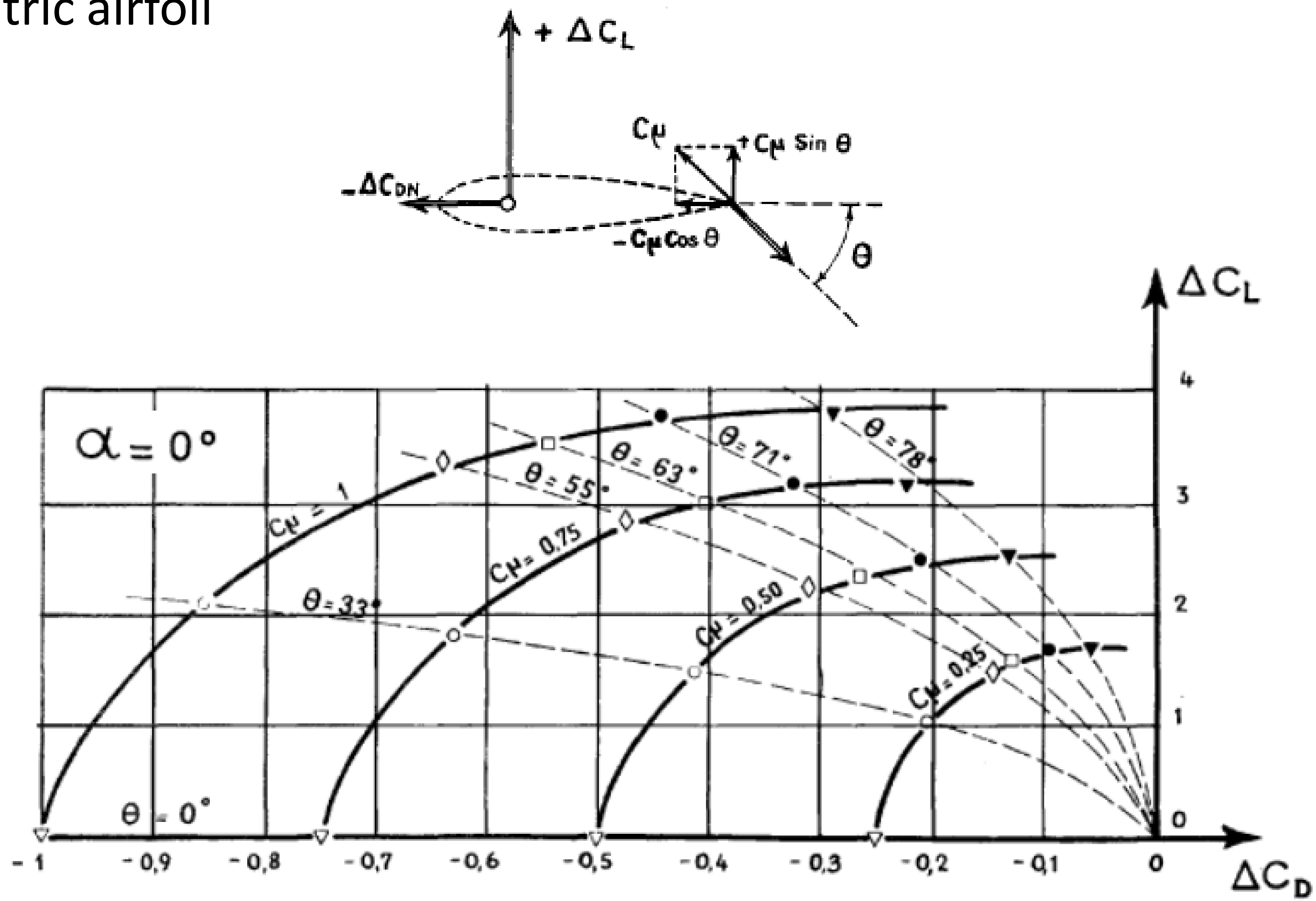

L. Malavard, P. Poisson-Quinton, and P. Jousserandot, "Theoretical and experimental investigations of circulation control," T.M. Berthoff and DC. Hazen (translators), Princeton University Department of Aeronautical Engineering, Report 356, 1956.

Flap 20 Lift and Drag Investigation

2D

α=6°, Re = 2.51E6, and Ma = 0.185

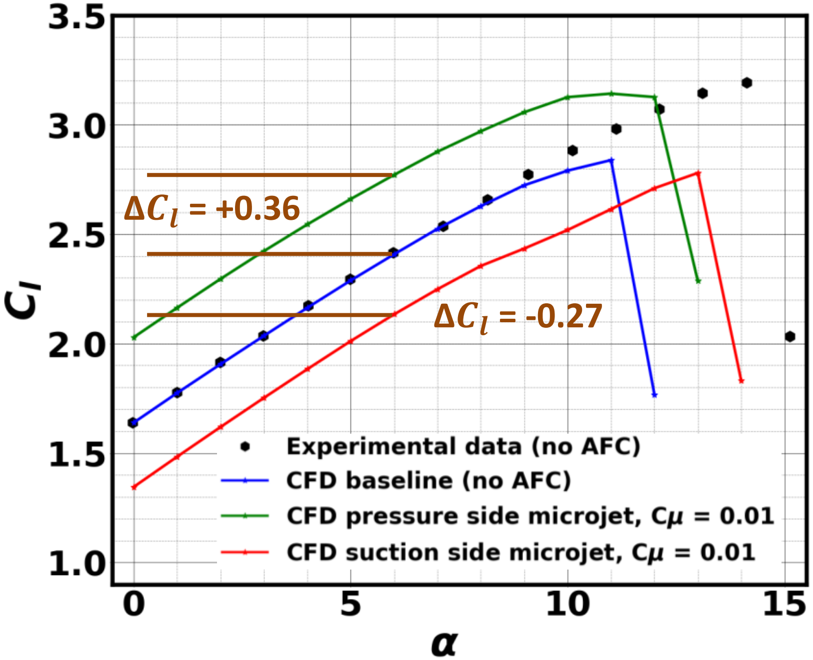

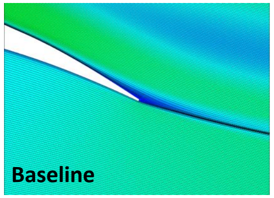

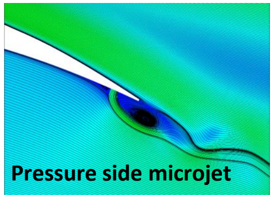

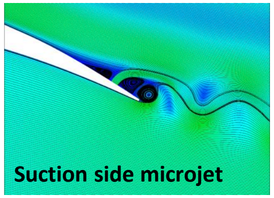

Microjet at 95% flap chord with a fixed width of 0.005 refence chord

$$\boldsymbol{F} = \int (-P\delta_{ij} + \tau_{ij})\, n_j \, dA + \int \rho u_i u_j \, n_j dA$$

$$L = -F_x sin\alpha + F_z cos\alpha$$

Flap 20 Lift and Drag Investigation

2D

α=6°, Re = 2.51E6, and Ma = 0.185

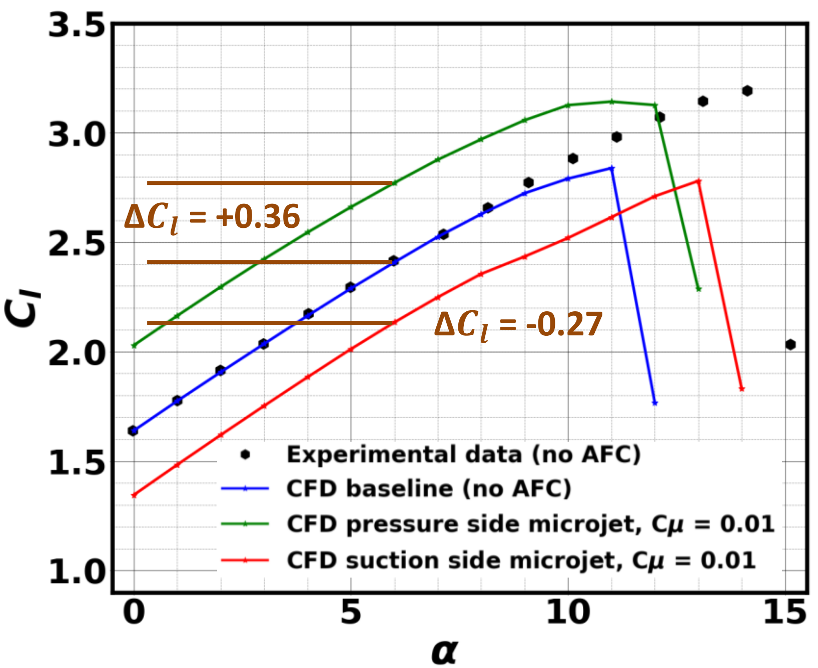

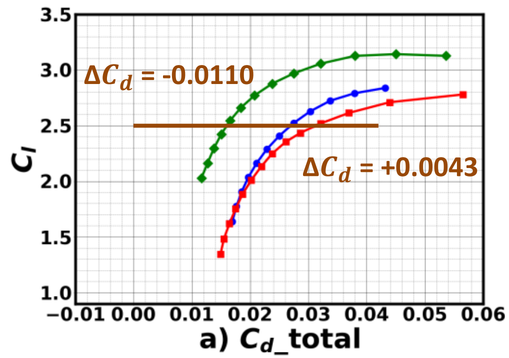

Microjet at 95% flap chord with a fixed width of 0.005 refence chord

$$\boldsymbol{F} = \int (-P\delta_{ij} + \tau_{ij})\, n_j\, dA + \int \rho u_i u_j\, n_j dA$$

$$L = -F_x sin\alpha + F_z cos\alpha$$

Flap 20 Lift and Drag Investigation

2D

α=6°, Re = 2.51E6, and Ma = 0.185

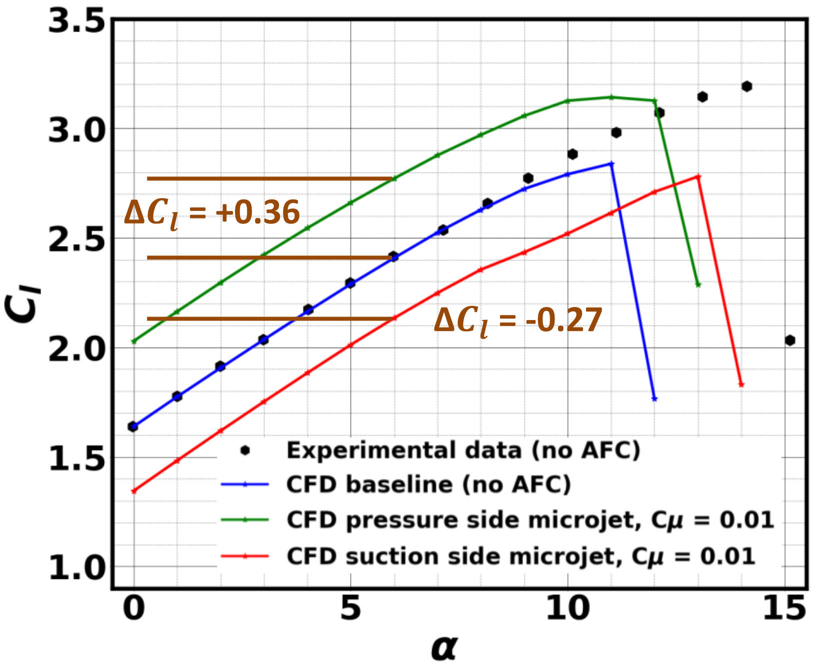

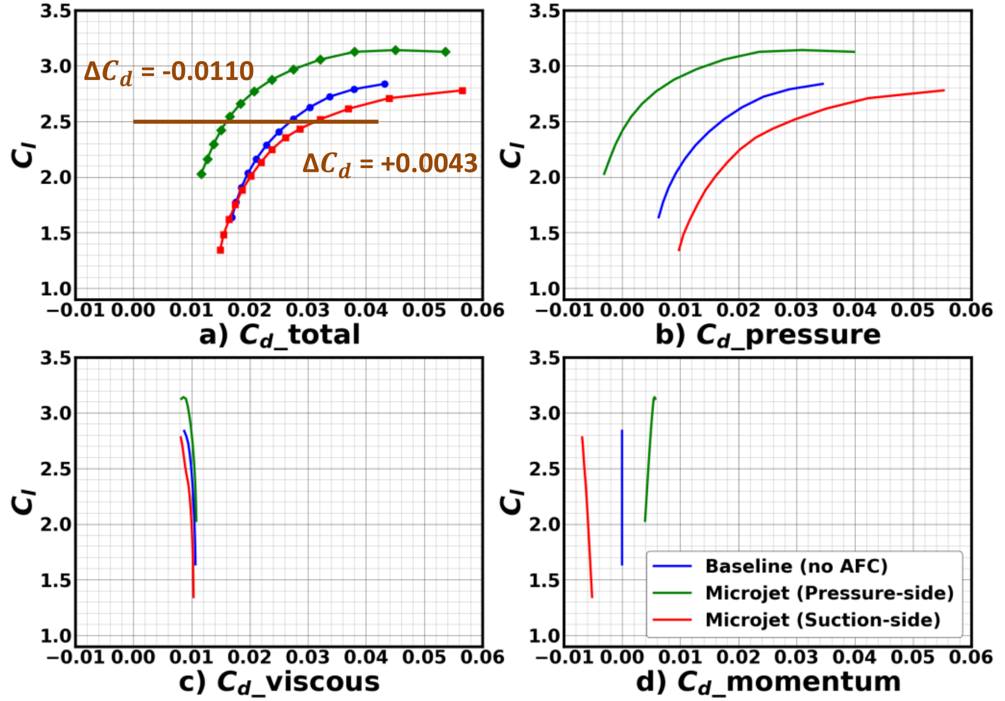

$$F = \int (-P\delta_{ij} + \tau_{ij})\, n_j\, dA + \int \rho u_i u_j\, n_j dA$$

$$D = F_x cos\alpha + F_z sin\alpha$$

$$L = -F_x sin\alpha + F_z cos\alpha$$

Flap 20 Lift and Drag Investigation

2D

α=6°, Re = 2.51E6, and Ma = 0.185

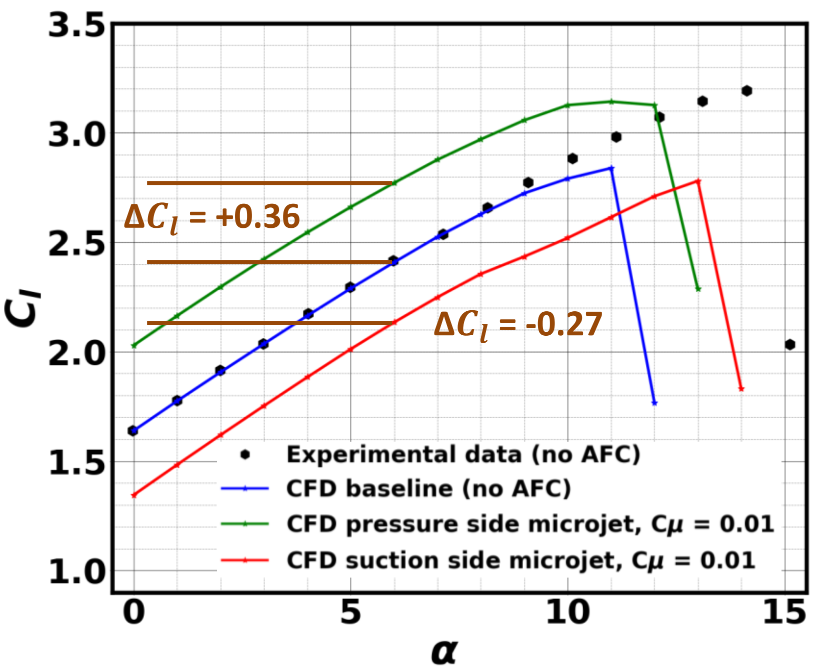

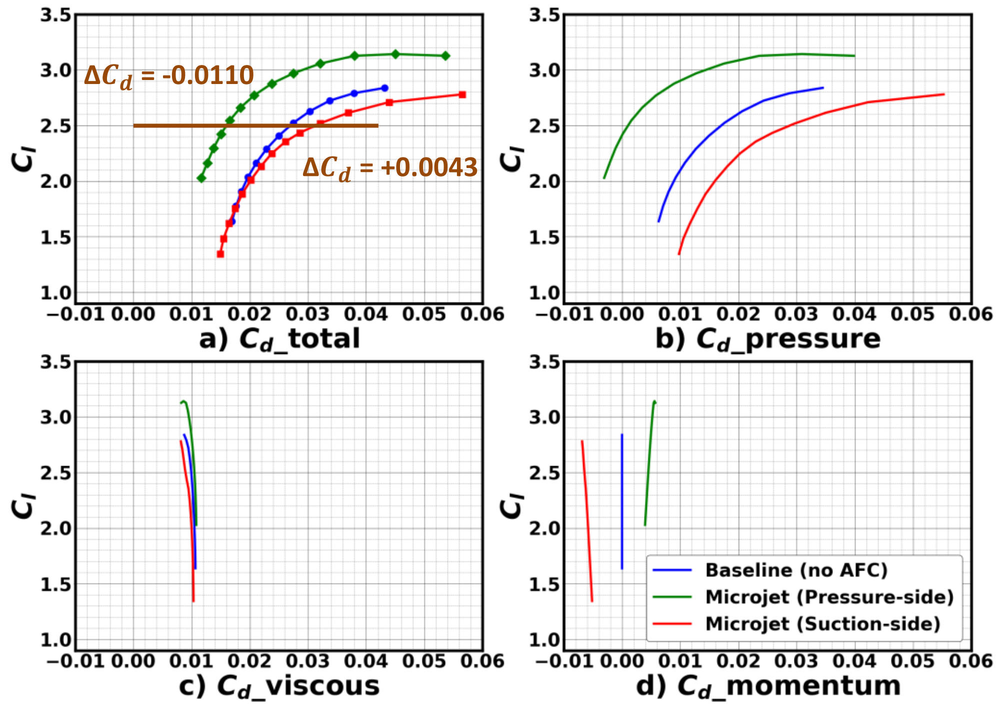

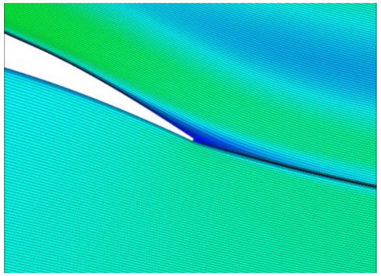

Baseline

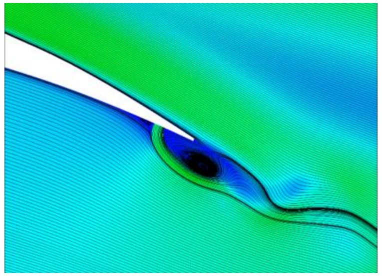

Pressure side microjet

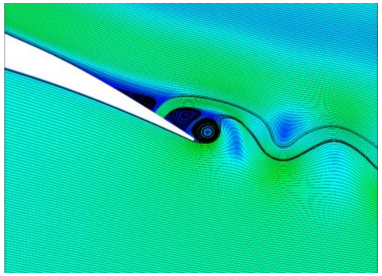

Suction side microjet

Microjet at 95% flap chord with a fixed width of 0.005 refence chord

Computational Studies

- Summary of the computational setup on baseline multi-element airfoil NLR7301
- 2D investigations on the NLR7301 flaps 20˚ and 30˚
- 2.5D (infinite sheared wing) the NLR7301 flap 30˚
- CRM-HL in landing configuration

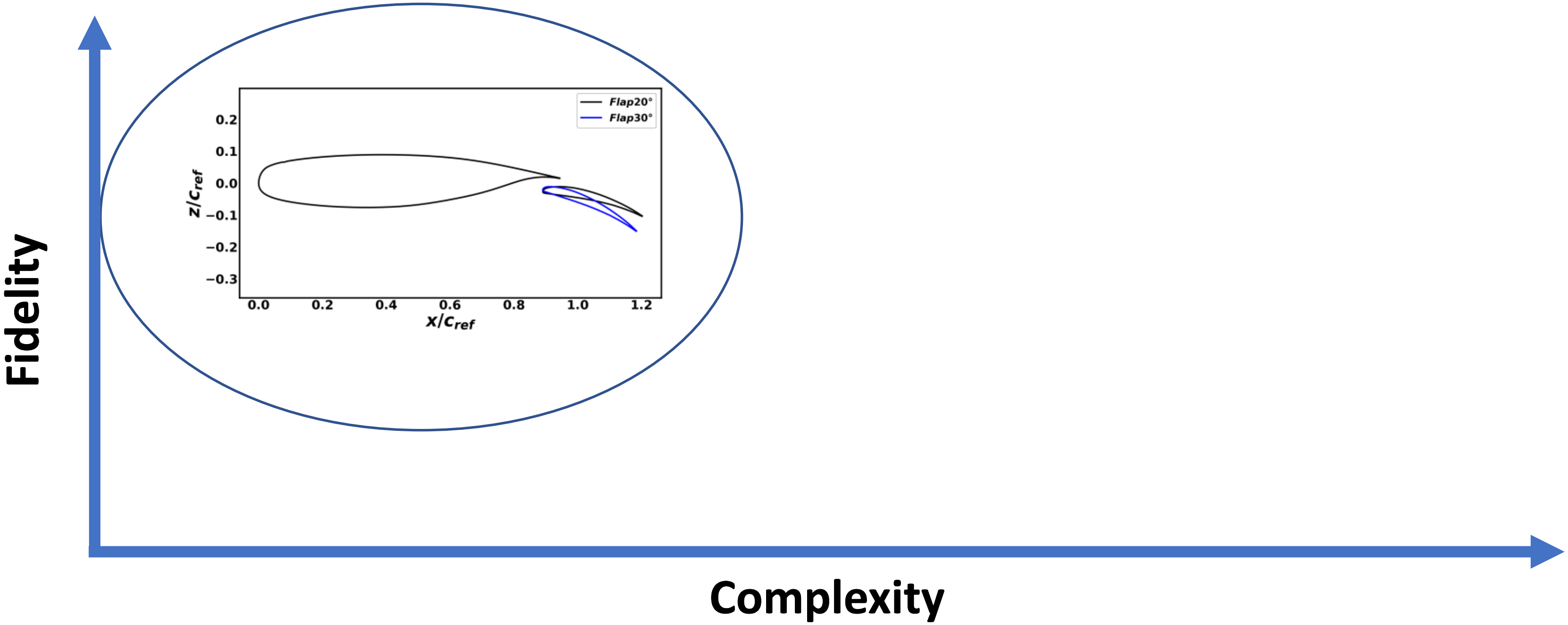

2D Investigations on the NLR7301 Flaps 20˚ and 30˚

- Sensitivity of microjet aerodynamic effectiveness to configuration:
  - Microjet chordwise location
  - Microjet width
  - Preliminary air supply analysis
  - Microjet transpiration velocity profile
  - Microjet modeling: plenums
  - Preliminary analysis of power requirements

Flap 20 Microjet Chordwise Location

α=6°, Re = 2.51E6, Ma = 0.185, $h_j = 0.005c_{ref}$, $C\mu$ = 0.01

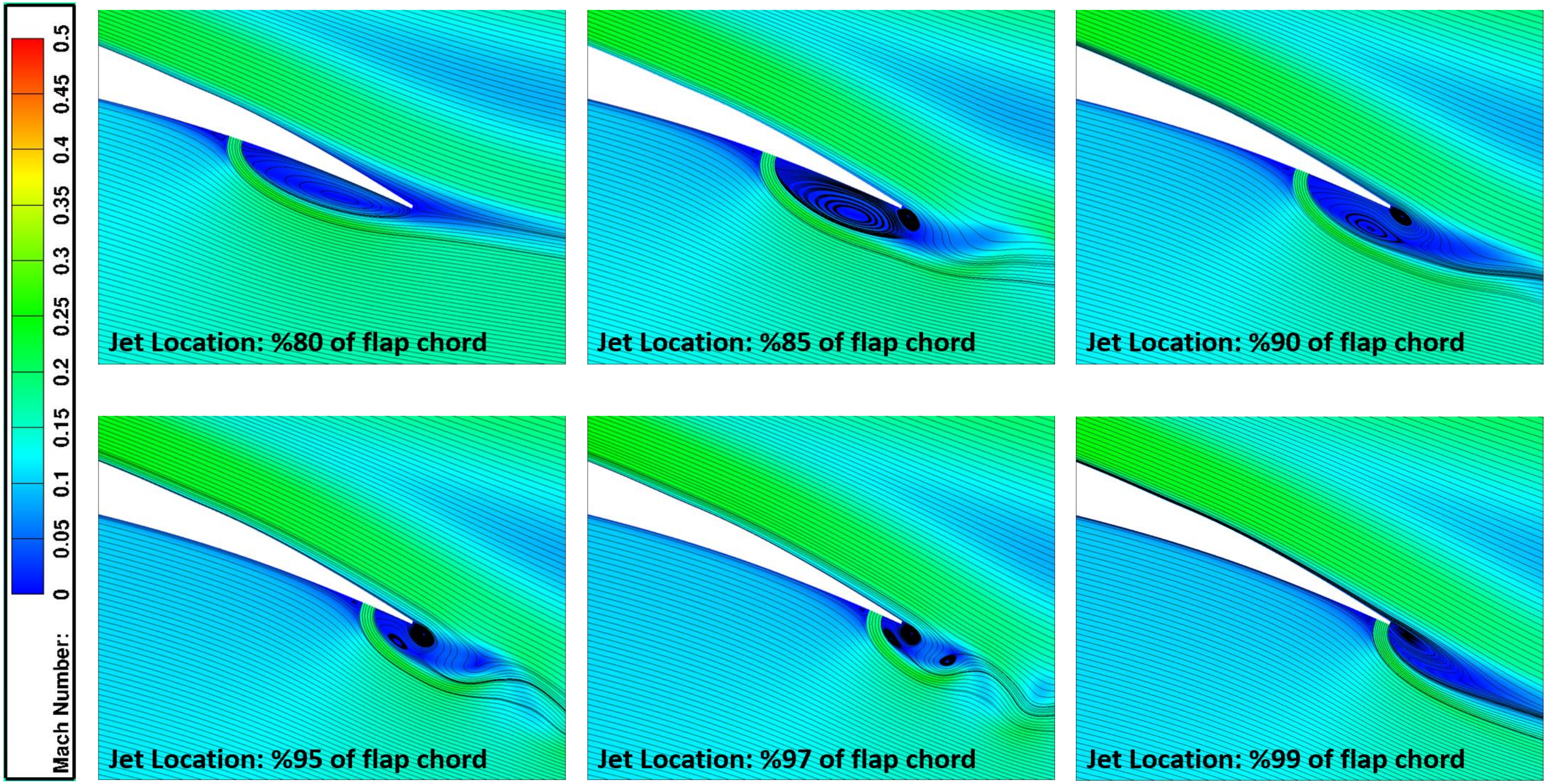

Flap 20 Microjet Chordwise Location

α=6°, Re = 2.51E6, Ma = 0.185, $C\mu$ = 0.01

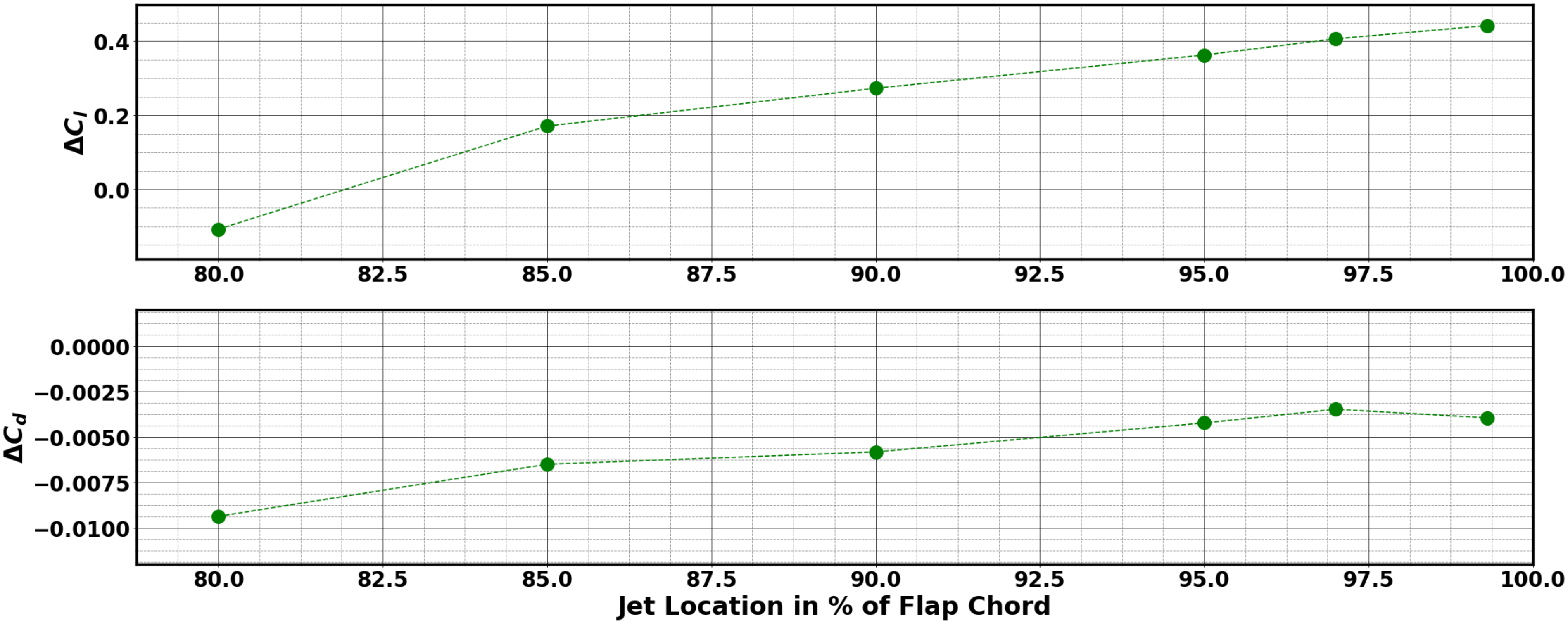

- Microjet lift enhancement increases as it gets closer to the trailing edge
- Microjet Drag reduction benefit decreases as it gets closer to the trailing edge

Flap 20 Microjet/Microtab Chordwise Location

2D

α=6°, Re = 2.51E6, Ma = 0.185

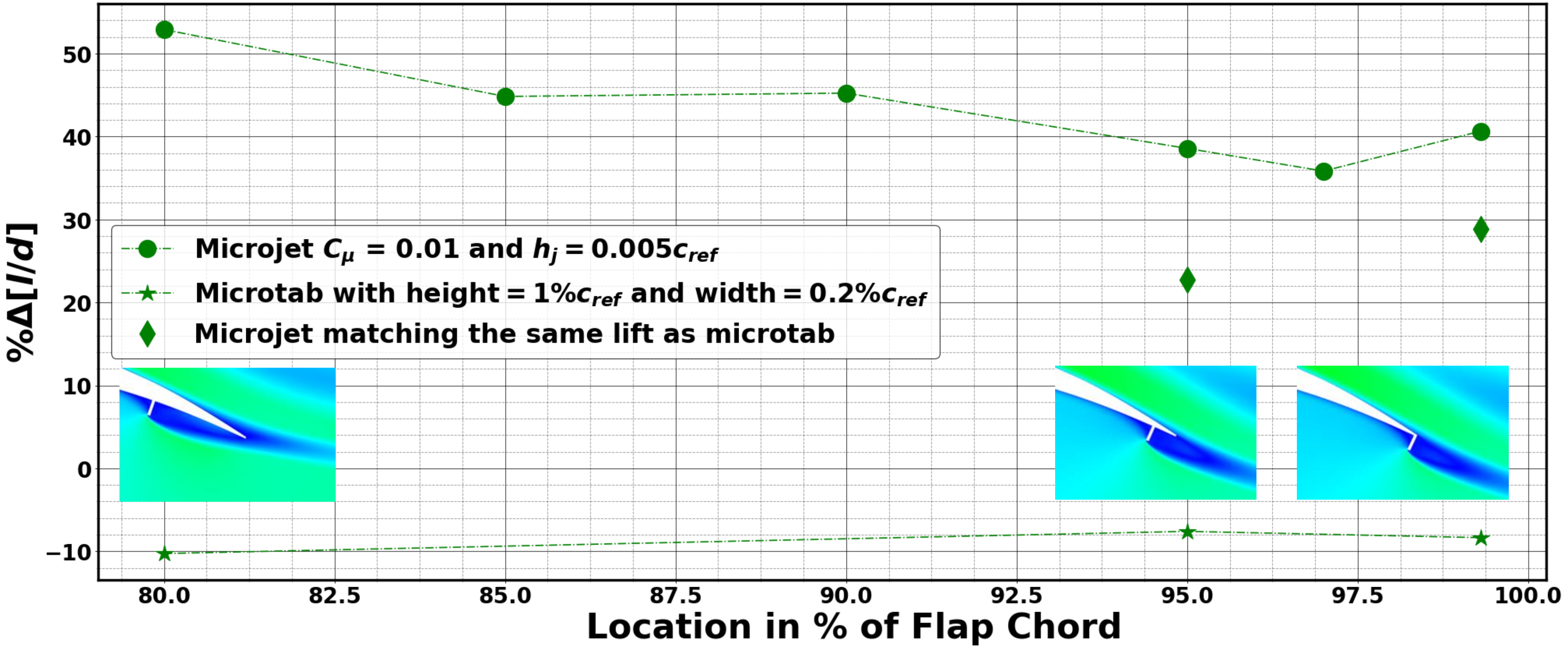

$Height_{microtab}$= 1%c_{ref}, $Thickness_{microtab}$= 0.2%c_{ref}

2D Investigations on the NLR7301 Flaps 20˚ and 30˚

- Sensitivity of microjet aerodynamic effectiveness to configuration:
  - Microjet chordwise location
  - Microjet width
  - Preliminary air supply analysis
  - Microjet transpiration velocity profile
  - Microjet modeling: plenums
  - Preliminary analysis of power requirements

Microjet Width Sensitivity Study

α=6°, Re = 2.51E6, Ma = 0.185, $C\mu$ = 0.01

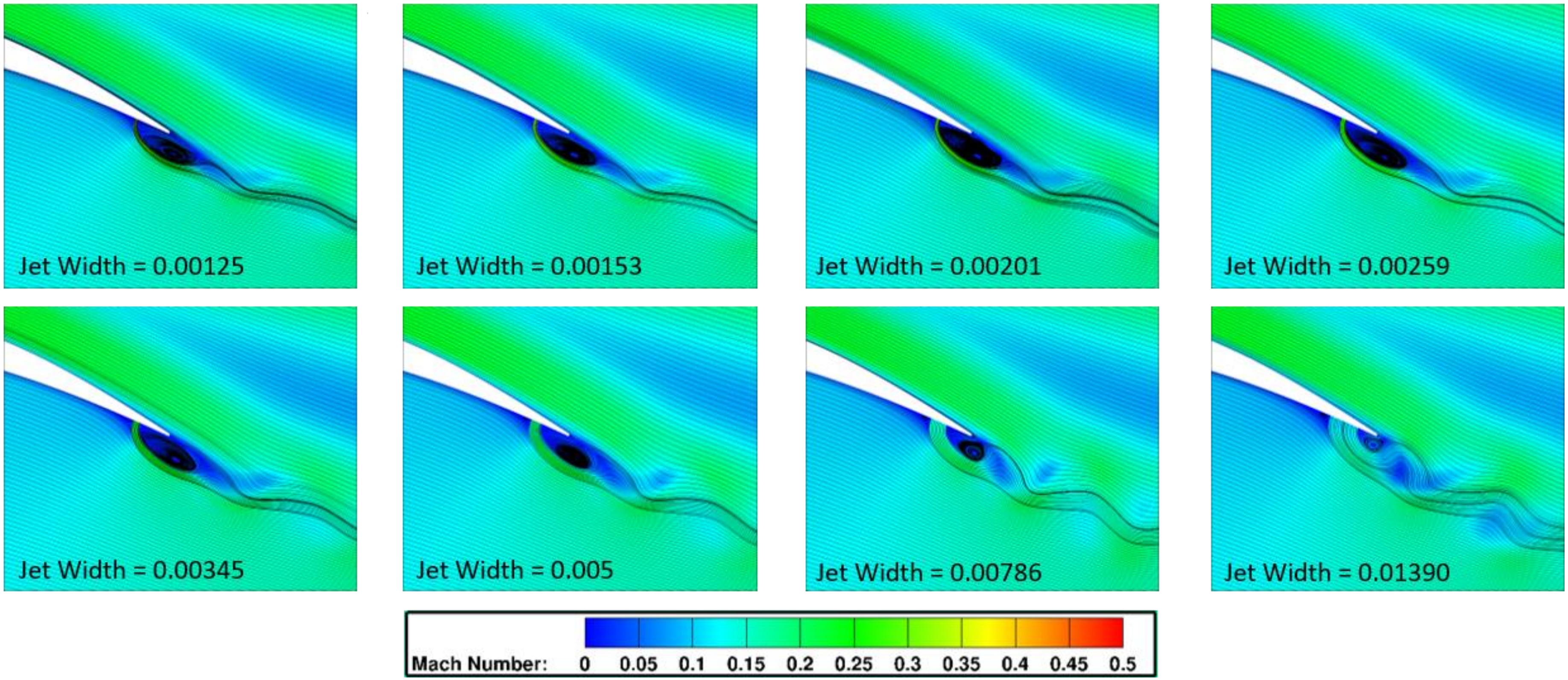

All the microjets are centered at 95% c_{flap} and all the widths are in % c_{ref}

Microjet Width Sensitivity Study

α=6°, Re = 2.51E6, Ma = 0.185, $C\mu$ = 0.01

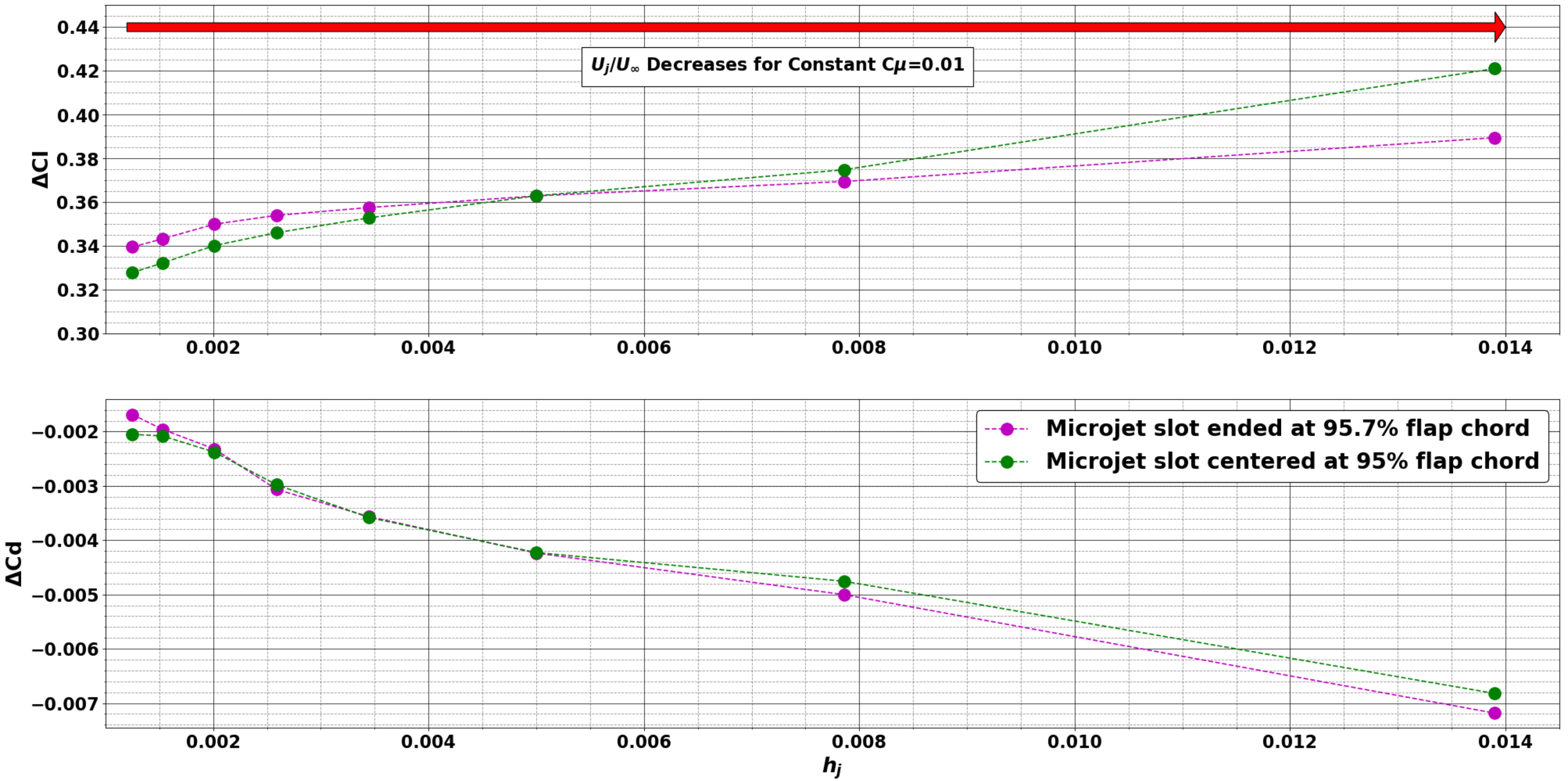

Flap 20 Microjet Width Sensitivity Study

2D

α=6°, Re = 2.51E6, Ma = 0.185, $C\mu$ = 0.01

Microjet is centered at 95% of the flap

Mass flow coefficient: $Cq = \dfrac{\dot{m}_j}{\rho_\infty U_\infty S_{ref}}$ $\Rightarrow$ $C_q = \dfrac{C_\mu}{2\dfrac{U_j}{U_\infty}}$

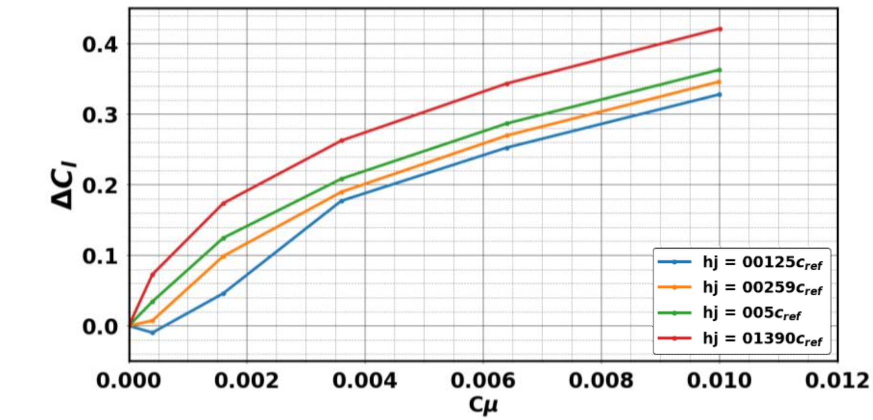

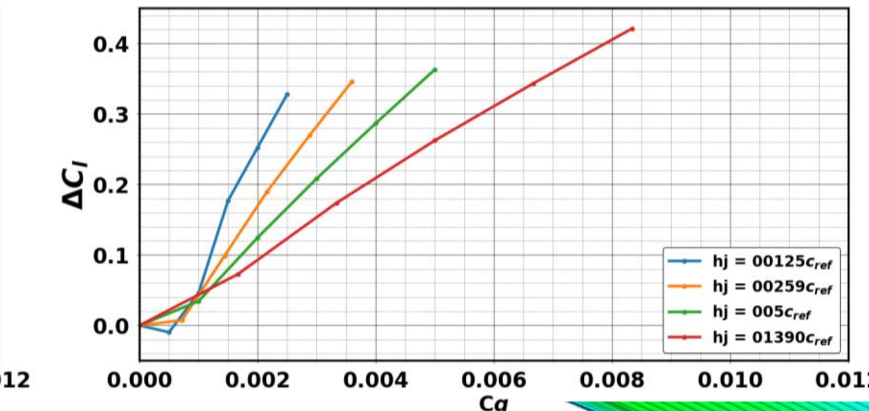

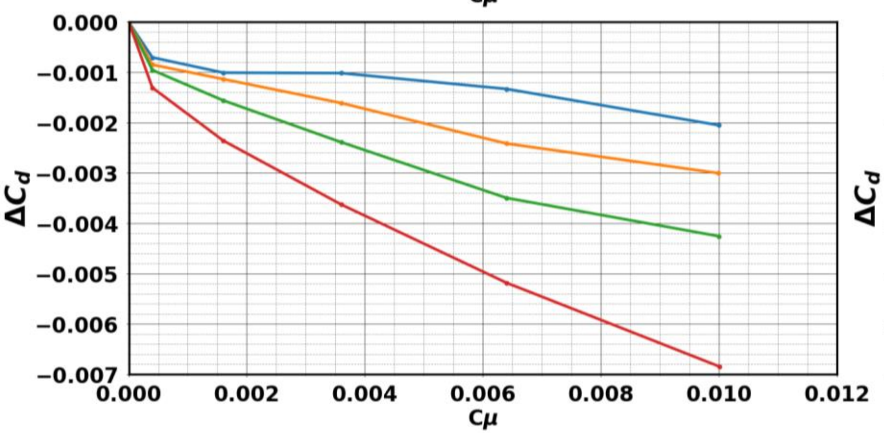

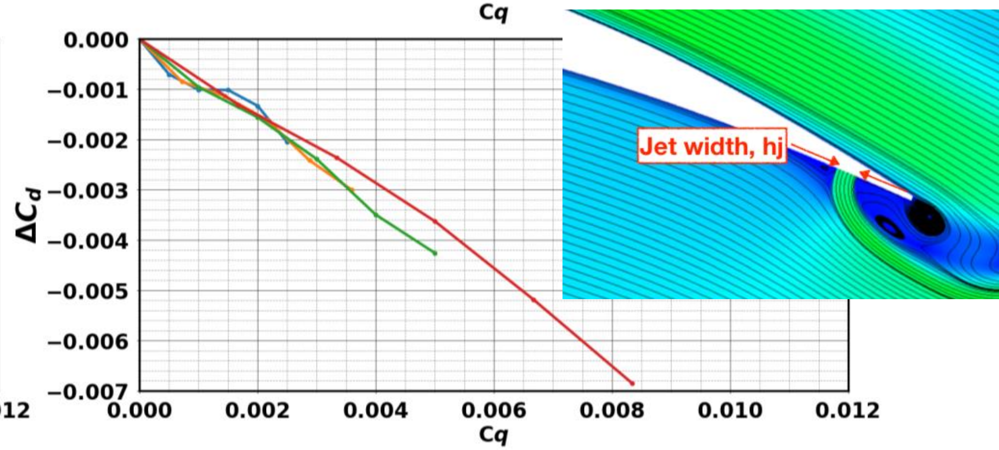

2D Investigations on the NLR7301 Flaps 20˚ and 30˚

- Sensitivity of microjet aerodynamic effectiveness to configuration:
  - Microjet chordwise location
  - Microjet width
  - Preliminary air supply analysis
  - Microjet transpiration velocity profile
  - Microjet modeling: plenums
  - Preliminary analysis of power requirements

Preliminary System Analysis: Air Supply

$$\dot{m} = 2\rho_\infty U_\infty \int_{\text{inboard flap root}}^{\text{outboard flap tip}} C_q c dy$$

$$\dot{m} = \frac{1}{2} C_\mu \left(\frac{U_\infty}{U_j}\right) \rho_\infty U_\infty c_{MAC} w_j$$

Reference chord:	c_{ref}	7	m
Airspeed:	U_∞	133	knots
Jet spanwise extent:	w_j	38	m

Initial Microjet Configuration

$\frac{h_j}{c_{ref}} = 0.005$

$\frac{U_j}{U_\infty} = 1.0$

$C_\mu = 0.01$

$\Delta C_l = 0.36$

111 kg/s

Reduce C_μ

$\frac{h_j}{c_{ref}} = 0.005$

$\frac{U_j}{U_\infty} = 0.6$

$C_\mu = 0.004$

$\Delta C_l = 0.23$

74 kg/s

Reduce h_j

$\frac{h_j}{c_{ref}} = 0.00125$

$\frac{U_j}{U_\infty} = 2.2$

$C_\mu = 0.012$

$\Delta C_l = 0.36$

61 kg/s

Further reductions?

- *Spanwise spacing*
- *Pulsed blowing*

Combine & optimize

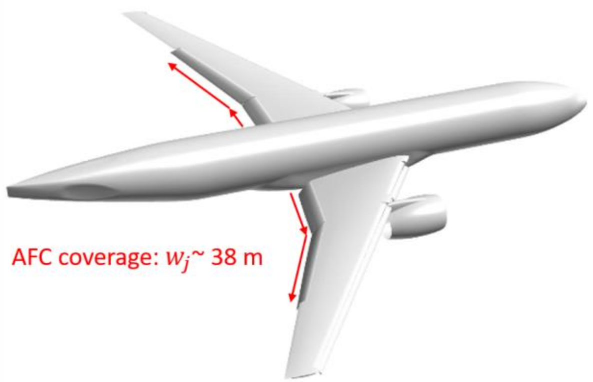

2D Investigations on the NLR7301 Flaps 20˚ and 30˚

- Sensitivity of microjet aerodynamic effectiveness to configuration:
  - Microjet chordwise location
  - Microjet width
  - Preliminary air supply analysis
  - Microjet transpiration velocity profile
  - Microjet modeling: plenums
  - Preliminary analysis of power requirements

Microjet Transpiration Velocity Profile Sensitivity

α=6°, Re = 2.51E6, Ma = 0.185, $C\mu$ = 0.01

	C_l	C_d
Baseline (no AFC)	2.408	0.02499
uniform BC, $C\mu$ = 0.01	2.223	0.02571
BC based on turbulent velocity profile, $C\mu$ = 0.01	2.640	0.02965
BC based on laminar velocity profile, $C\mu$ = 0.01	2.720	0.03080

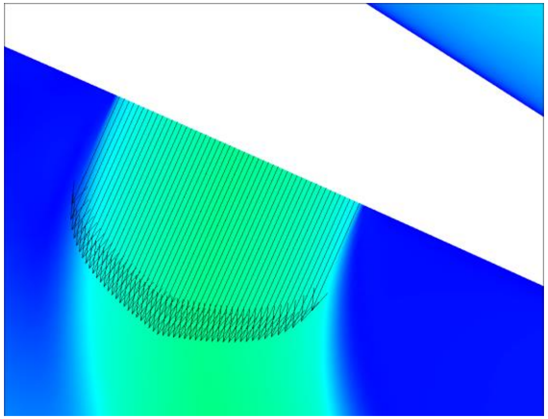

$$U = U_{max}[1 - \frac{r}{R}]^{1/n}$$

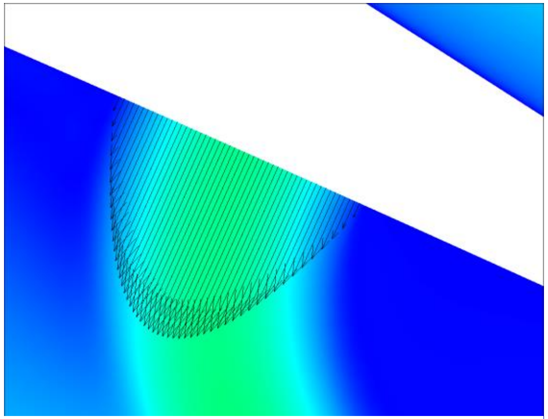

$$U = U_{max}\ [1-(\frac{r}{R})^2]$$

Lift coefficient is effected by less than 0.5% and drag coefficient by less than 4 counts. Using uniform BC is sufficient.

2D Investigations on the NLR7301 Flaps 20˚ and 30˚

- Sensitivity of microjet aerodynamic effectiveness to configuration:
  - Microjet chordwise location
  - Microjet width
  - Preliminary air supply analysis
  - Microjet transpiration velocity profile
  - Microjet modeling: plenums
  - Preliminary analysis of power requirements

Flap 20 Microjet Modeling: Plenum

2D

α=6°, Re = 2.51E6, Ma = 0.185, $C\mu$ = 0.01

Plenum A: $h_j = 0.005c_{ref}$

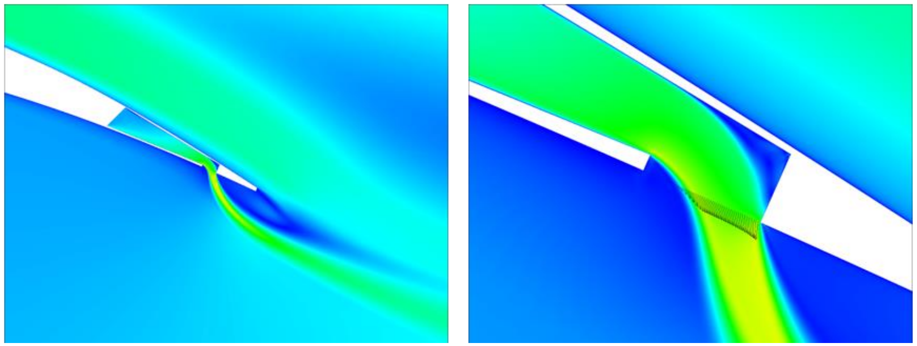

Plenum B: $h_j = 0.005c_{ref}$

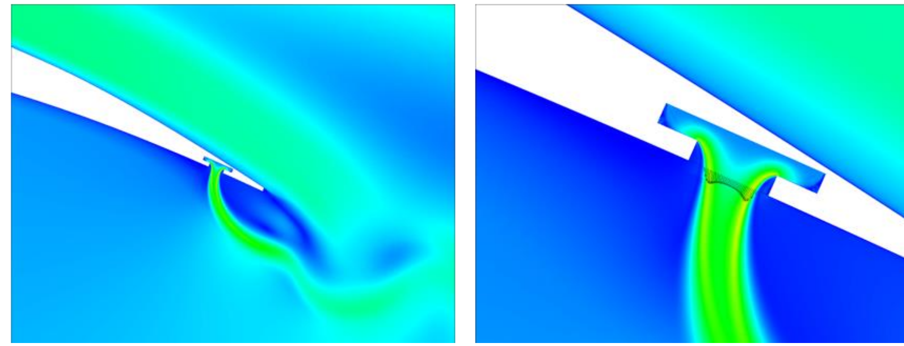

Plenum C: $h_j = 0.005c_{ref}$

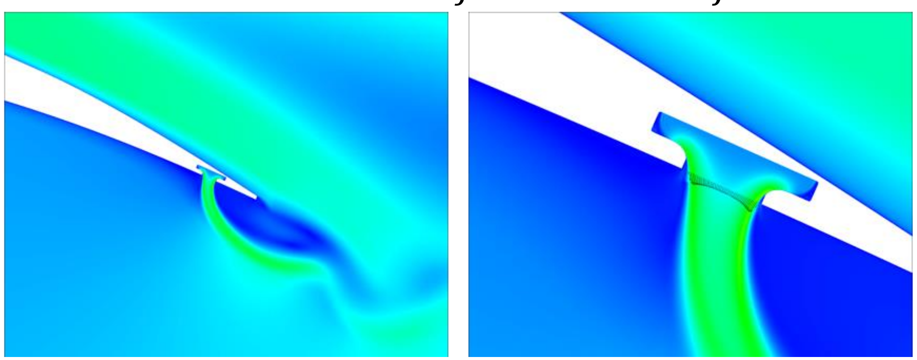

Plenum D: $h_j = 0.00125c_{ref}$

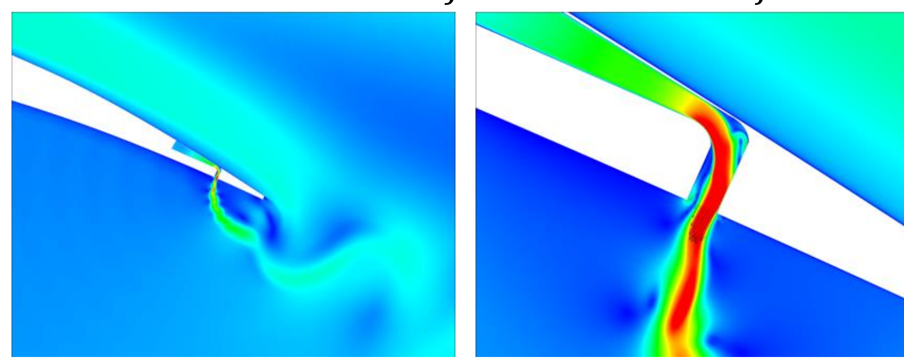

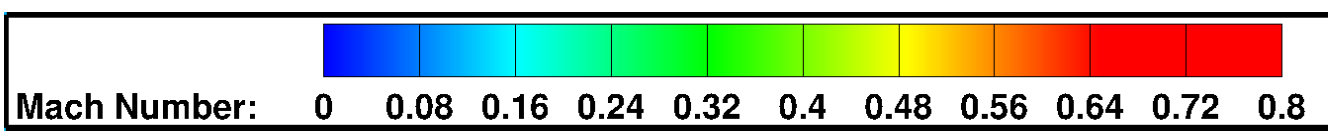

Flap 20 Microjet Modeling: Plenum

2D

α=6°, Re = 2.51E6, Ma = 0.185, $C\mu$ = 0.01

Plenum A: $h_j = 0.005c_{ref}$

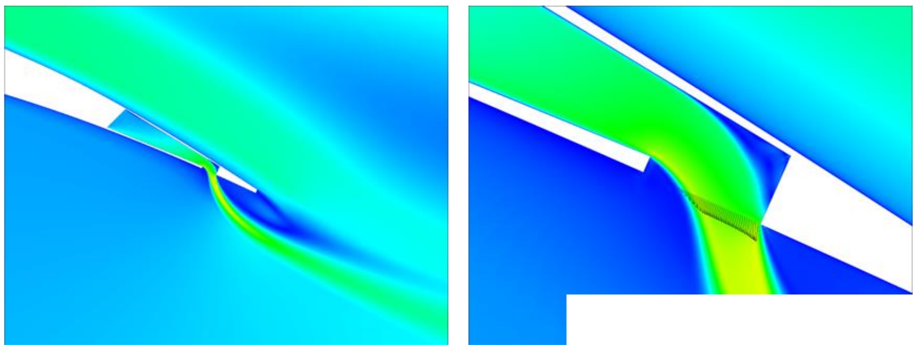

Plenum B: $h_j = 0.005c_{ref}$

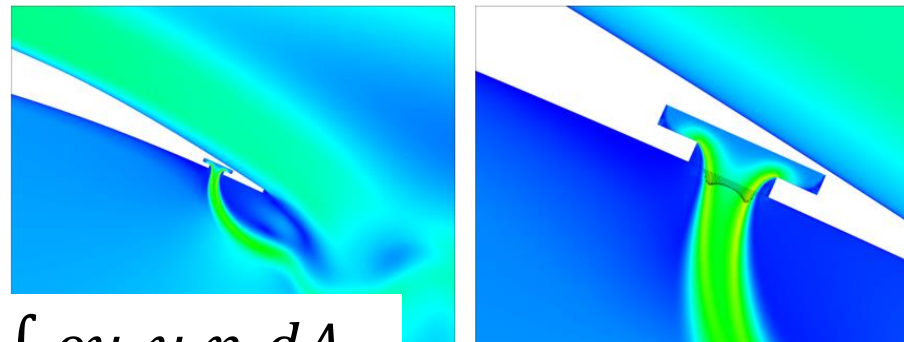

$$C_{\mu_{effective}} = \frac{\int \rho u_j u_i n_j dA}{\frac{1}{2}\rho_\infty U_\infty^2 A_{ref}}$$

Plenum C: $h_j = 0$

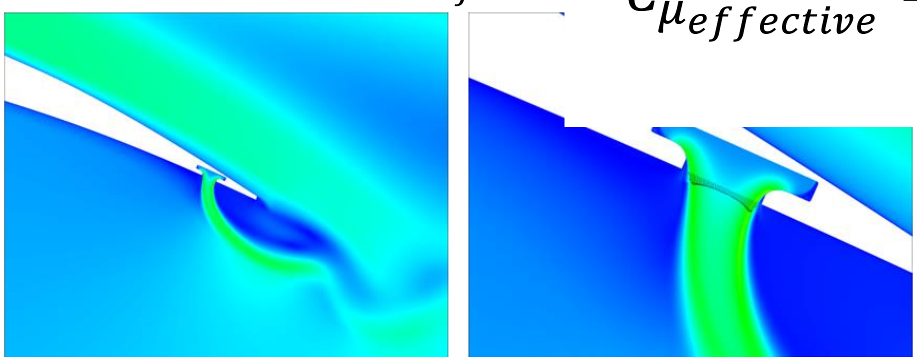

: $h_j = 0.00125c_{ref}$

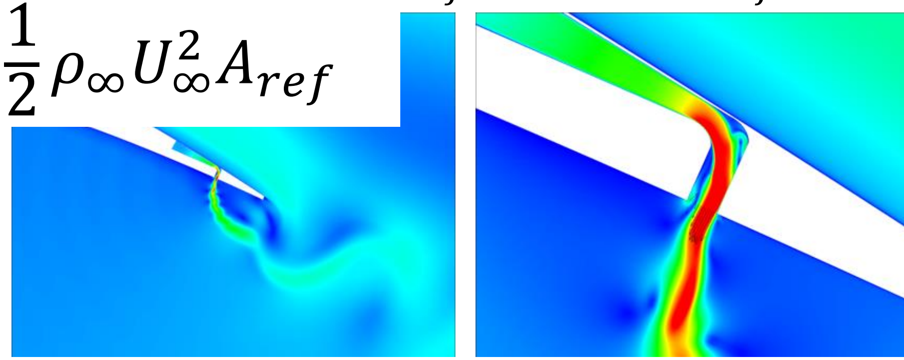

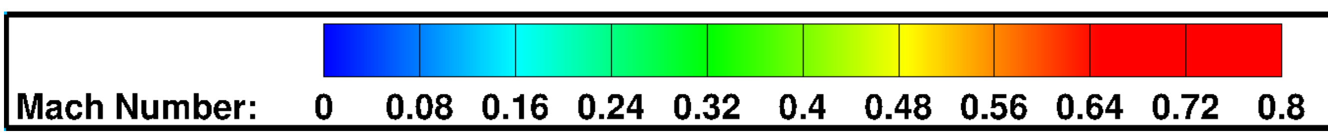

Equivalent Drag

α=6°, Re = 2.51E6, Ma = 0.185

Control volume analysis:

$$D_{eq.} = D_{Press.} + D_{vis.} + D_{\Delta mom.} + D_{power}$$
$$= D_{Press.} + D_{vis.} + \dot{m}U_\infty - D_{mom} + \frac{Power}{U_\infty}$$
$$= D_{comp} + \dot{m}U_\infty + \frac{\frac{1}{2}\dot{m}U_j^2}{U_\infty}$$

$$\boldsymbol{F} = \int (-P\delta_{ij} + \tau_{ij})\, n_j\, dA + \int \rho u_i u_j\, n_j dA$$

$$D_{comp} = F_x cos\alpha + F_z sin\alpha$$

Non-dimensional:

$$C_{d_{eq}} = C_{d_{comp}} + C_\mu \frac{U_j}{2U_\infty} + C_\mu \frac{U_\infty}{U_j}$$

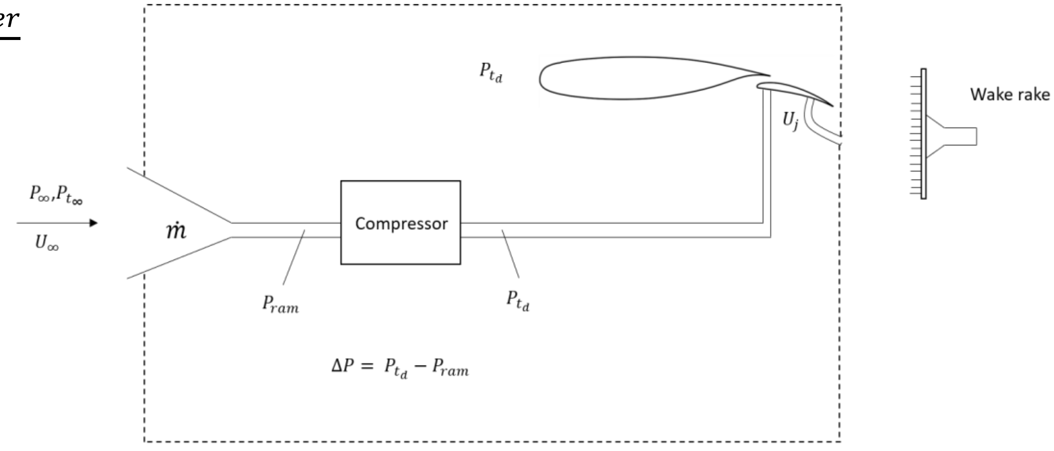

Control volume

Configuration	$\frac{U_j}{U_\infty}$	C_μ	C_l	$C_{d_{comp}}$	$C_{d_{eq}}$	$C_l/C_{d_{comp}}$
Baseline (no jet)	-	-	2.41	0.0250	0.0250	96.4
Initial microjet	1.0	0.010	2.77	0.0206	0.0356	134.5
1% microtab	-	-	2.64	0.0297	0.0297	88.9
Matched microjet	0.6	0.004	2.64	0.0223	0.0302	118.4

Minor vs. Moderate TE Flow Separation

- Flap 30° is set up with the same overlap and gap as flap 20°
  - No experimental data for 30° flap setting

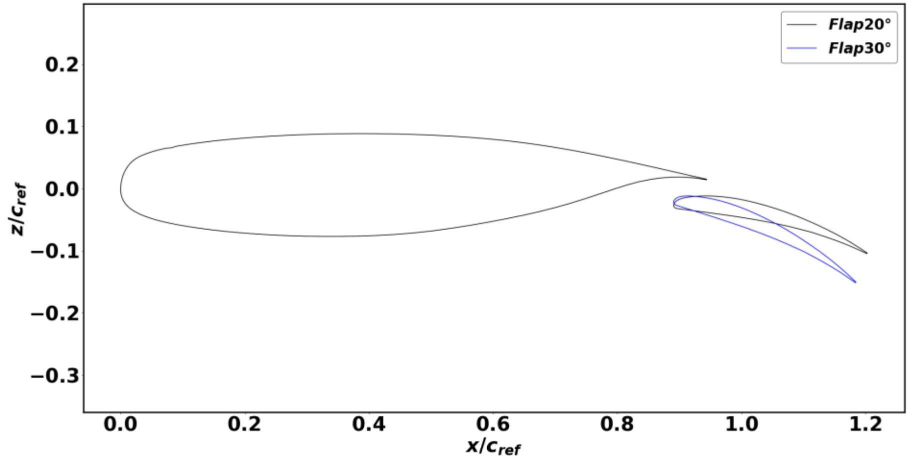

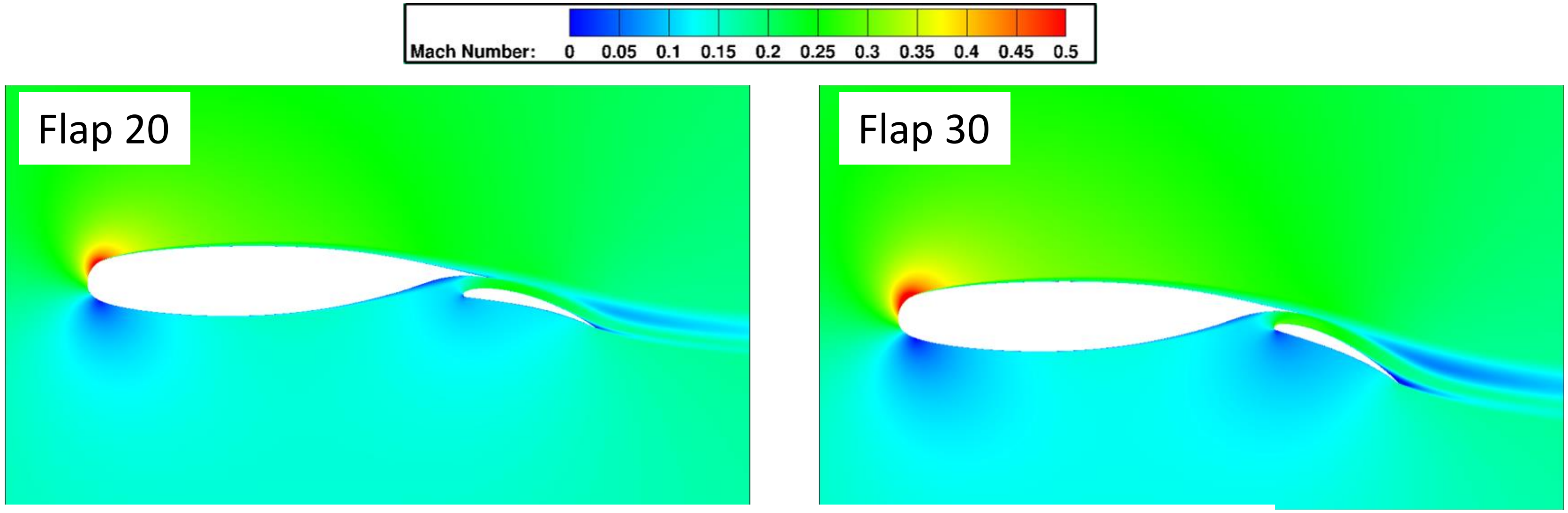

Minor vs. Moderate TE Flow Separation

2D

Re = 2.51E6, Ma = 0.185

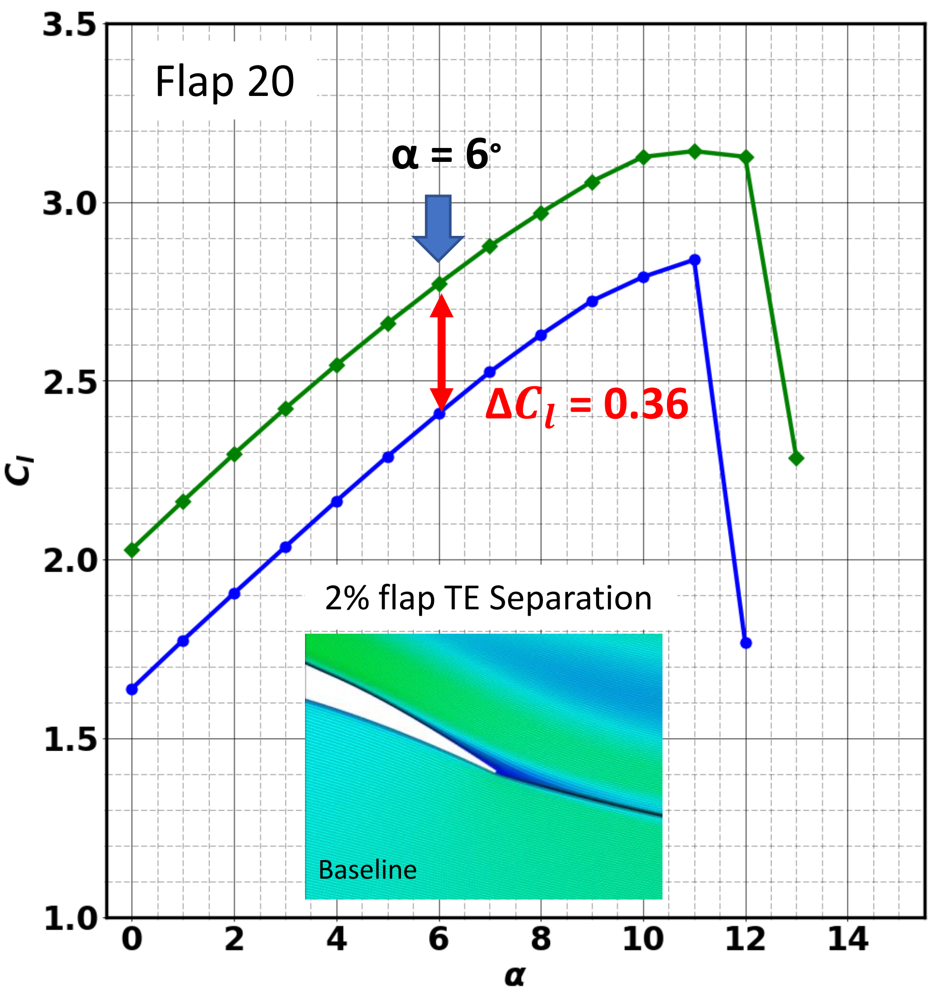

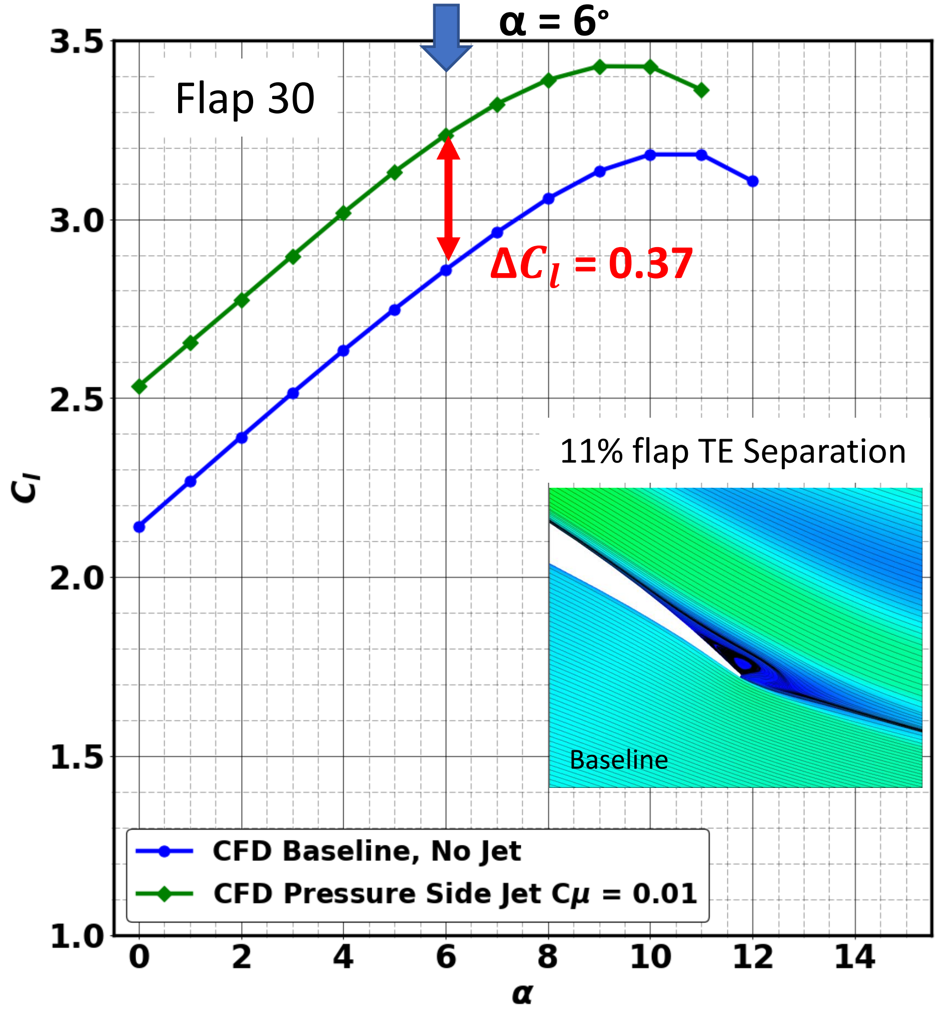

Minor vs. Moderate TE Flow Separation

2D

Re = 2.51E6, Ma = 0.185

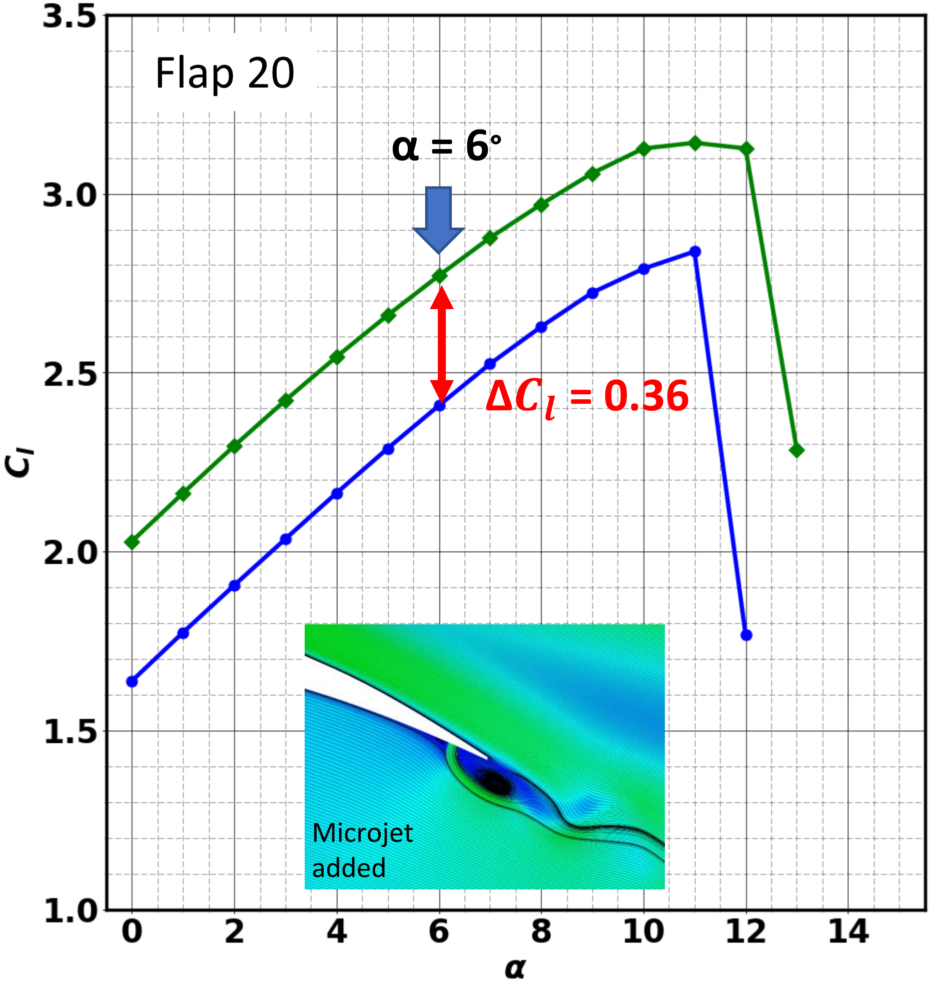

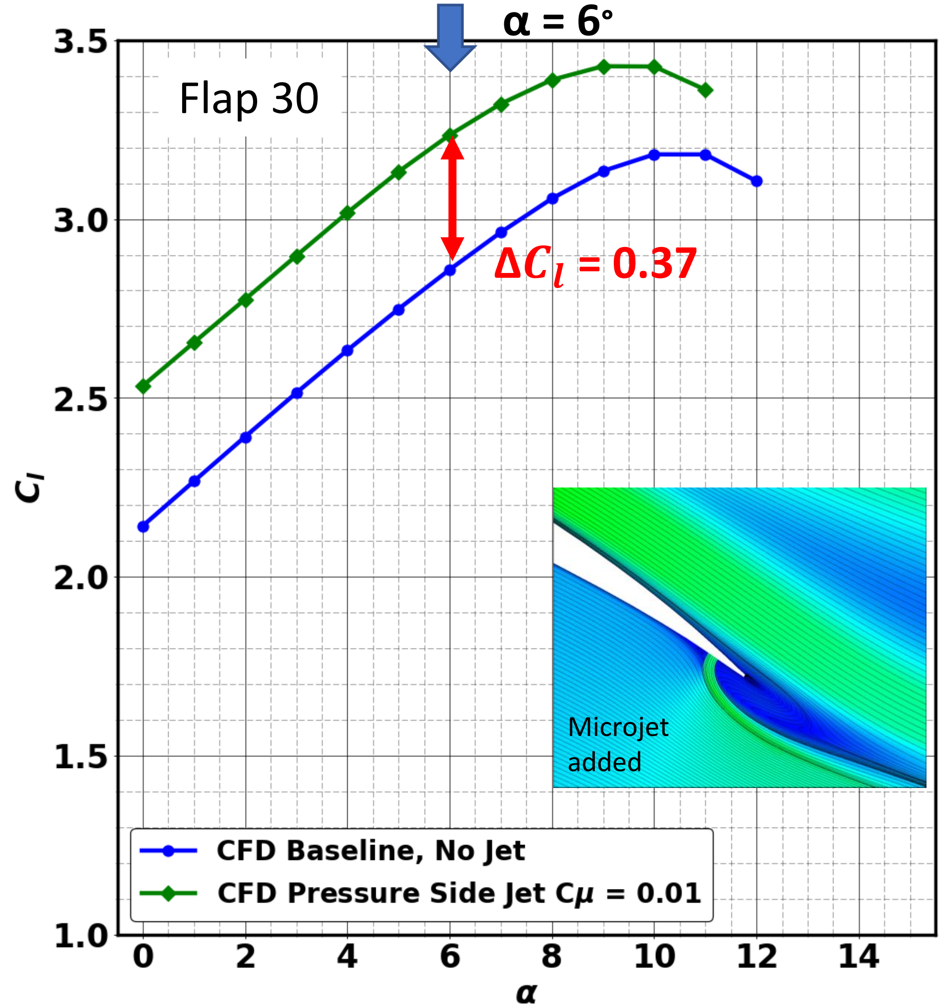

Flap 30 Drag Decomposition

2D

Re = 2.51E6, and Ma = 0.185 , $C\mu$ = 0.01

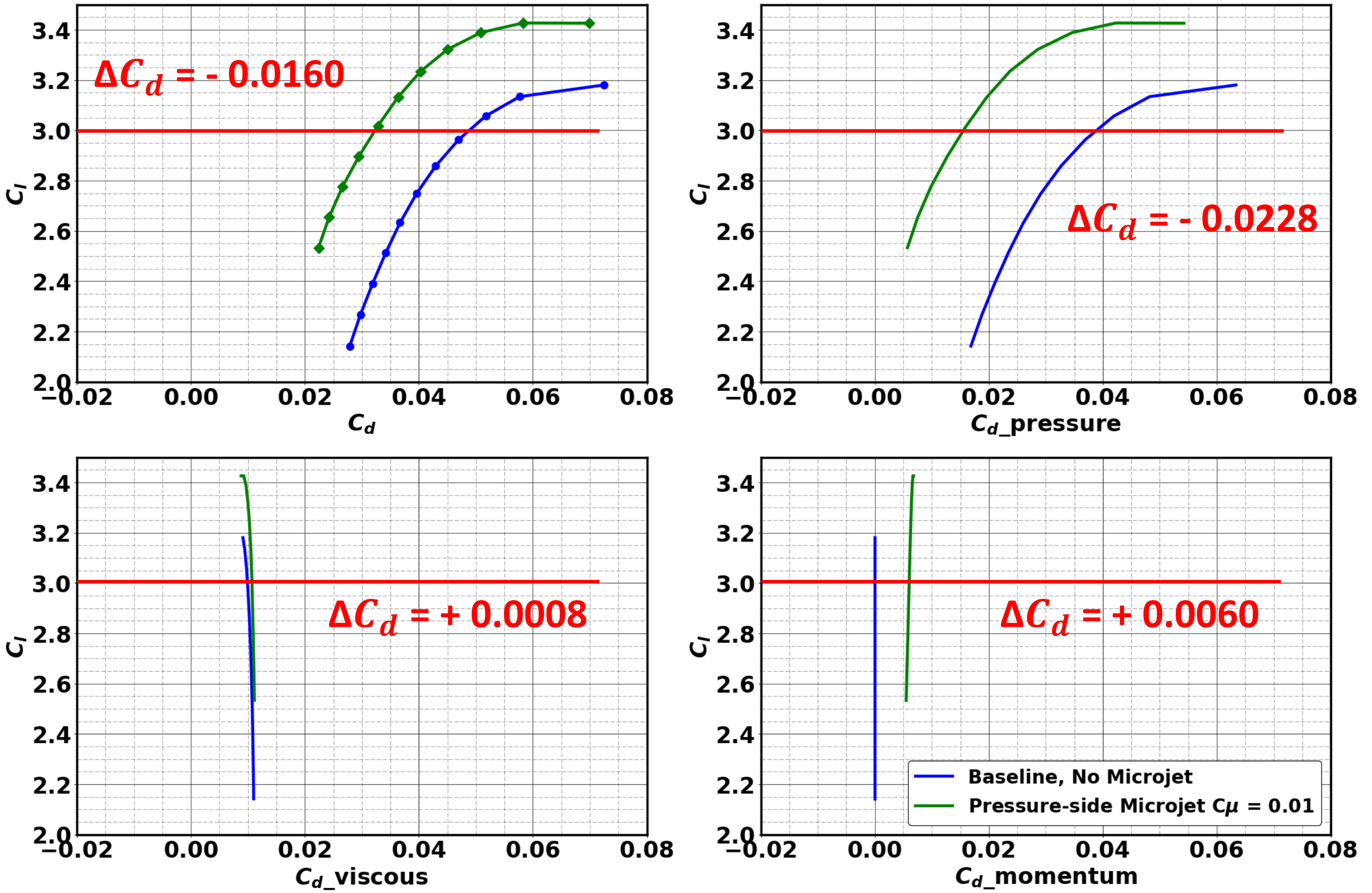

α=6°, Re = 2.51E6, Ma = 0.185

2D

Flap 20

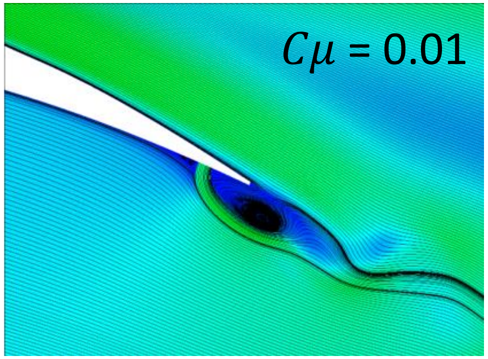

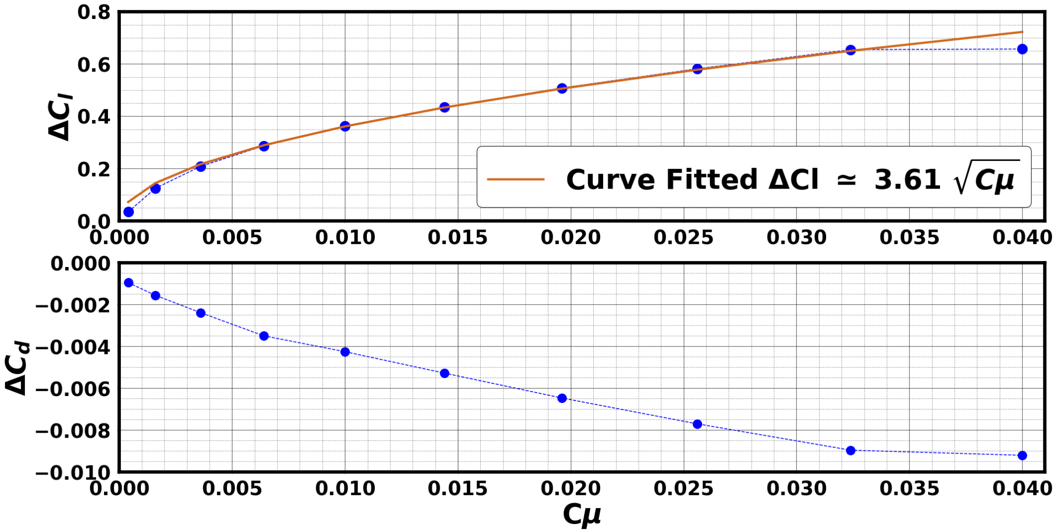

Flap 30

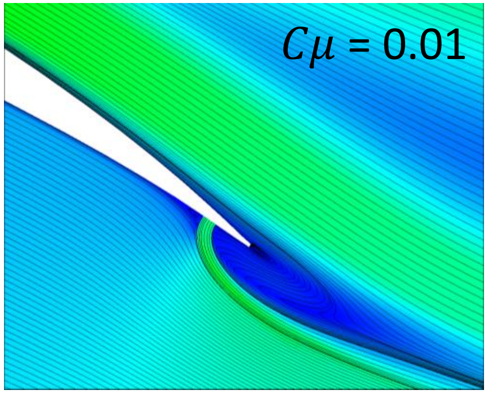

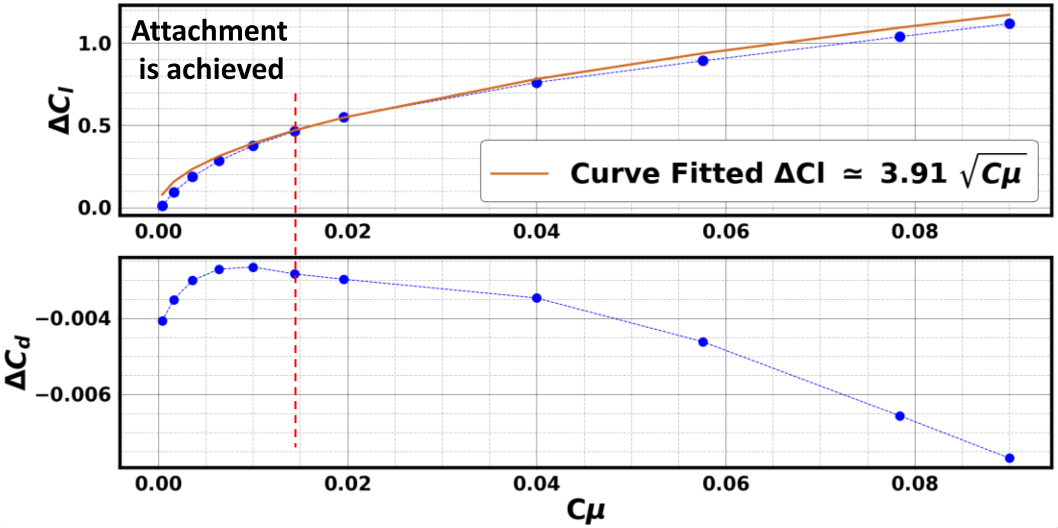

Flap 30, Momentum Coefficient Sensitivity

2D

α=6°, Re = 2.51E6, and Ma = 0.185, Microjet width: $h_j = 0.005c_{ref}$

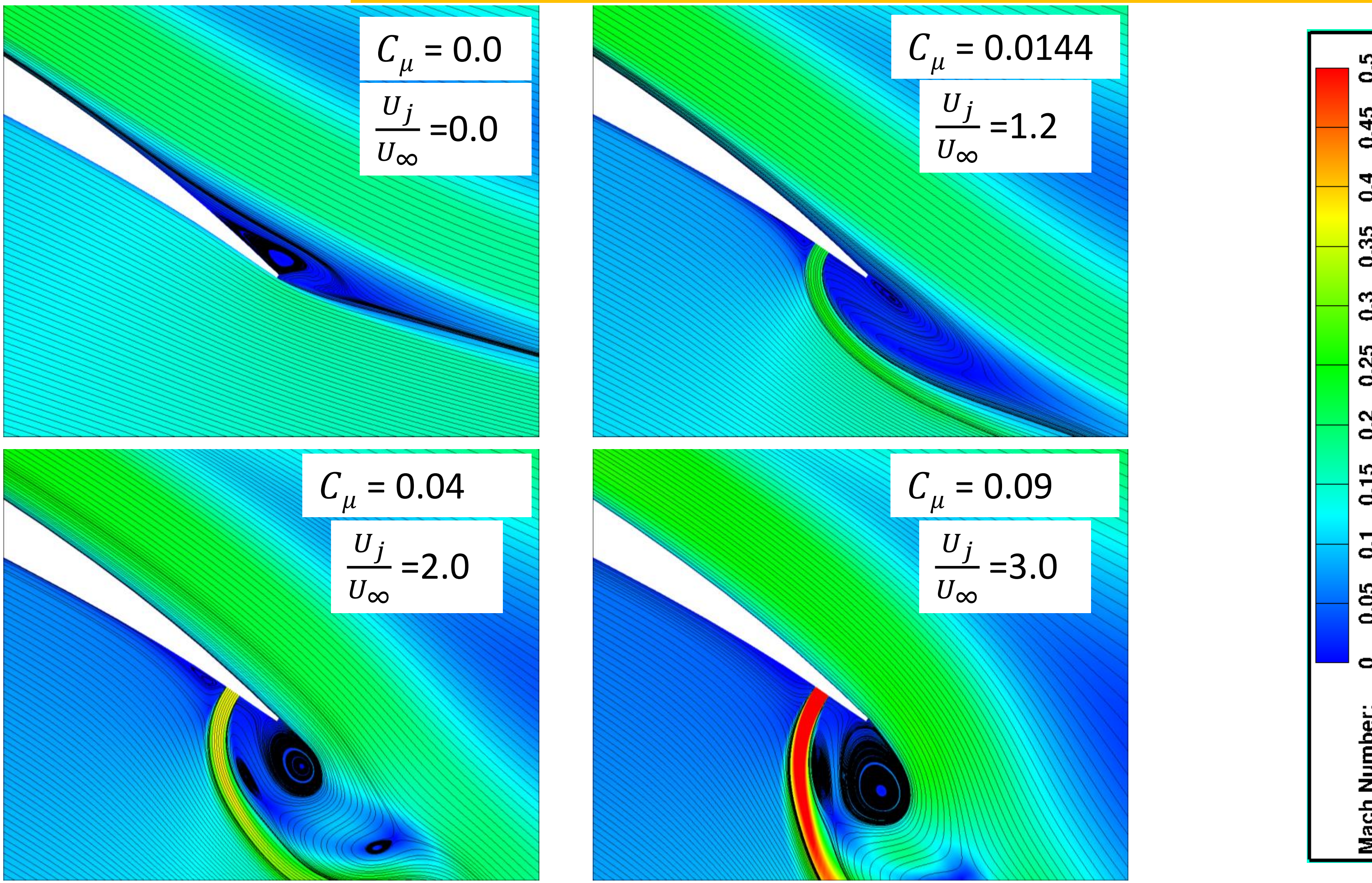

Minor vs. Moderate TE Flow Separation

2D

Re = 2.51E6, and Ma = 0.185

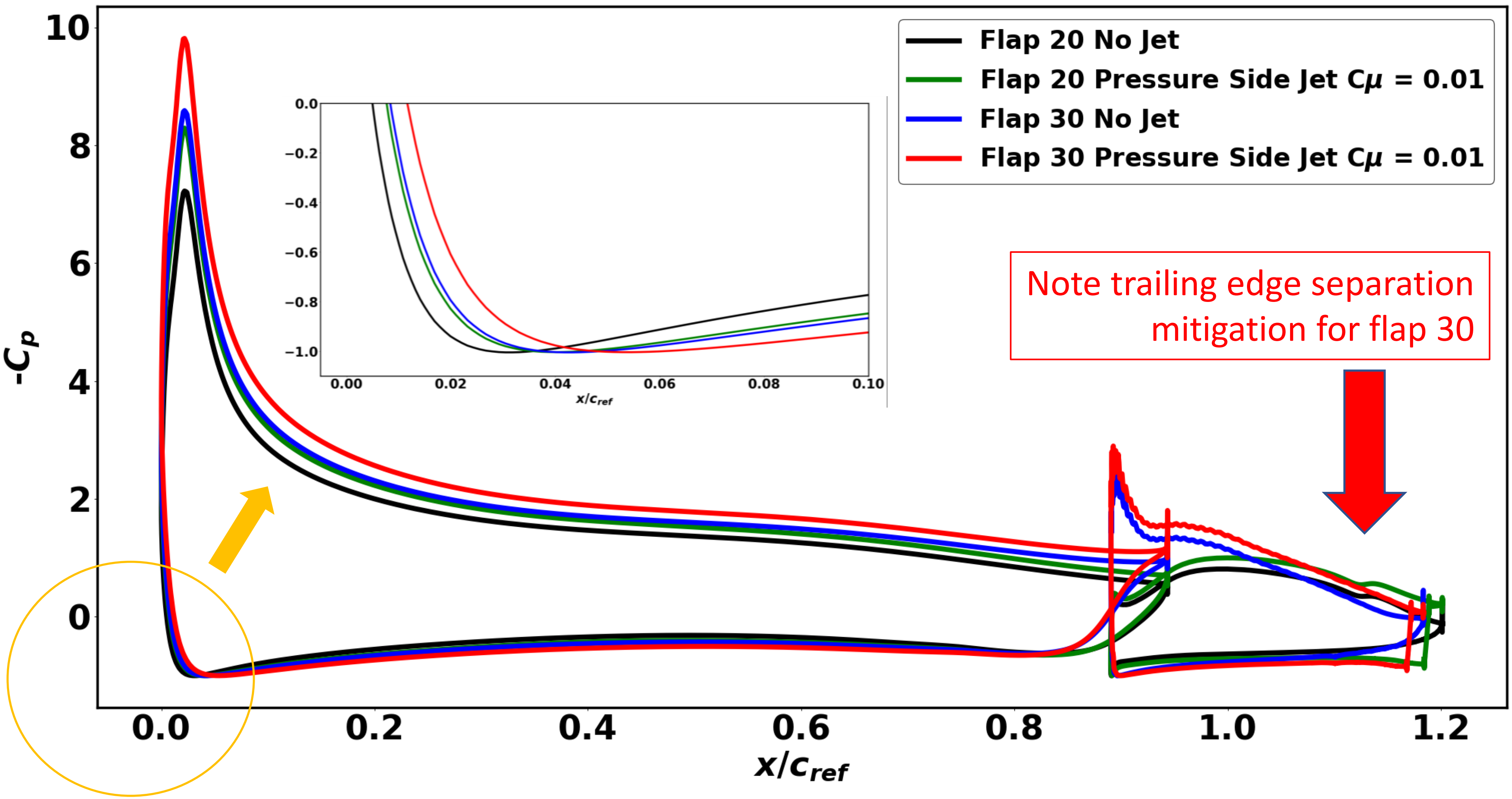

Baseline: Re = 2.51E6, and Ma = 0.185

2D

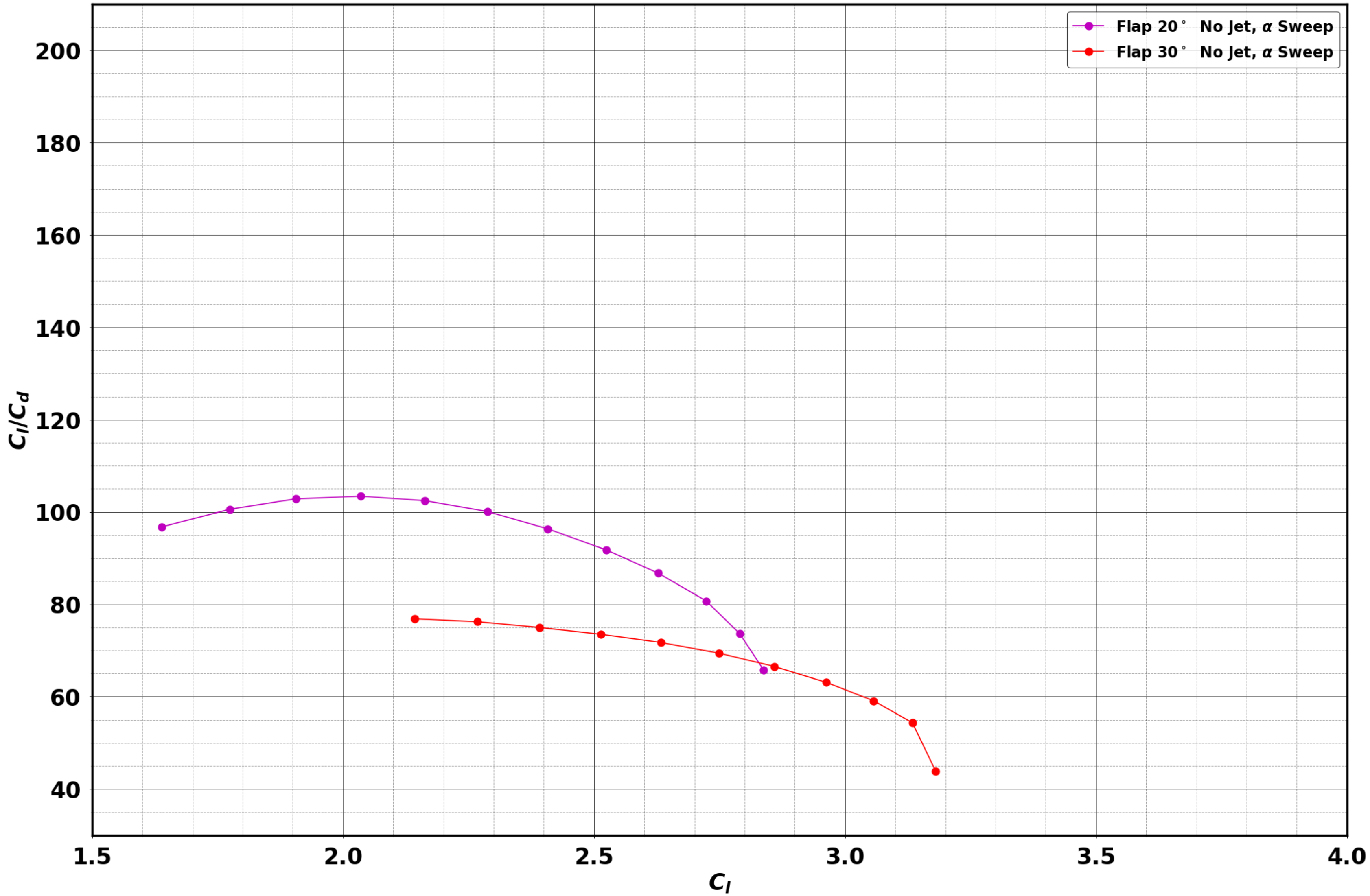

Re = 2.51E6, and Ma = 0.185, Cμ = 0.01, Microjet width: $h_j = 0.005c_{ref}$

2D

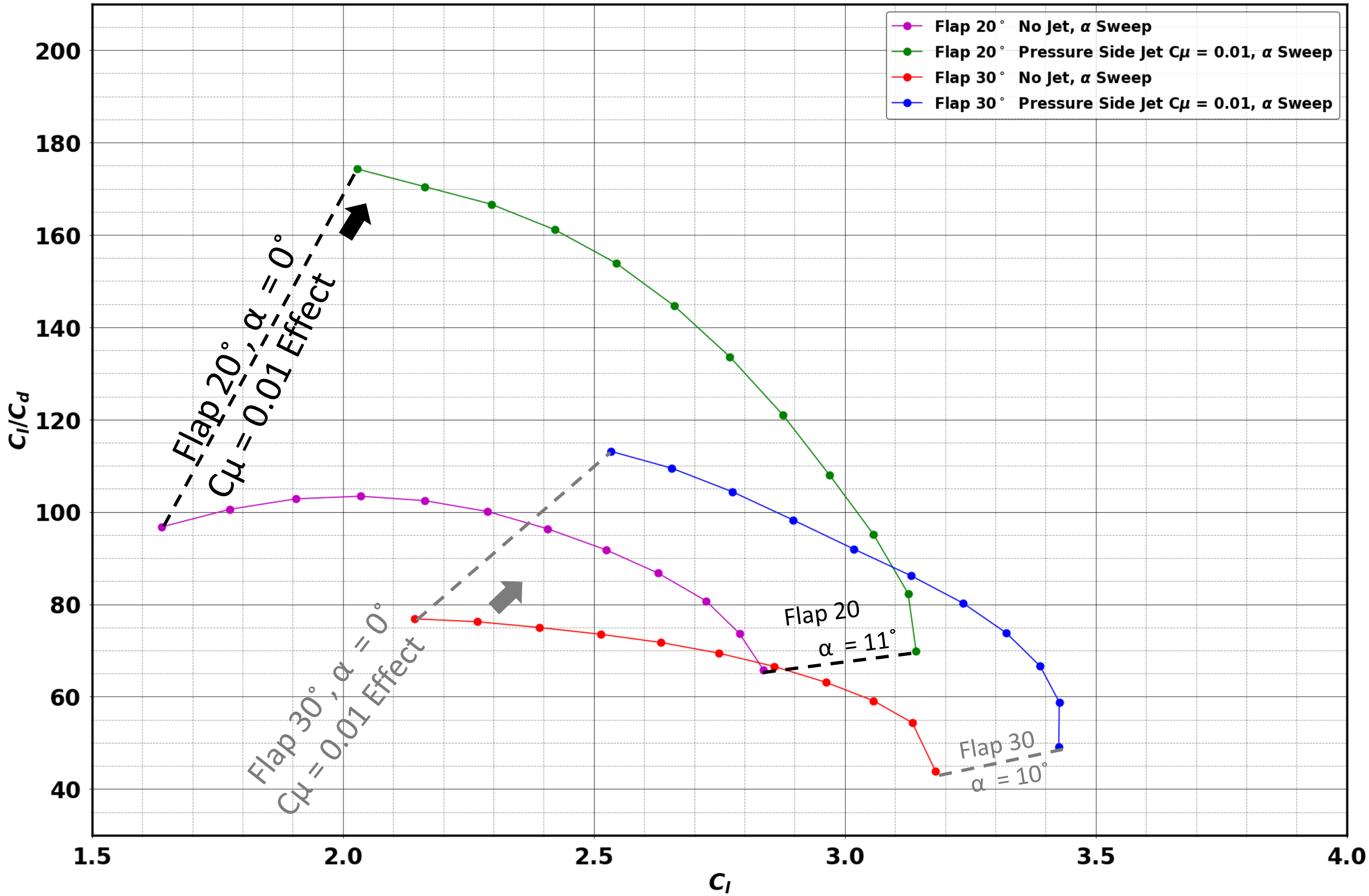

Re = 2.51E6, and Ma = 0.185, Cμ sweep, Microjet width: $h_j = 0.005c_{ref}$

2D

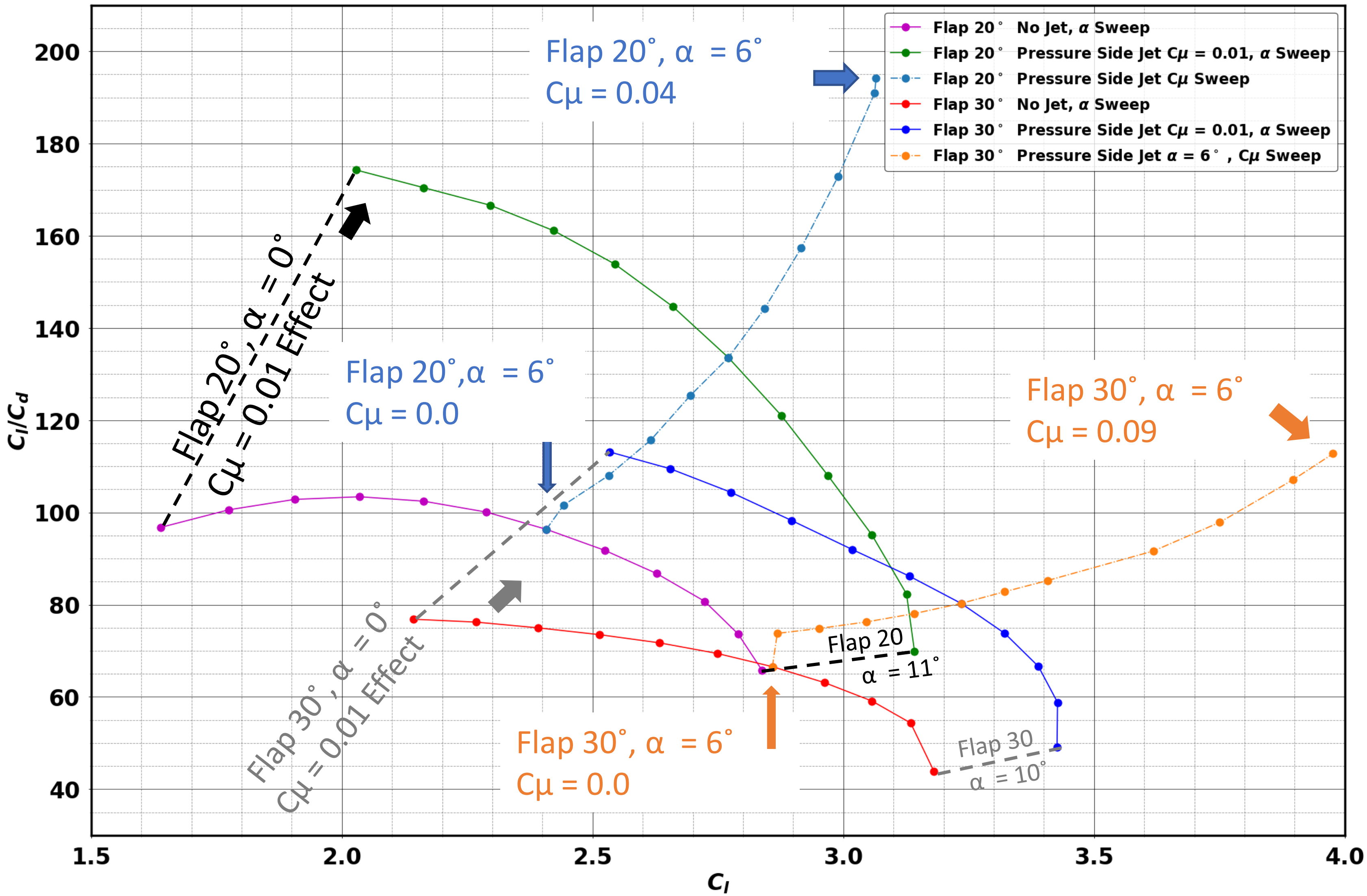

Flap 30°, Steady vs. Pulsed Blowing

2D

α=6°, Re = 2.51E6, and Ma = 0.185, Microjet width: $h_j = 0.005c_{ref}$

Constant Blowing Umax = 1, Umin = 1,

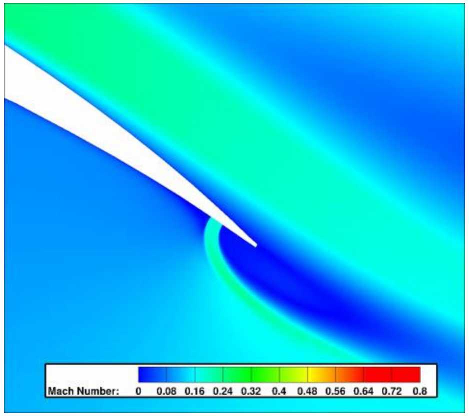

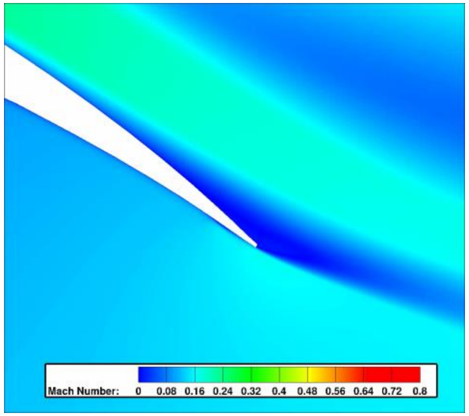

F+ = 0.02, Umax = 1, Umin = 0

$f = 37.3\ [Hz]$

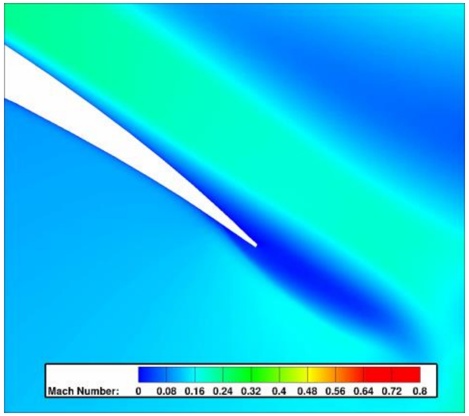

F+ = 0.08, Umax = 1, Umin = 0

$f = 186.5\ [Hz]$

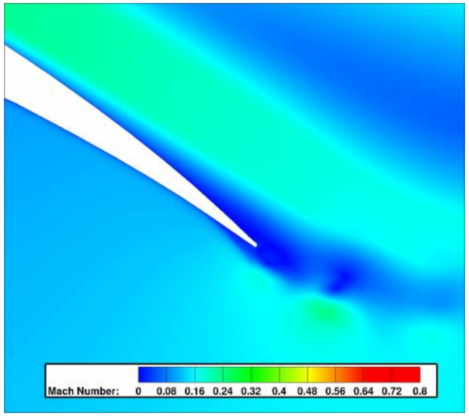

F+ = 0.2, Umax = 1, Umin = 0

$f = 373.0\ [Hz]$

Time is: 0-0.027[s]

Flap 30°, Steady vs. Pulsed Blowing

2D

α=6°, Re = 2.51E6, and Ma = 0.185, Microjet width: $h_j = 0.005c_{ref}$

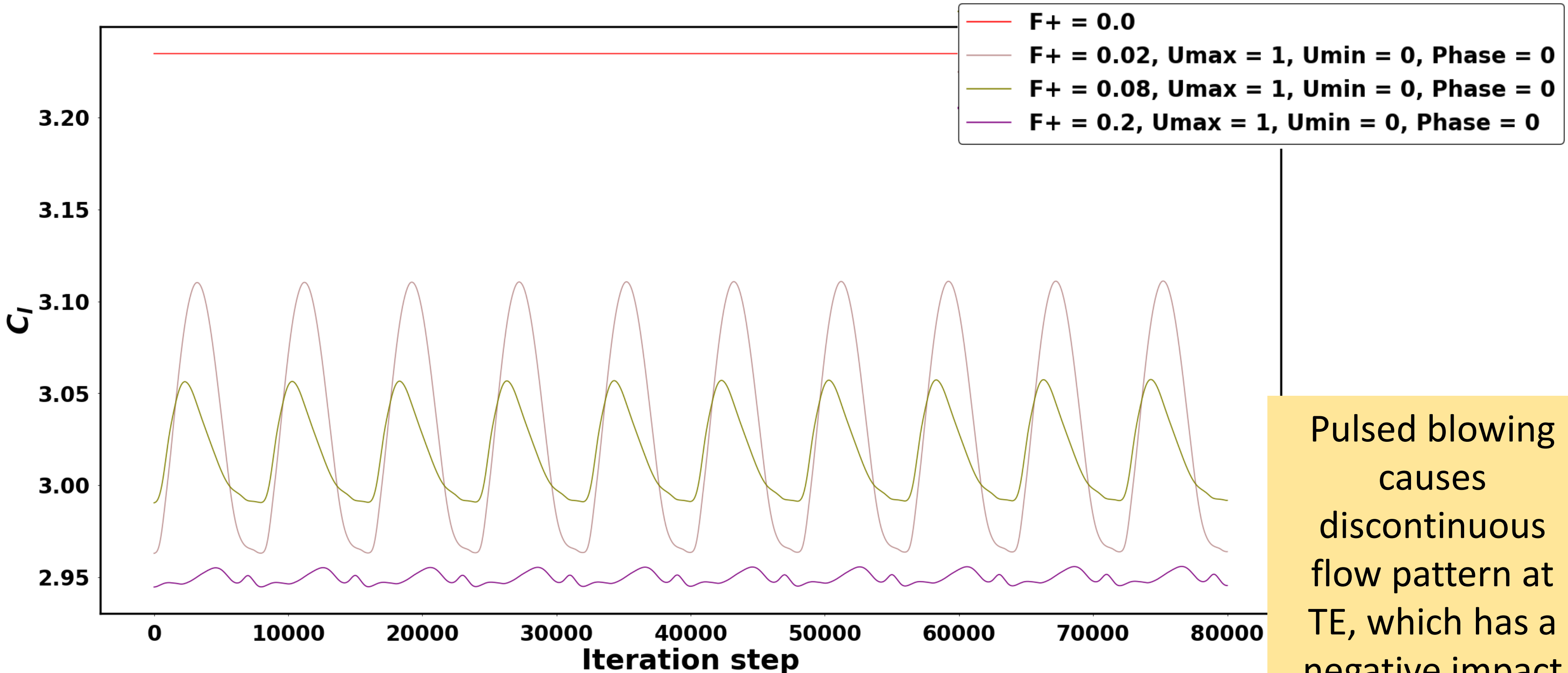

Pulsed blowing causes discontinuous flow pattern at TE, which has a negative impact on microjet effectiveness.

Flap 30° Mach and Re # Sensitivity

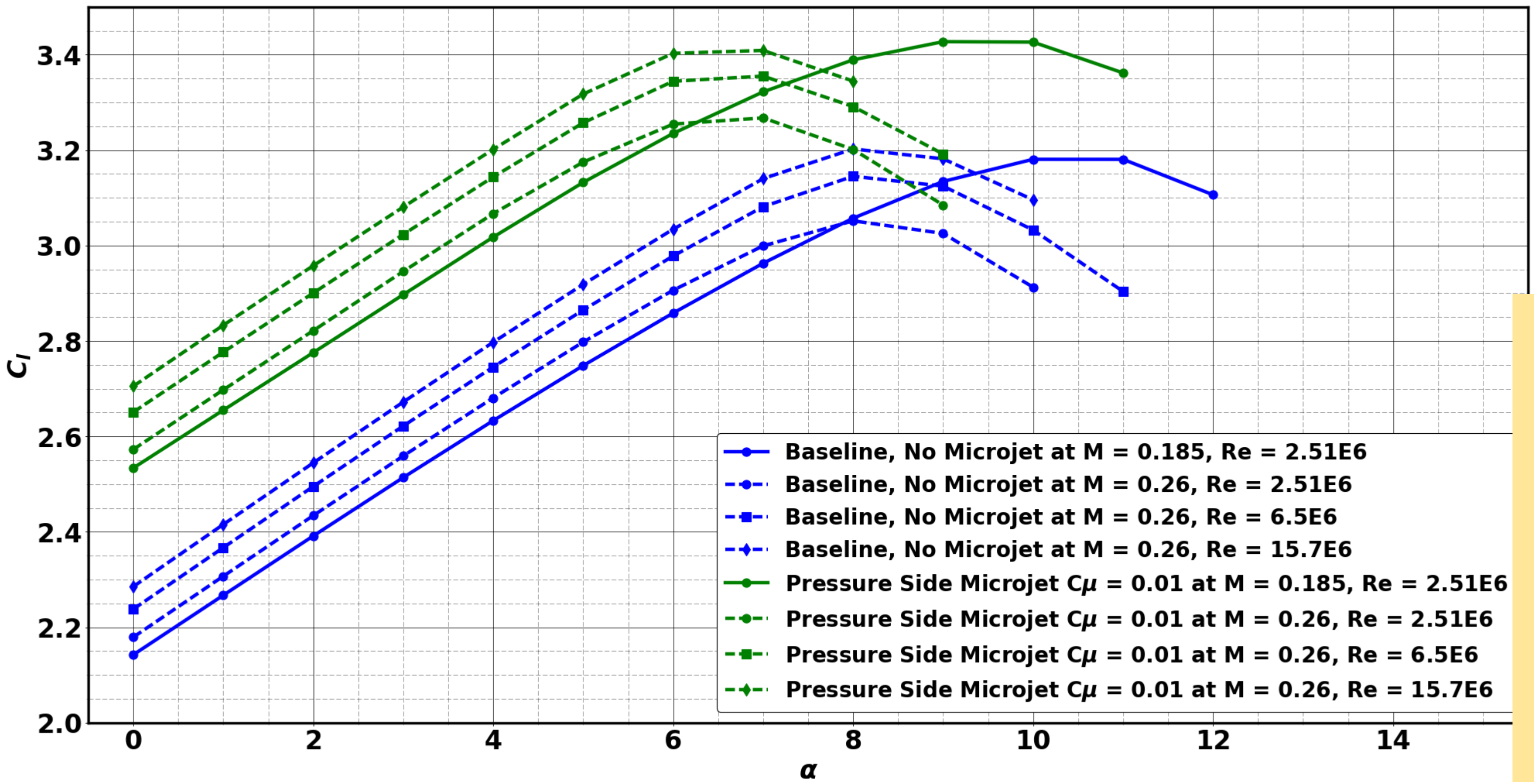

	ΔC_l @ α=6°
M = 0.185, Re = 2.51E6	0.38
M = 0.26, Re = 2.51E6	0.35
M = 0.26, Re = 6.5E6	0.36
M = 0.26, Re = 6.5E6	0.36

Results at higher Mach number (0.26) and Reynolds number (15.7 million) indicate microjet effectiveness in linear regime not affected by compressibility and Reynolds number effects.

Computational Studies

- Summary of the computational setup on baseline multi-element airfoil NLR7301
- 2D investigations on the NLR7301 flaps 20˚ and 30˚
- 2.5D (infinite sheared wing) the NLR7301 flap 30˚
- CRM-HL in landing configuration

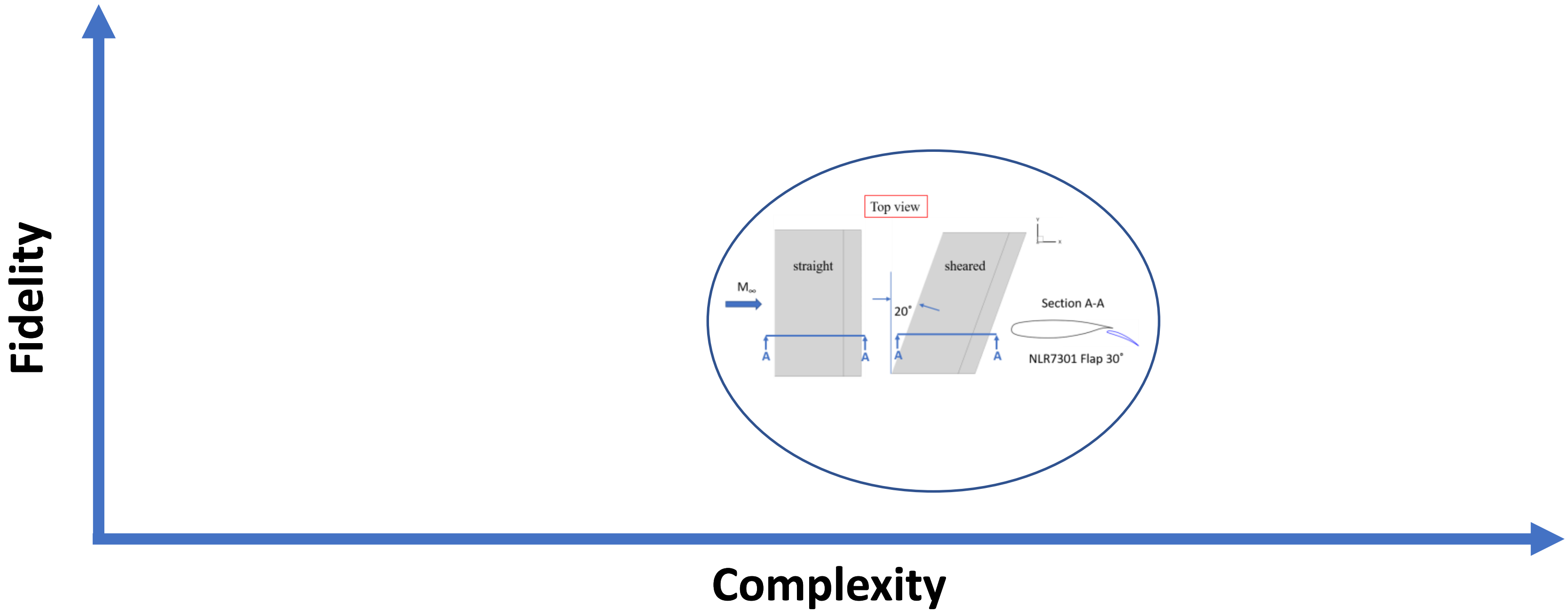

Flap 30° Infinite Wing Study

- Infinite wing allows for study more detailed jet effects (compared to 2D airfoil)
- Infinite wing is constructed from the 2D grid
- URANS (OVERFLOW), same as the 2D study
- 3rd order accurate and ARC3D diagonalized approximate factorization with matrix artificial dissipation
- SST turbulence model

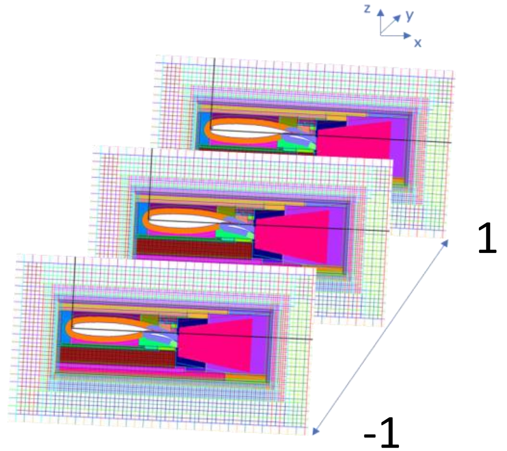

Straight infinite wing
- Wall boundary condition sensitivity
- Spanwise resolution

20° Sheared infinite wing
- Wall boundary condition sensitivity
- Spanwise resolution
- Microjet effect

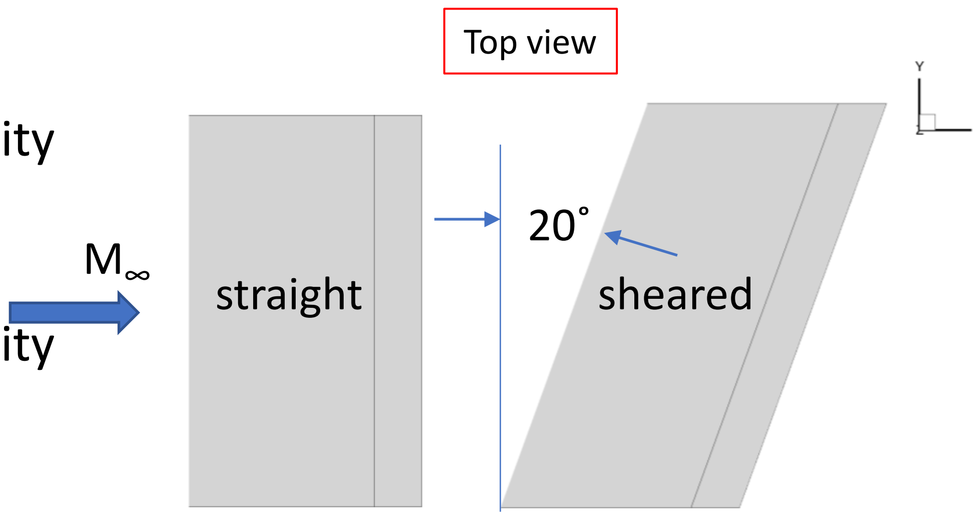

Flap 30° Sheared Wing Lift and Drag Investigation 2.5D

α=6°, Re = 2.51E6, and Ma = 0.185

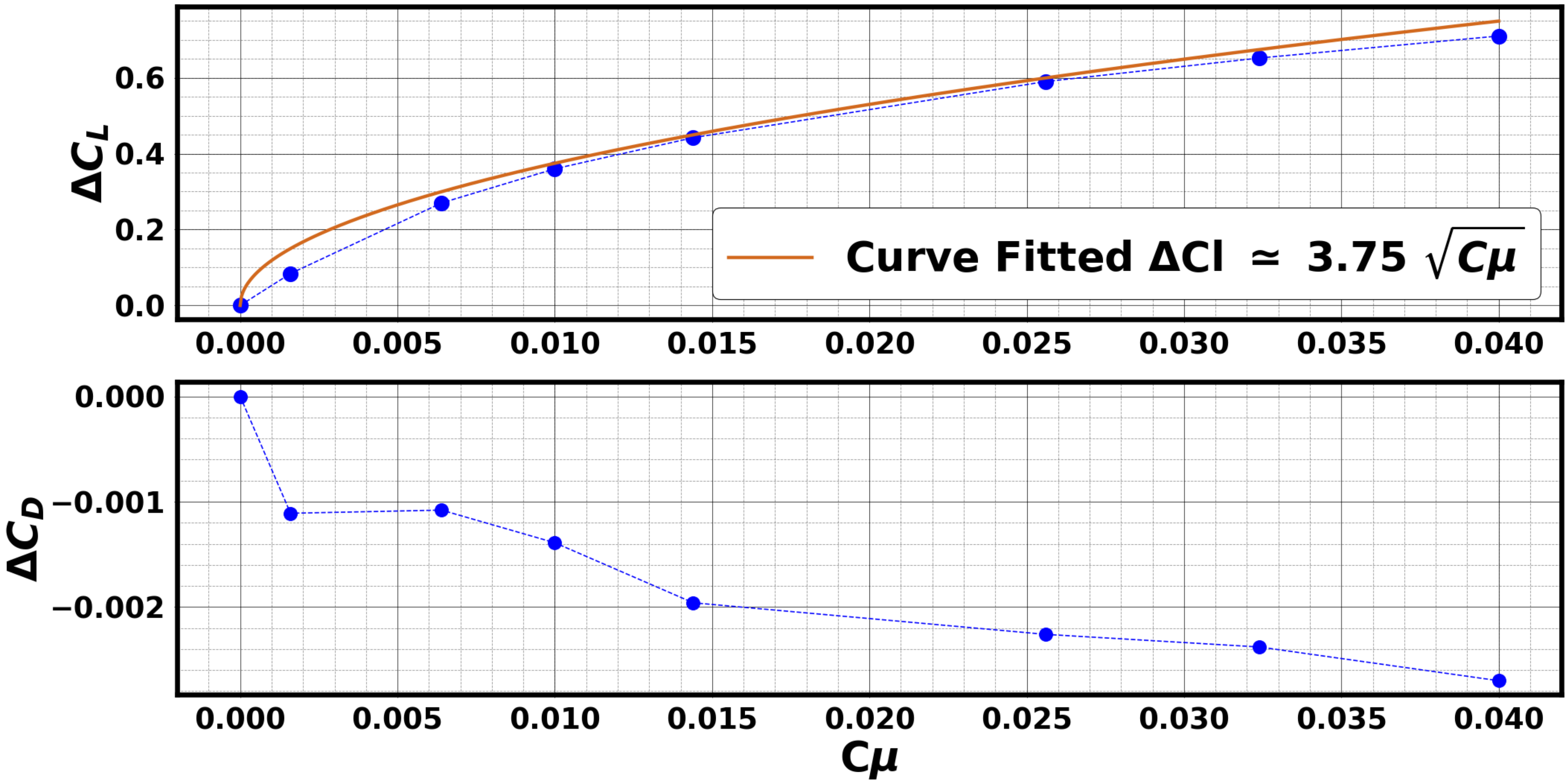

- C_μ effect on C_l and C_d corresponds well with two-dimensional results

Flap 30° Sheared Wing Lift and Drag Investigation 2.5D

α=6°, Re = 2.51E6, and Ma = 0.185

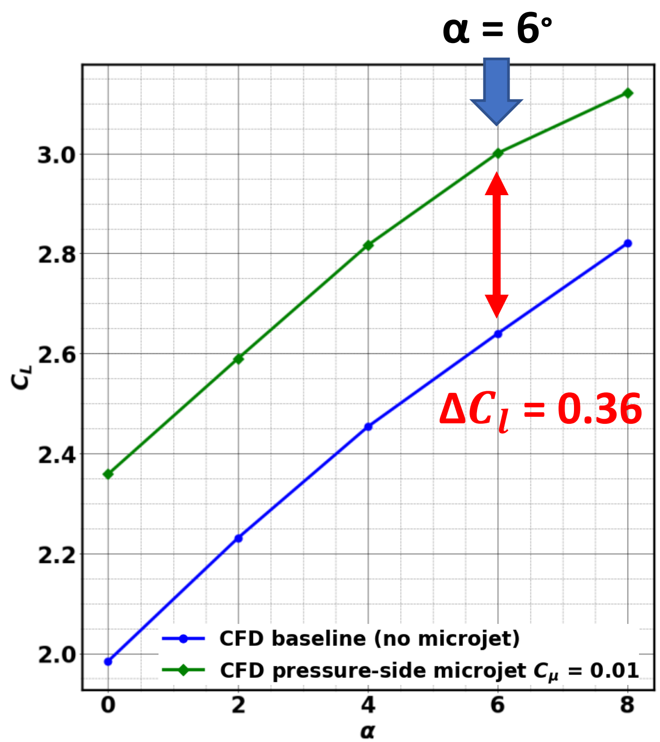

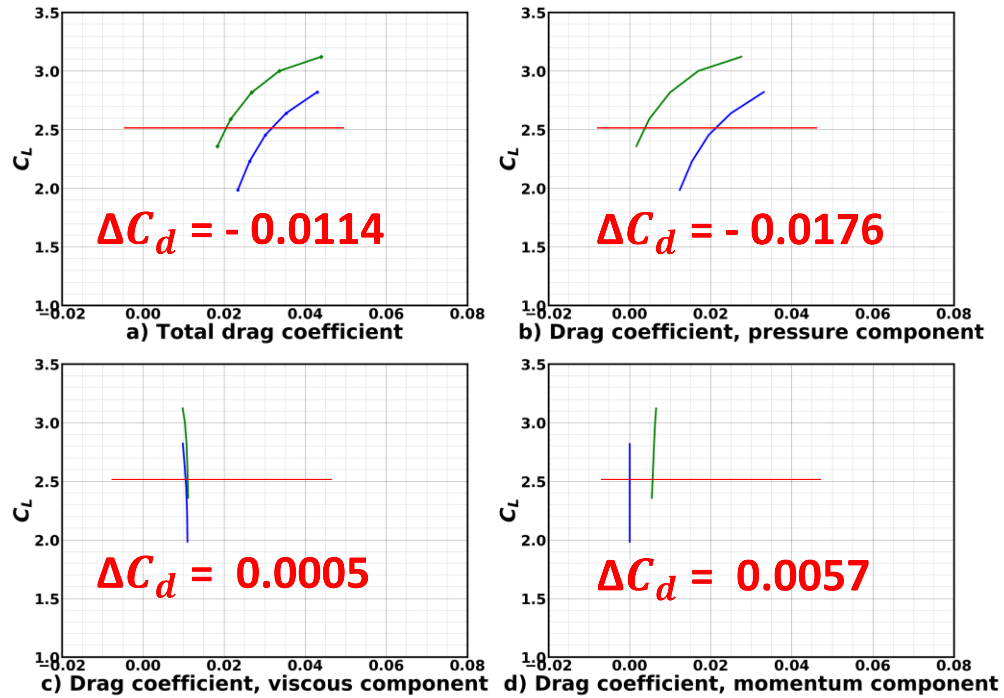

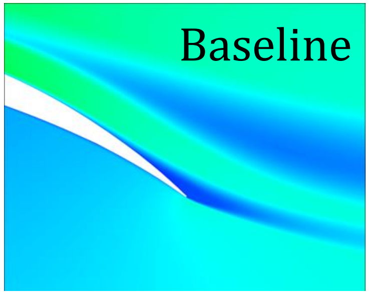

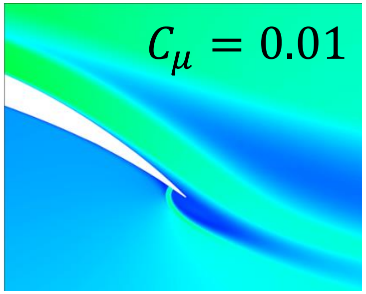

Microjet at 95% flap chord with a fixed width of 0.005 refence chord

Flap 30° Sheared Wing Separation Mitigation

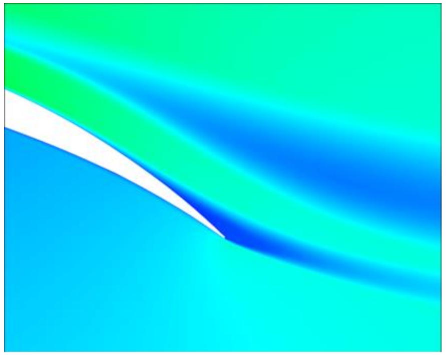
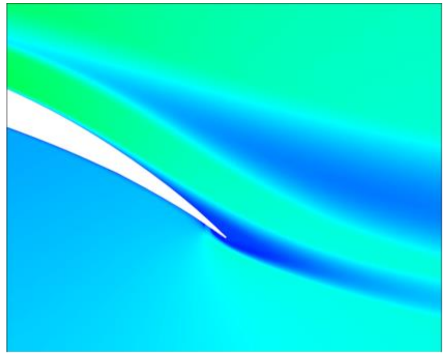
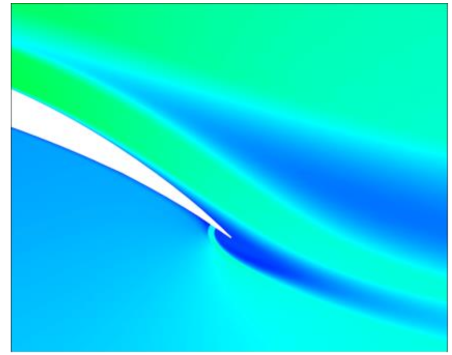
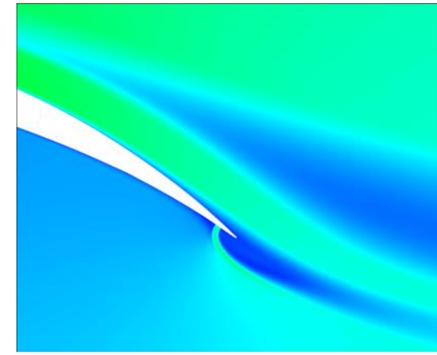

a) $C_\mu = 0.0000$ b) $C_\mu = 0.0016$ c) $C_\mu = 0.0064$ d) $C_\mu = 0.0100$

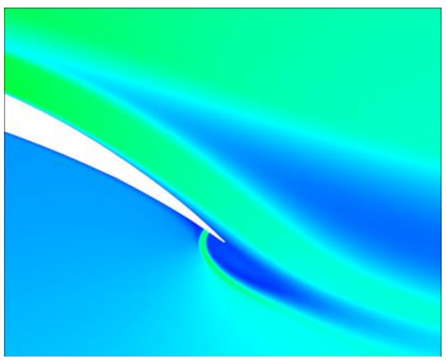
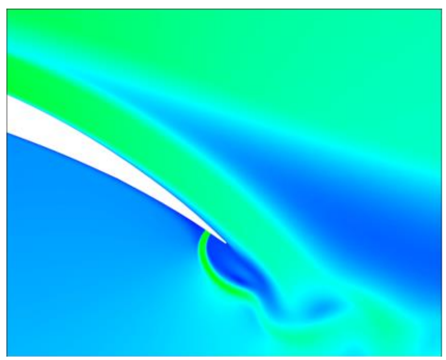
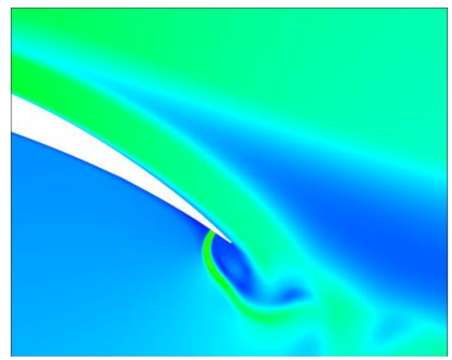
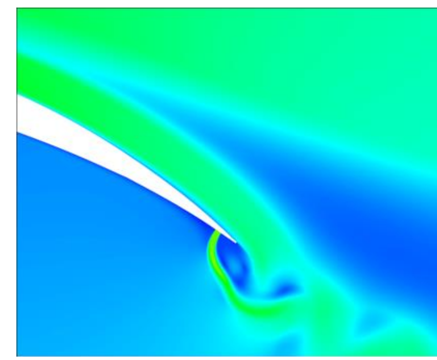

e) $C_\mu = 0.0144$ f) $C_\mu = 0.0256$ g) $C_\mu = 0.0324$ h) $C_\mu = 0.0400$

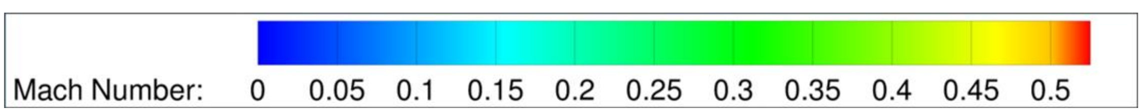

Computational Studies

- Summary of the computational setup on baseline multi-element airfoil NLR7301
- 2D investigations on the NLR7301 flaps 20˚ and 30˚
- 2.5D (infinite sheared wing) the NLR7301 flap 30˚
- CRM-HL in landing configuration

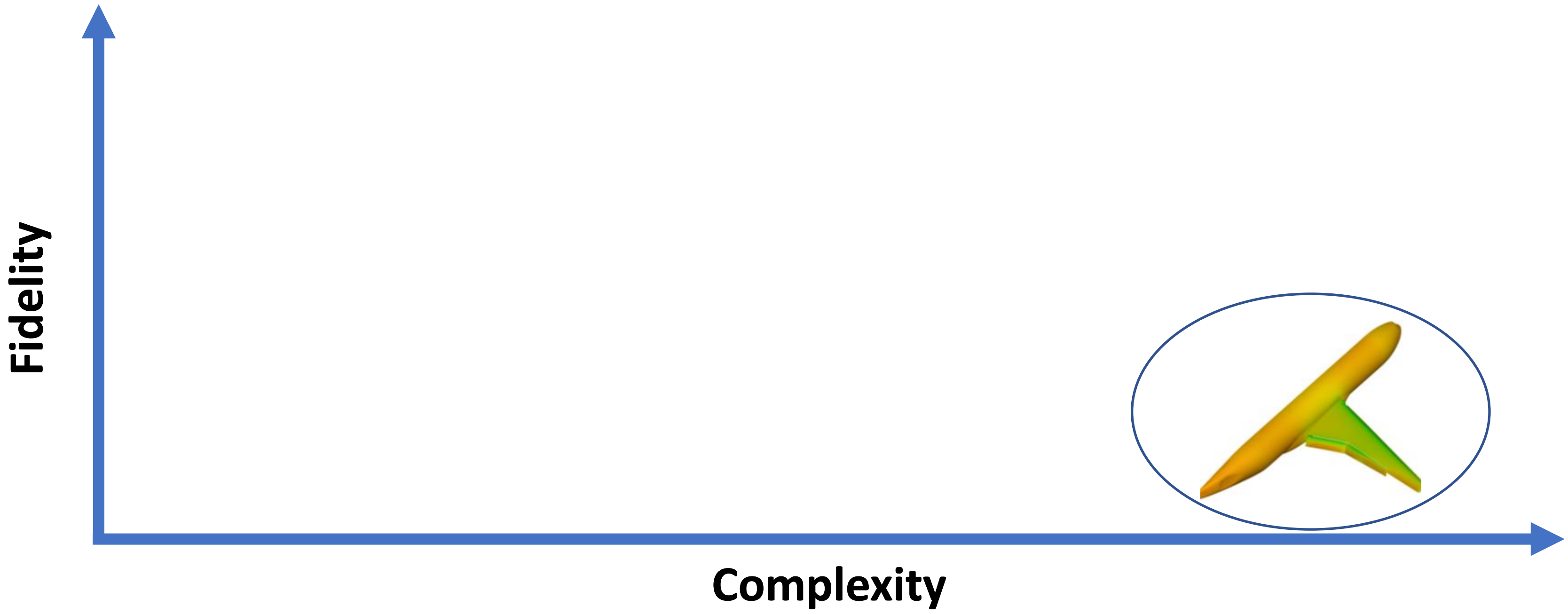

CRM High-Lift

3D

Geometry:

- CRM_HL is wing body configuration adapted from HiLiftPW-3. Slat and flaps are deployed at 30˚ and 37 ˚ respectively, without nacelle, pylon, tail or support brackets. The Full Chord Gap configuration is chosen for the microjet study.

Flow condition:

- Mach number = 0.2
- α = 8 ˚
- Reynold number based on MAC = 3.26 million
- MAC = 275.8 inches full scale
- Domain Connectivity Function routines
- Roe upwind scheme for spatial discretization
- F3D Steger-Warming 2-factor
- SA-RC turbulent model
- RANS simulations on 432 Haswell processors

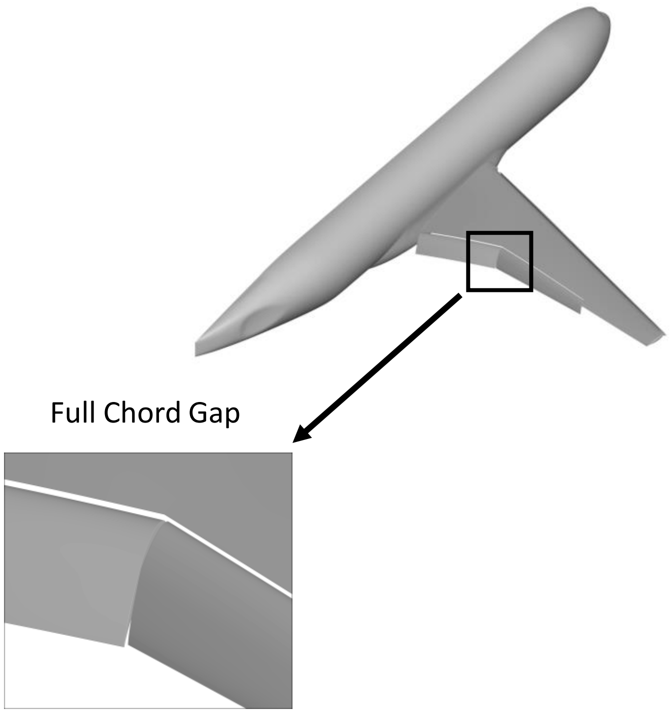

CRM High-Lift: Grid Refinement

3D

α=8°, Re_{MAC} = 3.26E6, and M = 0.2

	Number of cells
Original medium grid by William Chan	65,423,213
Refined grid for this study	68,538,927

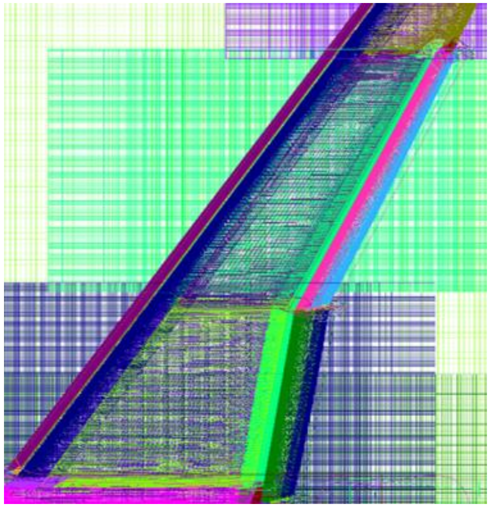

a) HiLiftPW-3 original medium grid

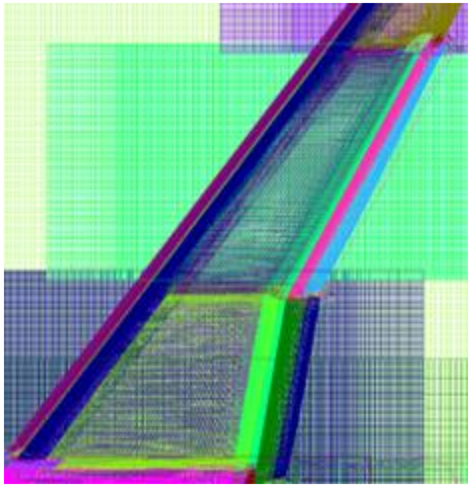

b) refined grid for this study

CRM High-Lift: Original vs. Refined Grid Solutions 3D

α=8°, Re$_{MAC}$ = 3.26E6, and M = 0.2

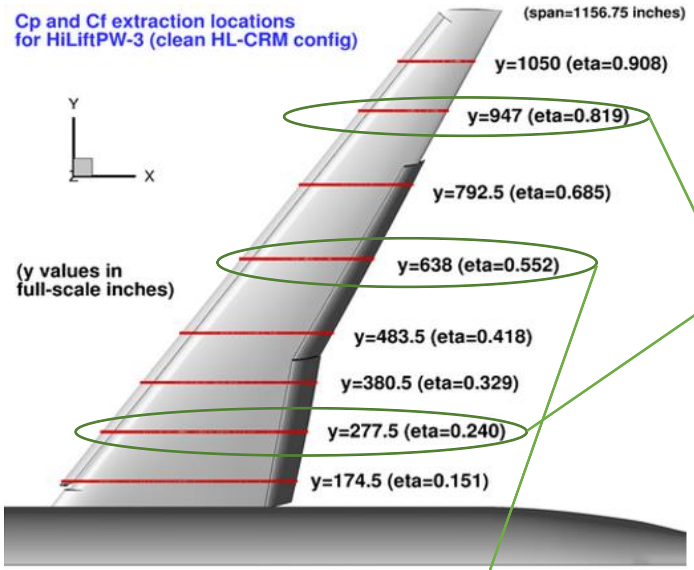

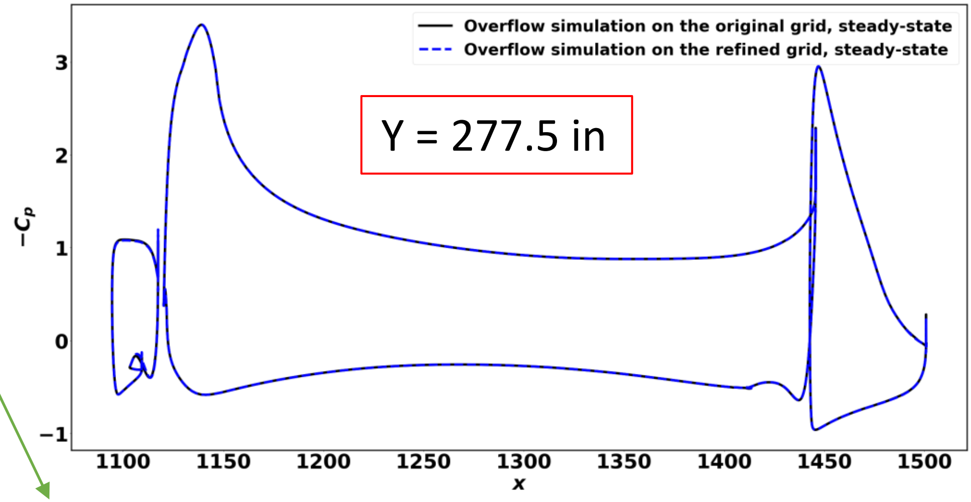

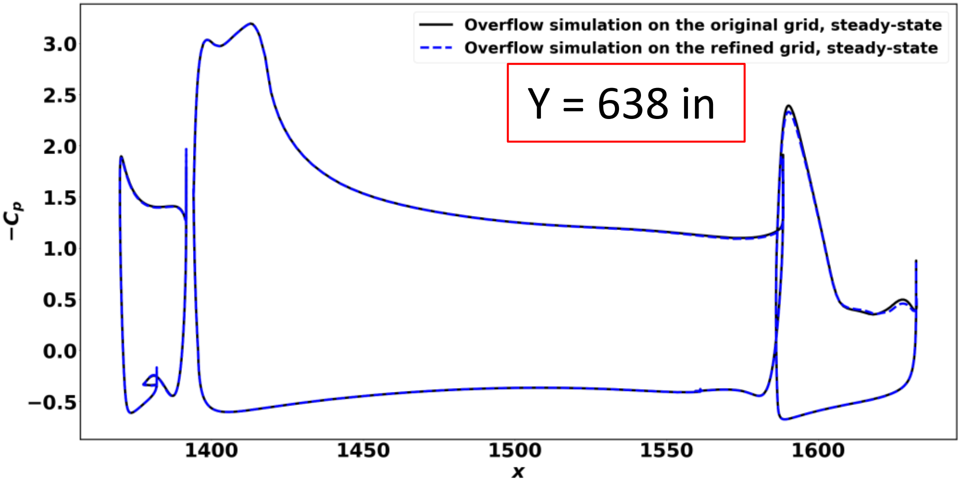

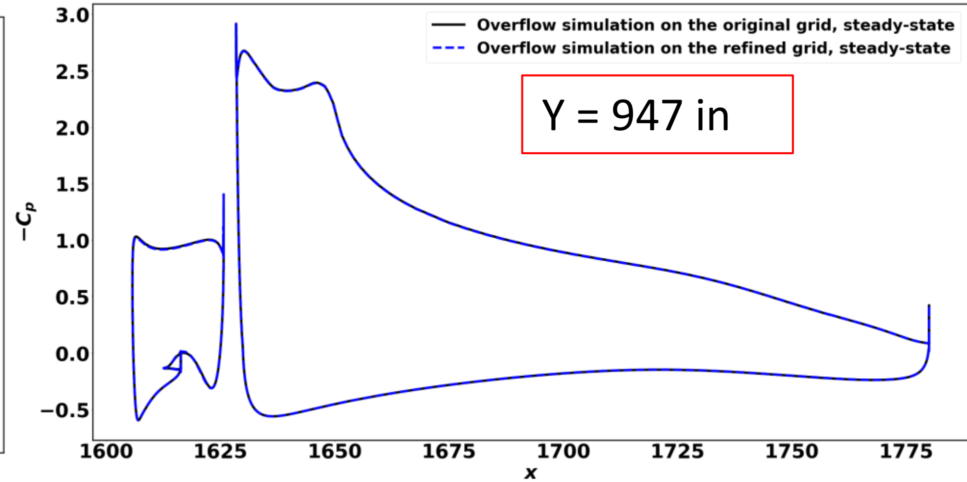

CRM High-Lift: Original vs. Refined Grid Solutions

3D

α=8°, Re_{MAC} = 3.26E6, and M = 0.2

	C_L	C_D
Overflow simulation using the HiLiftPW-3 original medium grid	1.752	0.1701
Overflow simulation using the refined medium grid	1.753	0.1700

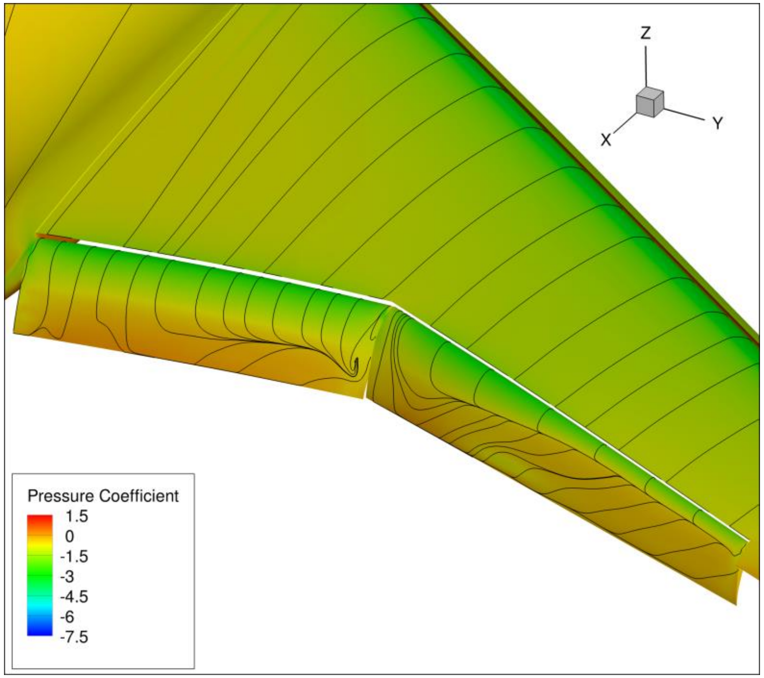

a) Overflow simulation using the HiLiftPW-3 original medium grid

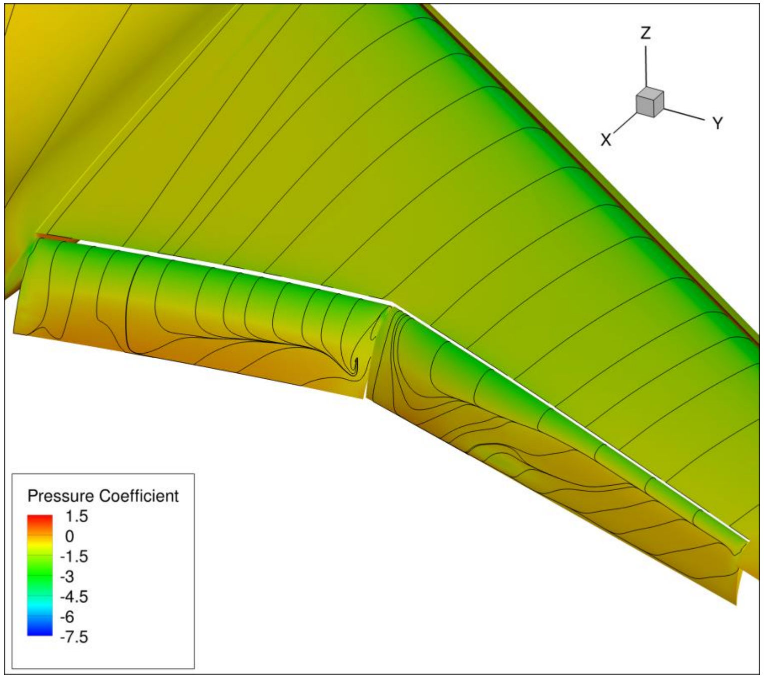

b) Overflow simulation using the refined medium grid for this study

CRM High-Lift: Preliminary Microjet Study

3D

α=8°, Re_{MAC} = 3.26E6, and M = 0.2

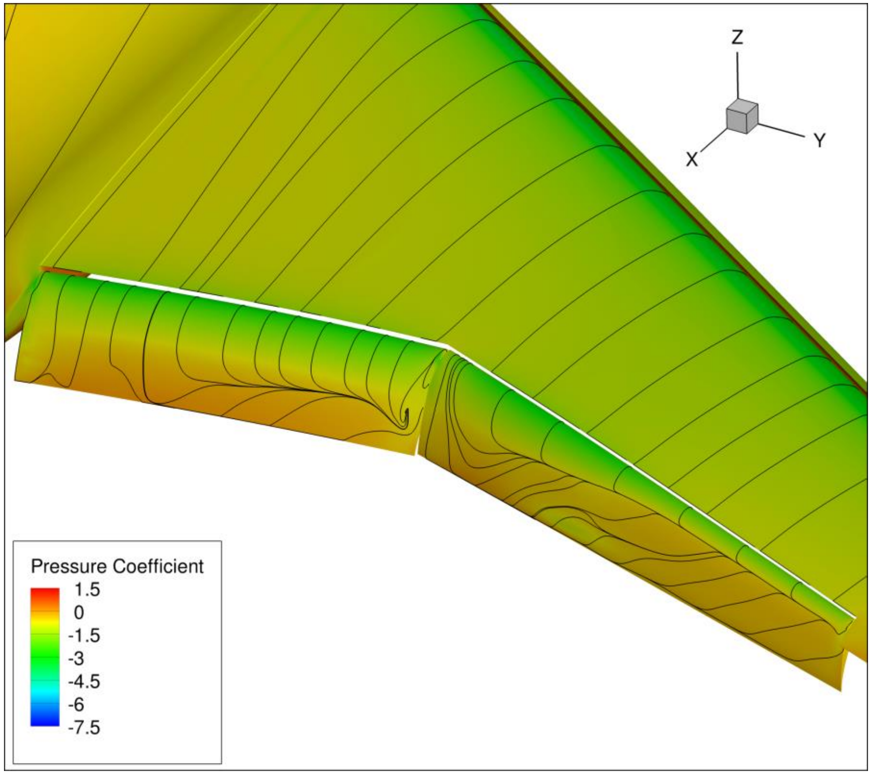

Baseline

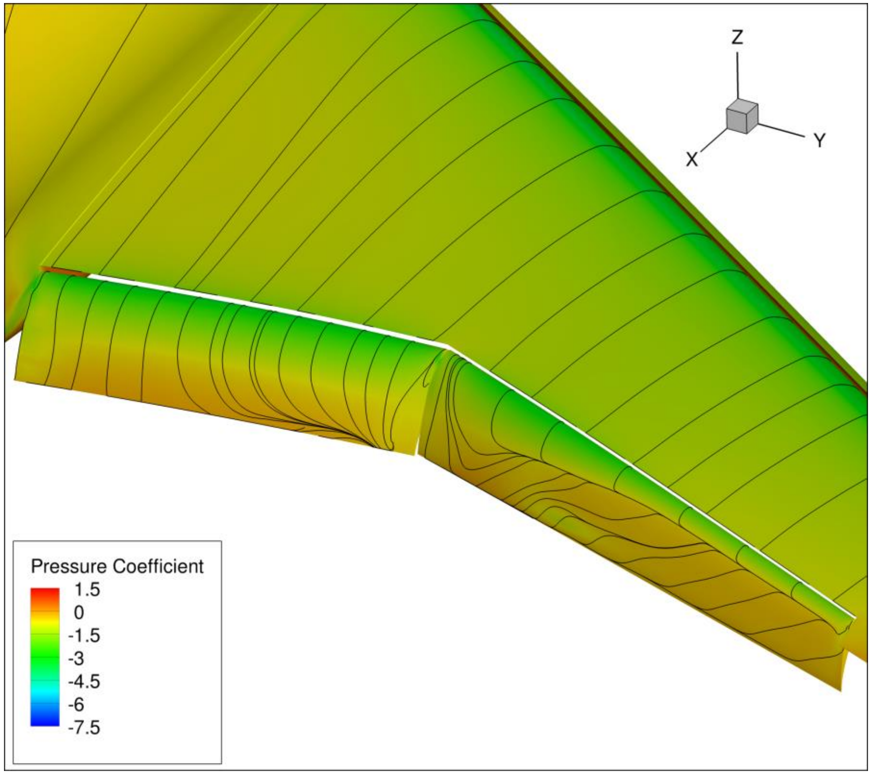

Inboard microjet at 95% c_{flap} and U_j/U_∞ = 1.0
No microjet on outboard flap

CRM High-Lift: Preliminary Microjet Study

3D

α=8°, Re_{MAC} = 3.26E6, and M = 0.2

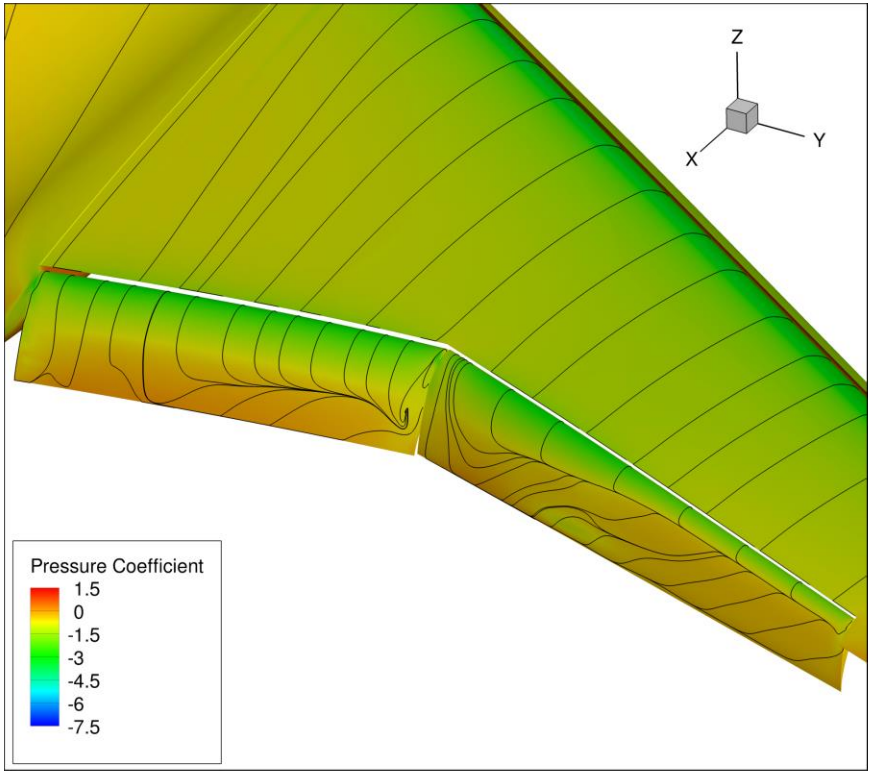

Baseline

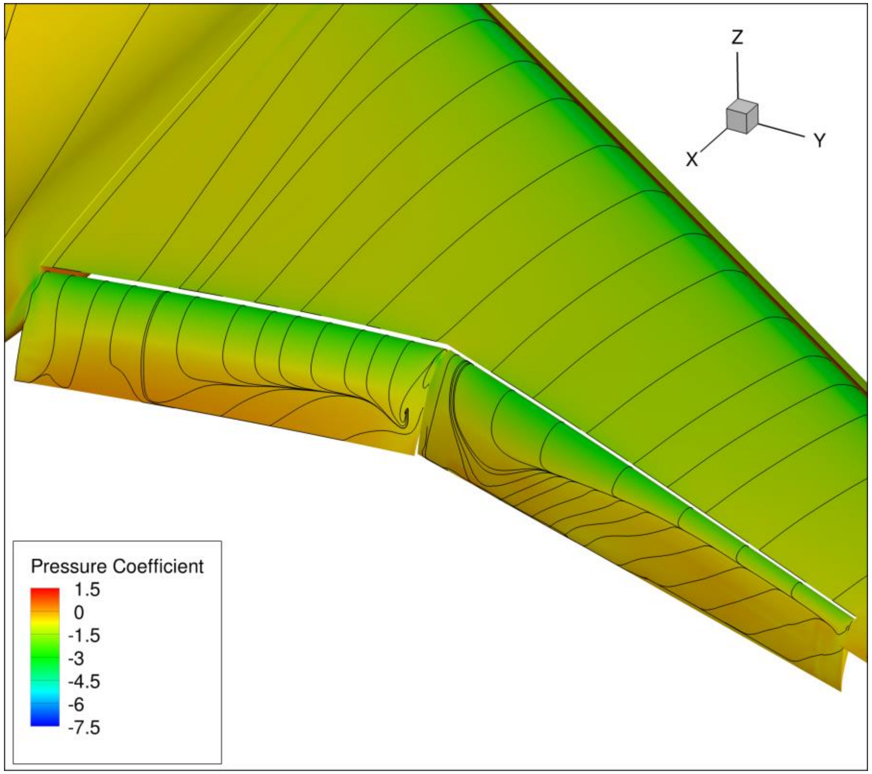

Outboard Microjet at 95% c_{flap} and U_j/U_∞ = 1.0. No microjet on inboard flap

CRM High-Lift: Preliminary Microjet Study

3D

α=8°, Re_{MAC} = 3.26E6, and M = 0.2

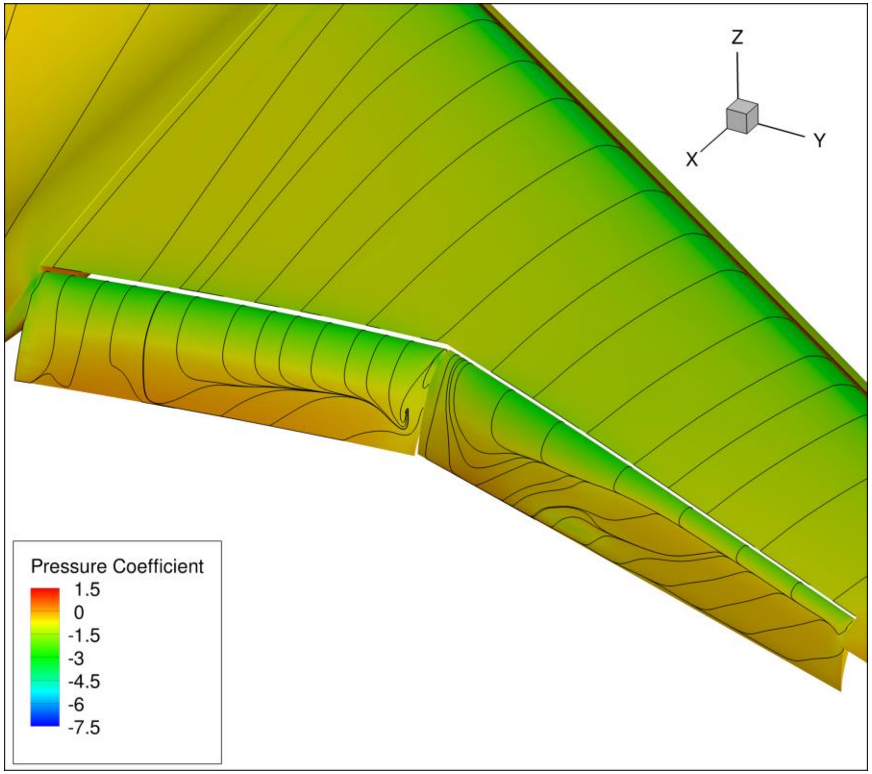

Baseline

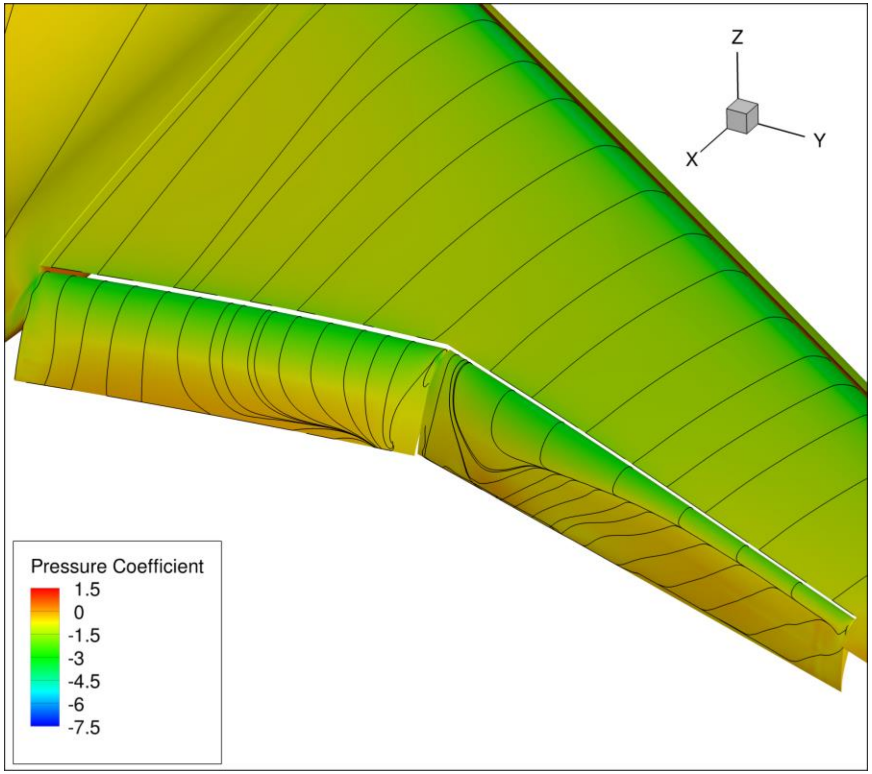

Inboard and outboard Microjet at 95% c_{flap} and U_j/U_∞ = 1.0

CRM High-Lift: Preliminary Microjet Study

3D

α=8°, Re_{MAC} = 3.26E6, and M = 0.2

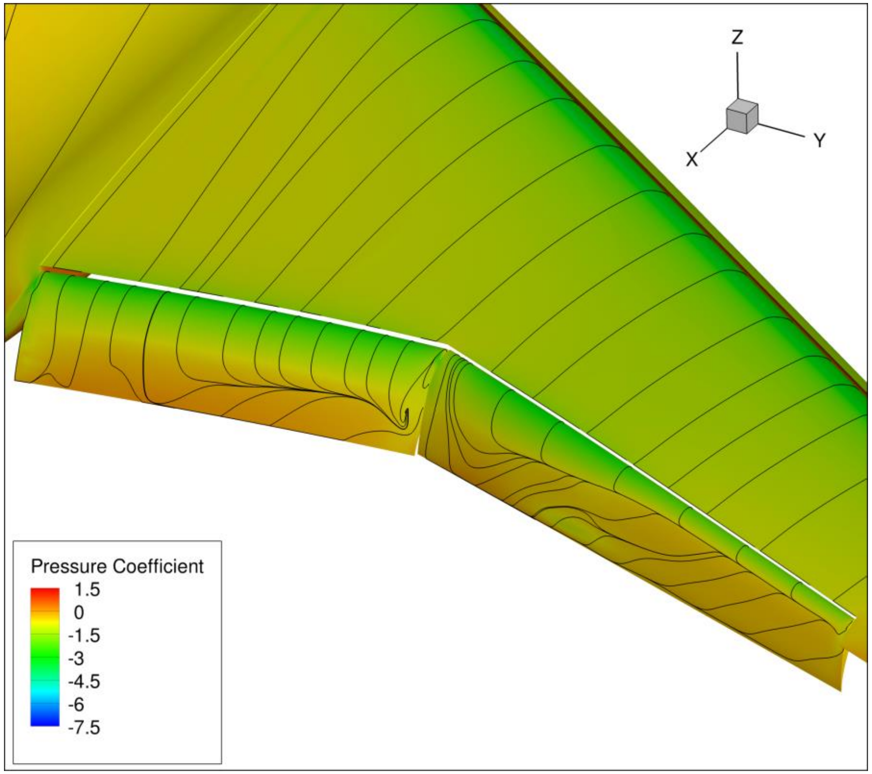

Baseline

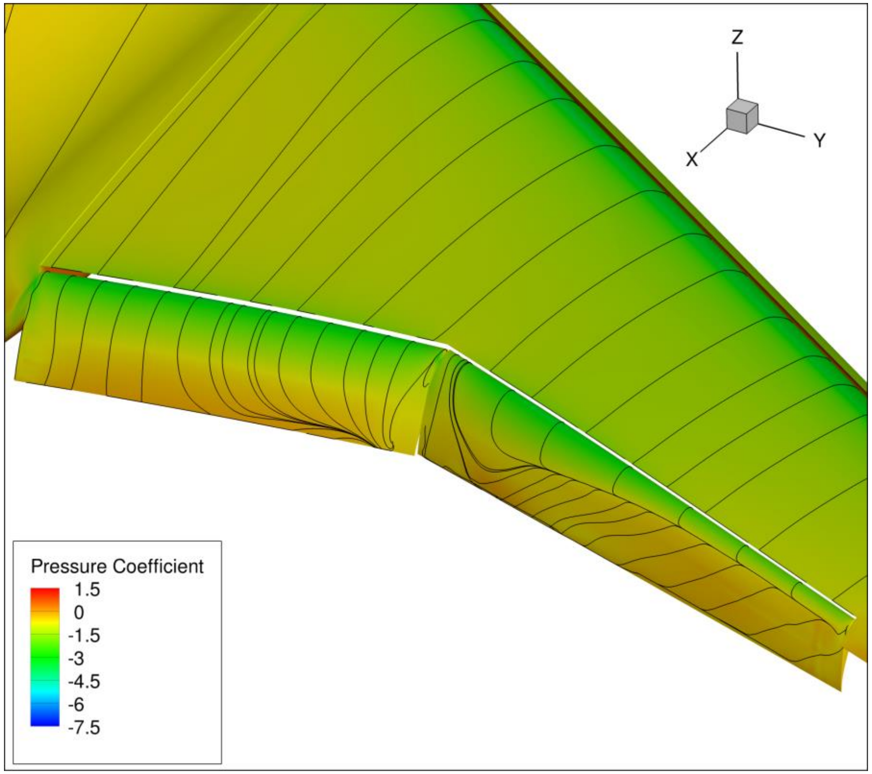

Inboard and outboard Microjet at 95% c_{flap} and U_j/U_∞ = 1.0

CRM High-Lift: Preliminary Microjet Study

3D

α=8°, Re_{MAC} = 3.26E6, M = 0.2, U_j/U_∞ = 1.0

	C_L	ΔC_L	C_D	ΔC_D
Baseline (no microjet)	1.752	-	0.1698	-
Pressure-side microjet on the inboard flap	1.832	0.080	0.1864	0.0166
Pressure-side microjet on the outboard flap	1.789	0.037	0.1743	0.0045
Pressure-side microjet on the inboard and outboard flaps	1.866	0.114	0.1903	0.0205

The drag coefficient associated with the microjet is thought to be dominated by the induced drag due to lift enhancement and spanwise load distribution modification, ($\frac{C_L^2}{\pi ARe}$)

CRM High-Lift: Inboard Microjet

3D

α=8°, Re_{MAC} = 3.26E6, M = 0.2, U_j/U_∞= 1.0

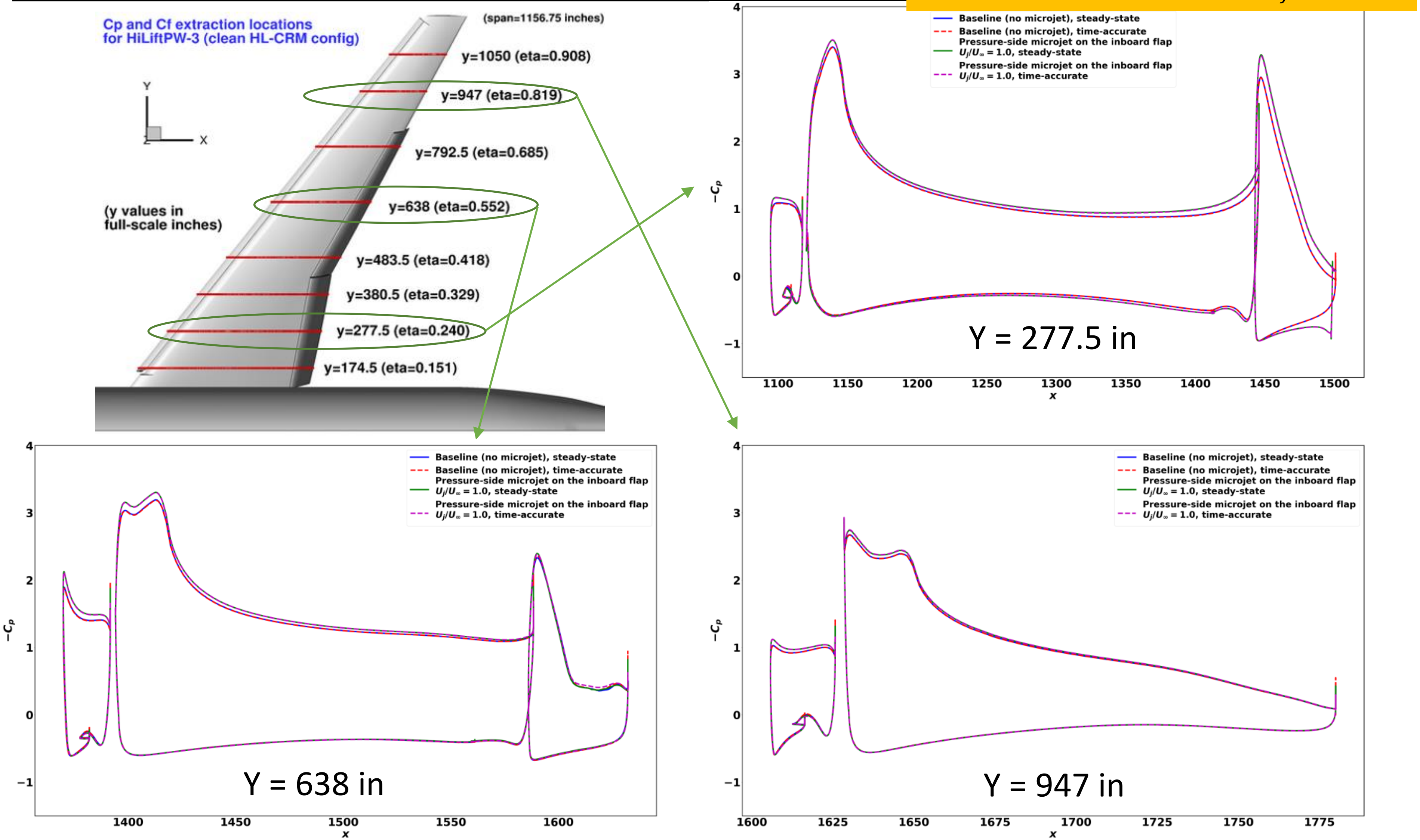

CRM High-Lift: Momentum Coefficient Sensitivity 3D

α=8°, Re_MAC = 3.26E6, and M = 0.2

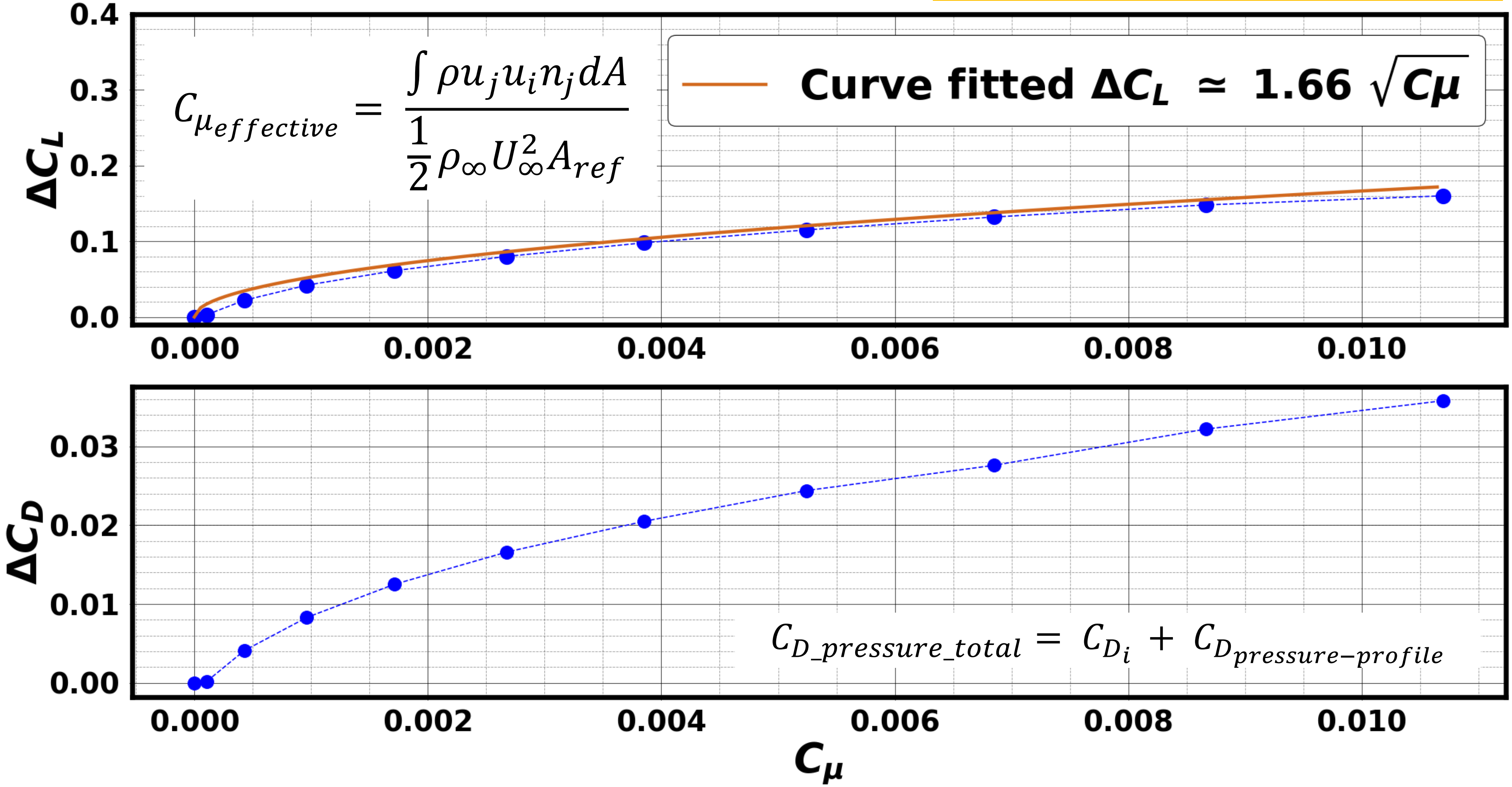

CRM High-Lift: Lift and Drag, Inboard Microjet

3D

Re_{MAC} = 3.26E6, and M = 0.2

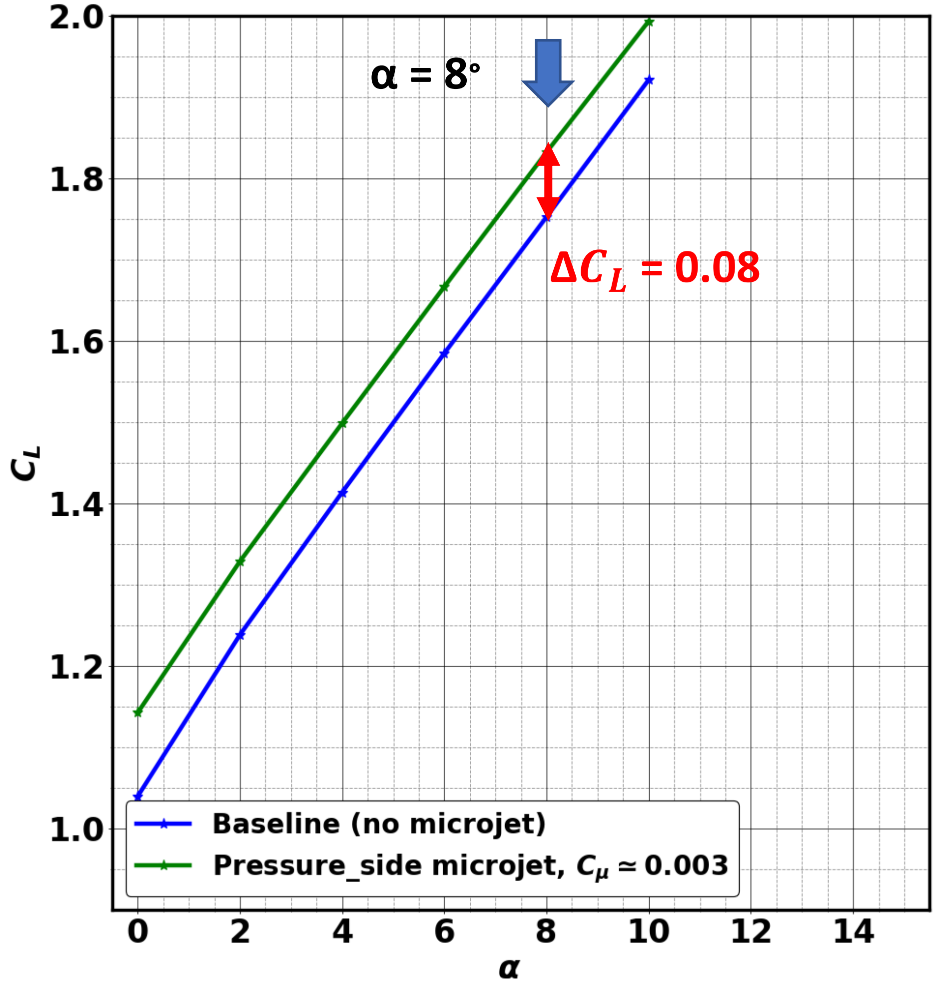

+0.10 ΔC_L *
∝ 14 in reduction in
$h_{landing\ gear}$
∝ 1400 lb (~7 passenger)

* P. Meredith, "Viscous phenomena affecting high-lift systems and suggestions for future CFD development. High-lift System Aerodynamics," AGARD CP 515, pp. 19(1)–19(8), 1993.

Conclusions and Contributions

- Proposed microjet as an AFC concept for lift enhancement and separation mitigation for high-lift systems
- Extensive study conducted on the various microjet characteristics in a building block approach (2D to 3D) addressing microjet effects on both lift and drag
- Confirmed that the investigated trailing edge microjets can provide significant control and produce improvements in high-lift characteristics of an airfoil, including
  - Lift enhancement and reduction (modulation in lift curve)
  - Lift enhancement in terms of $\Delta C_l \propto K\sqrt{C_\mu}$
  - Separation mitigation
  - Possible pressure drag reduction

Conclusions and Contributions

- Proposed mic … lift enhancement and separation mi
- Extensive stu … us microjet characteristics … building block approach (2D to 3D) addressing mi
- Confirmed tha … edge microjets can provide signifi … ments in high-lift characteris
  - Lift enhan … in lift curve)
  - Lift enhan
  - Separatio
  - Possible

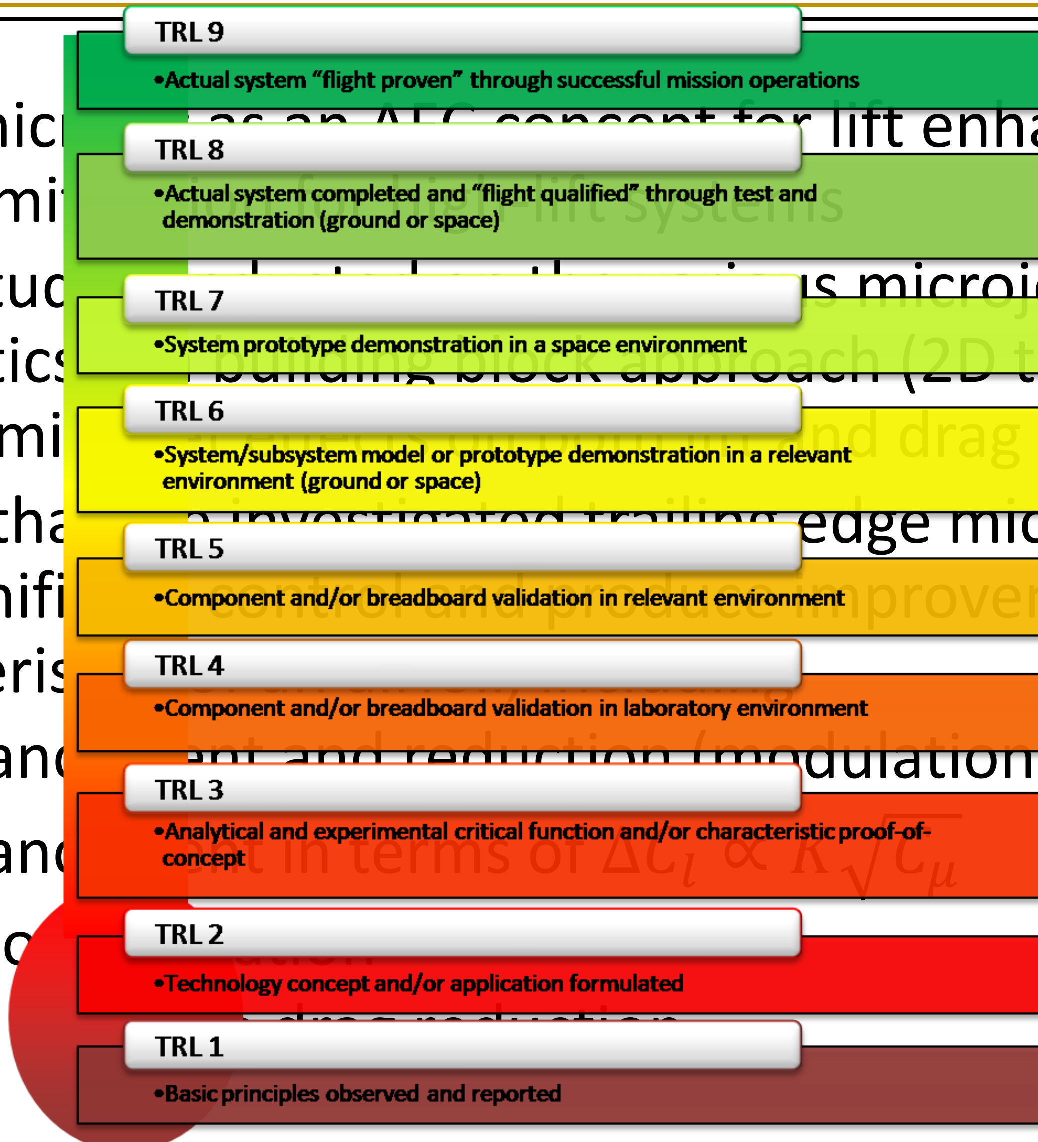

Follow-on Efforts - I

- CFD
  - 3D CRM-HL
    - Investigate the pressure drag behavior
    - Microjet configuration studies
    - Solidity ratio sensitives combined with momentum coefficient sensitivity and pulsed blowing
    - Upper surface blowing
    - Takeoff configuration for reduced flap flow separation
  - Modeling of flap internal flow paths and microjets
    - Predict pressure losses, determine minimum loss configurations
    - Study ram-air options
    - Study hybrid flow (ram-air + pressurized air) options

Follow-on Efforts – II and III

- Wind Tunnel
  - Test at TAMU
  - Use NLR 7301 2-element airfoil model
  - Study focused on jet characteristics and impact on airfoil aerodynamic characteristics
    - Determine characteristics of jet flow, including jet angle, exit pressure and velocity profile, mass flow rate and associated power requirement
- System analysis
  - How best to apply this technology?
  - Synergism - focus has been on high lift but how effective can this system then be in cruise?
  - Aerodynamic load control - tab versus blowing (or both?)
  - Industry involvement

*

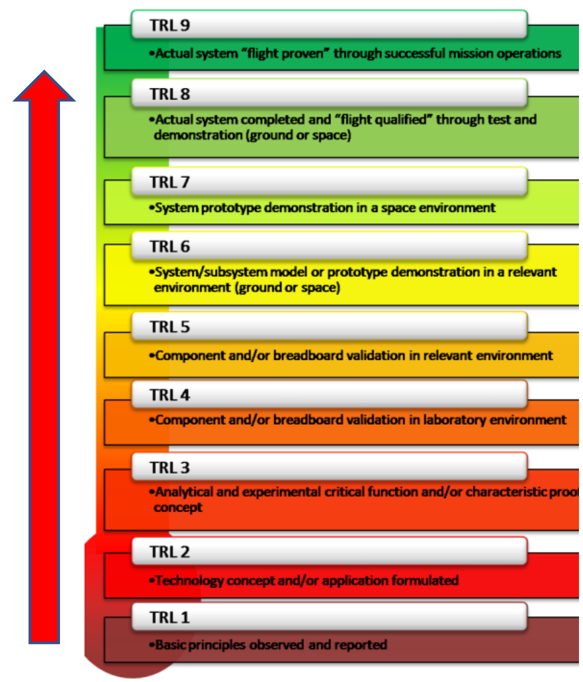

* https://www.nasa.gov/directorates/heo/scan/engineering/technology/txt_accordion1.html

Acknowledgment

- The research reported in this presentation was partially funded by Boeing Commercial Airplanes (BCA), The Boeing Company, and NASA's Advanced Air Transport Technology (AATT) project. The computing resources were provided by the NASA Ames Research Center (ARC).
- The authors acknowledge the help and inputs by Dr. Paul Vijgen, BCA, and Dr. William Chan and Dr. Thomas Pulliam, NASA ARC.

Thank you for listening